UNIVERSIDADE FEDERAL DE UBERLÂNDIA
INSTITUTO DE GENÉTICA E BIOQUÍMICA
PÓS-GRADUAÇÃO EM GENÉTICA E BIOQUÍMICA

CARACTERIZAÇÃO FUNCIONAL DE UMA LIPASE/ESTERASE SECRETADA POR *Xylella fastidiosa* COMO FATOR DE VIRULÊNCIA CHAVE NA PATOGÊNESE DA DOENÇA DE PIERCE

Aluno: Rafael Nascimento

Orientador: Luiz Ricardo Goulart Filho
Co-orientador: Abhaya M. Dandekar

UBERLÂNDIA – MG
2012

UNIVERSIDADE FEDERAL DE UBERLÂNDIA
INSTITUTO DE GENÉTICA E BIOQUÍMICA
PÓS-GRADUAÇÃO EM GENÉTICA E BIOQUÍMICA

CARACTERIZAÇÃO FUNCIONAL DE UMA LIPASE/ESTERASE SECRETADA POR *Xylella fastidiosa* COMO FATOR DE VIRULÊNCIA CHAVE NA PATOGÊNESE DA DOENÇA DE PIERCE

Aluno: Rafael Nascimento

Orientador: Luiz Ricardo Goulart Filho

Co-orientador: Abhaya M. Dandekar

Tese apresentada à Universidade Federal de Uberlândia como parte dos requisitos para obtenção do título de Doutor em Genética e Bioquímica (Área Genética).

UBERLÂNDIA – MG
2012

Dados Internacionais de Catalogação na Publicação (CIP)

Sistema de Bibliotecas da UFU, MG, Brasil.

N244c 2013

Nascimento, Rafael, 1983-

Caracterização funcional de uma lipase/esterase secretada por *Xylella fastidiosa* como fator de virulência chave na patogênese da Doença de Pierce/ Rafael Nascimento. -- 2013.

136 f. : il.

Orientador: Luiz Ricardo Goulart Filho.

Co-orientador: Abhaya M. Dandekar.

Tese (doutorado) - Universidade Federal de Uberlândia, Programa de Pós-Graduação em Genética e Bioquímica.

Inclui bibliografia.

1. Genética - Teses. 2. Genética molecular - Teses. 3. Microorganismos - Genética - Teses. I. Goulart Filho, Luiz Ricardo, 1962- . II. Dandekar, Abhaya M. III. Universidade Federal de Uberlândia. Programa de Pós-Graduação em Genética e Bioquímica. IV. Título.

CDU: 575

Palavras-chave: *Xylella fastidiosa*, Doença de Pierce, lipase, esterase, LipA.

UNIVERSIDADE FEDERAL DE UBERLÂNDIA
INSTITUTO DE GENÉTICA E BIOQUÍMICA
PÓS-GRADUAÇÃO EM GENÉTICA E BIOQUÍMICA

CARACTERIZAÇÃO FUNCIONAL DE UMA LIPASE/ESTERASE SECRETADA POR *Xylella fastidiosa* COMO FATOR DE VIRULÊNCIA CHAVE NA PATOGÊNESE DA DOENÇA DE PIERCE

ALUNO: Rafael Nascimento

COMISSÃO EXAMINADORA

Presidente: Dr. Luiz Ricardo Goulart Filho

Examinadores:

Dr. Helvécio Della Coletta Filho
Dr. Marcos Antônio Machado
Dr. Paulo Adriano Zaini
Dr. Matheus de Souza Gomes

As sugestões da Comissão Examinadora e as normas da PGGB para o formato da Tese foram contempladas.

_____

Dr. Luiz Ricardo Goulart Filho

Dedico aos meus pais, Solange e Nilson,
e às minhas irmãs, Emília e Mariana.

"Não sabendo que era impossível,
ele foi lá e fez"
Jean Cocteau

AGRADECIMENTOS

Aos professores Luiz Ricardo Goulart Filho e Abhaya M. Dandekar, pelo incentivo, pelas oportunidades e por acreditarem no meu trabalho.

Aos meus colegas de trabalho: Alice Vieira, Ana Paula Carneiro, Ana Carolina Siquieroli, Ana Paula Freschi, Carolina Reis, Carlos Prudêncio, Carlos Ueira, Fabiana Santos, Fausto Capparelli, Galber Araújo, Guilherme Lino, Karina Marangoni, Janaína Lobato, Lara Vecchi, Larissa Goulart, Luciana Bastos, Luciana Calábria, Patrícia Terra, Rone Cardoso, Thaíse Araújo, Washington Carvalho e muitos outros... muito obrigado por compartilharem comigo todo esse tempo!

Aos meus colegas de trabalho no Laboratório do professor Dandekar (Dept. Plant Sciences, UC Davis - CA): David Dolan, Elenor Castillo, Sandie Uratsu, Ana Maria Ibanez, Quyen Tran, Hyrum Gillespie, Russel Reagan, Marta Bjornson, Timothy Butterfield, Aye Tu e My Phu... muito obrigado por fazerem parte dessa importante experiência pessoal e profissional!

Aos meus amigos Tisciane e Rafael Hermes, pela grande ajuda nos primeiros meses fora de casa!

Aos meus colegas de trabalho Darren Weber e Diana Tran (UC Davis Proteomics Core Facility) pela grande ajuda, afinal de contas LC-MSMS não é tão simples quanto parece!

Aos pesquisadores Dario Cantu, Sandeep Chakraborty e Paul Alexander, que tanto me ajudaram na reta final deste trabalho!

Ao professor Dr. George Bruening (UC Davis, Dept. of Plant Pathology), por um dos maiores ensinamentos científicos: ciência se faz na bancada, mesmo depois de se tornar Emeritus Faculty.

À minha amiga Mona Gouran, pelos momentos de descontração.

À todos os professores que, desde os primeiros anos, me mostraram que a educação é o melhor caminho.

Aos membros da Banca Examinadora, que gentilmente aceitaram o convite para avaliarem este trabalho.

Ao povo brasileiro, que por meio da UFU, da CAPES e do CNPq, investiu em minha educação e formação científica. Espero retribuir essa confiança!

E um agradecimento muito especial:

À minha família, especialmente aos meus pais, Nilson e Solange, e às minhas irmãs, Mariana e Emília: muito obrigado pelo apoio, cuidado e dedicação durante todos esses anos! Não há palavras que exprimam a minha gratidão... amo vocês! Aos meus cunhados, Alessandro Gomes e João Felício... muito obrigado, especialmente por fazerem minhas irmãs felizes! Aos meus avós, que já se foram, mas que deixaram uma boa lembrança! Aos tios e tias, primos e primas, muito obrigado pelo incentivo!

Ao Pedro Pablo S. Martins, que me acompanhou incondicionalmente durante os momentos mais difíceis, quando tudo parecia sem solução, e nos momentos de muita alegria, que se intensificaram com sua presença! Muito obrigado pela paciência, pela compreensão, pela companhia e pelo carinho nos momentos em que eu mais precisava... isso fez a diferença e nunca será esquecido! Você faz parte dessa conquista tanto quanto eu!

À família Martins: Ari, Simone, Juliano, João Lucas, Lara, Henrique, Patrícia, Diego, Kriscia, Lívia, Natália e Edinha... muito obrigado pelo incentivo e pelos momentos de descontração!

Ao meu grande amigo Marco Lara, companheiro de muitos anos... muito obrigado! Sem tudo o que você fez por mim, essa conquista não seria possível. Você tem e sempre terá um lugar especial no meu coração!

Aos meus amigos: José Geraldo Gomes, Adriana Sousa, Luciana Paranahyba, Jocimar Tavares, Sandro Melo, Ricardo Pereira, Rômulo Nascimento, Francisco Arantes, Frederico Mameri, Francisco Resende, Brian Flach, Melvin Malapitan, Emerson Rasera, Adriano Gosuen, Ludmilla Dell'Isola,

Kátia Alessandra e Gabi Maravilha. Muito obrigado pela amizade... vocês fazem grande diferença na minha vida!

Às amigas Paula Cristina e Paula Souza... cada uma a seu tempo, vocês fizeram e fazem parte da minha história. Muito obrigado pelas risadas, pelos momentos de alegria e por tornar o dia-a-dia muito melhor!

Ao meu amigo Hossein Gouran, que tanto ajudou na difícil adaptação à vida em outro país. Agradeço todo o seu empenho e boa vontade. Muito obrigado por compartilhar comigo de todo esse tempo e por tornar a minha experiência nos EUA ainda mais gratificante! Tenho certeza que essa jornada foi de grandes mudanças, desafiadoras para ambos, mas que saímos mais fortes dessa batalha!

À amiga Ângela Sena, que compartilhou comigo de momentos difíceis, onde só se ouvia o canto dos corvos, e de momentos de felicidade, onde o sol realmente parecia mais brilhante. Nossos “dog days are over”, mas fico muito feliz em saber que superá-los juntos nos fez grandes amigos!

À amiga Yara P. Maia, muito obrigado pela consideração e pelo apoio... te admiro!

Às amigas Patrícia Fujimura e Juliana Franco, pela colaboração dentro e fora do laboratório! Admiro muito o empenho e dedicação de ambas em ajudar a todos... muito obrigado!

À Deus, pela vida!

LISTA DE FIGURAS

CAPÍTULO I

CAPÍTULO II

LISTA DE TABELAS

CAPÍTULO II

LISTA DE ABREVIATURAS E SÍMBOLOS

°C	Grau Celsius
Å	Ångström
ABC	ATP Binding Cassette
Abs.	Absorbance
ACN	Acetonitrile
Ala	Alanina / Alanine
AmBic	Ammonium Bicarbonate
Asp	Aspartato / Aspartate
BHL	N-Butyryl-Homoserine Lactone
BOG	β-Octil Glicosídeo
BSA	Bovine Serum Albumin
$CaCl_2$	Calcium Chloride
cDNA	Complementary DNA
Chaps	3-[(3-cholamidopropyl)dimethylammonio]-1-propanesulfonate
CLS	Coffee Leaf Scorch
cRAP	Common Repository of Adventitious Proteins
CVC	Clorose Variegada dos Citros / Citrus Variegated Chlorosis
CWDE	Cell Wall Degrading Enzyme
Da	Dalton
DNA	Deoxyribonucleic Acid
DSF	Diffusible Signaling Factor
DTT	Dithiothreitol
E.C.	Enzyme Commission
e.g.	Exempli gratia
EDTA	Ethylenediaminetetraacetic Acid
EF-Tu	Elongation-Factor Tu
EGase	Endo-1,4-β-glucanase
ELISA	Enzyme-Linked Immunosorbent Assay
EPS	Exopolysaccharide
EUA	Estados Unidos da América
g	Gram
GFP	Green Fluorescent Protein

Glu	Glutamato / Glutamate
Gly	Glicina / Glycine
h	Hour
HCl	Hydrochloric Acid
His	Histidina / Histidine
HR	Hypersensitive Response
HRP	Horseradish Peroxidase
i.e.	Id est
IM	Inner Membrane
IPTG	Isopropyl β-D-1-thiogalactopyranoside
KCl	Potassium Chloride
kDa	Kilodalton
KV	Kilovolt
LB	Luria Broth
LC/MSMS	Liquid Chromatography Mass Spectrometry
LPS	Lipopolisacarídeos
M	Molar
m/z	Mass-to-charge Ratio
MAMP	Microbe-Associated Molecular Patterns
mg	Milligram
min	Minute
mL	Milliliter
mM	Millimolar
ms/ms	Tandem Mass Spectrometry
NaCl	Sodium Chloride
NCBI	National Center for Biotechnology Information
ng	Nanogram
NI	Non-Infected
nm	Nanometro
OD	Optical Density
OLS	Oleander Leaf Scorch
OM	Outer Membrane
OMP	Outer Membrane Protein
OMV	Outer Membrane Vesicle

ORF	Open Reading Frame
PAMP	Pathogen-Associated Molecular Pattern
pb	Par de base
PBS	Phosphate-Buffered Saline
PBS-M	PBS plus Non-fat Dried Milk
PBS-T	PBS plus Tween 20
PD	Doença de Pierce / Pierce's Disease
PEG	Polyethylene Glycol
PG	Poligalacturonase
pH	Potential of Hydrogen
PMSF	Phenylmethylsulfonyl Fluoride
pNP-C4	p-Nitrophenyl Butyrate
PVPP	Polyvinylpolypyrrolidone
RNA	Ribonucleic Acid
rpm	Revolutions per Minute
rRNA	Ribosomal Ribonucleic Acid
RT	Room Temperature
RT-PCR	Reverse Transcription Polymerase Chain Reaction
SDS	Sodium Monododecyl Sulfate
SDS-PAGE	Sodium Dodecyl Sulfate Polyacrylamide Gel Electrophoresis
SEM	Scanning Electronic Microscopy
Ser	Serina / Serine
SSPs	Soluble Supernatant Proteins
T2SS	Type II Secretion System
T3SS	Type III Secretion System
TEM	Transmission Electronic Microscopy
TFA	Trifluoroacetic Acid
TMB	3,3′,5,5′-tetramethylbenzidine
TP	Total Proteins
Tris	Tris(hydroxymethyl)aminomethane
USA	United States of America
v/v	Volume/volume
W	Watt
w/v	Weight/volume

w/w	Weight/weight
wpi	Week Post Innoculation
WT	Wildtype
Xcc	*Xanthomonas campestris* pv. campestris
Xcv	*Xanthomonas campestris* pv. vesicatoria
Xf	*Xylella fastidiosa*
Xf-CVC	*Xylella fastidiosa* 9a5c
Xf-PD	*Xylella fastidiosa* Temecula 1
Xff	*Xylella fastidiosa fastidiosa*
XLB	Xylem-Limited Bacteria
Xoo	*Xanthomonas oryzae* pv. oryzae
Xps	Xanthomonas Protein Secretion
μg	Microgram
μL	Microliter

SUMÁRIO

APRESENTAÇÃO

Xylella fastidiosa (*Xf*) é uma bactéria fitopatogênica responsável por diversas doenças em um amplo espectro de hospedeiros de grande importância econômica. A transmissão deste patógeno é mediada por insetos e a população bacteriana é restrita aos tecidos do xilema no hospedeiro vegetal. Duas doenças causadas por *X. fastidiosa*, a Doença de Pierce (PD) da videira (*Vitis vinifera* L.) e a Clorose Variegada dos Citros (CVC), são epidemias importantes nos Estados Unidos e Brasil, respectivamente. O alto impacto econômico causado pelo CVC no cultivo da laranja doce levou à reunião da comunidade científica brasileira que, num esforço substancial, sequenciou o genoma completo da linhagem 9a5c de *X. fastidiosa*, sendo este o primeiro genoma de uma bactéria fitopatogênica a ser elucidado. O genoma da linhagem Temecula 1, causadora da PD, foi então sequenciado pelo mesmo grupo.

A PD é um problema crônico na indústria da uva na Califórnia, nos Estados Unidos, e têm se tornado ainda mais devastador devido à introdução de uma nova espécie de inseto transmissor (*glassy-winged sharpshooter*), capaz de transmitir *X. fastidiosa* mais eficientemente do que os vetores nativos. *X. fastidiosa* é transmitida durante a ingestão da seiva por insetos transmissores, seguido pela multiplicação a partir do ponto de inoculação e subsequente colonização do xilema.

Os principais sintomas observados na PD são caracterizados pela queima de porções da lâmina foliar bem como pela colonização extensiva dos vasos do xilema pelo biofilme bacteriano, composto por células e pelo material secretado na matriz extracelular. Três hipóteses gerais têm sido propostas para explicar o desenvolvimento dos sintomas da PD em plantas infectadas por *X. fastidiosa*, sendo elas: i) proliferação bacteriana sistêmica e o bloqueio dos vasos do xilema por agregados de células, o que resultaria na redução do fluxo de água e no estresse hídrico; ii) reação sistêmica do hospedeiro em reposta à infecção bacteriana como, por exemplo, desequilíbrio nos reguladores de crescimento; e iii) fitotoxina(s) produzida(s) por *X. fastidiosa* que desempenharia(m) papel na virulência bacteriana e na patogênese da PD. Diversas evidências suportam a idéia de que os sintomas da PD sejam o resultado do comprometimento do fluxo de água pela oclusão dos vasos do xilema e o conseqüente estresse hídrico em

plantas altamente infectadas. Entretanto, tais evidências não suportam totalmente esta hipótese, que têm sido amplamente questionada por pesquisadores especialistas na doença.

Neste estudo, apresentamos evidências que suportam a terceira hipótese acima mencionada. Neste sentido, defendemos a ideia de que uma fitotoxina secretada por *X. fastidiosa* seja um fator essencial à virulência bacteriana e à patogênese da PD. O primeiro indicativo de que *X. fastidiosa* secrete tal fator foi obtido pela análise do repertório de proteínas secretadas durante o crescimento bacteriano em cultura. Essa análise proteômica, também conhecida por secretoma, levou à identificação de uma proteína hipotética, codificada pelo gene PD1703, como sendo a proteína mais abundantemente secretada por *X. fastidiosa* Temecula 1 *in vitro*. Análises *in silico* revelaram que o gene PD1703 codifica uma lipase/esterase ortóloga à enzima LipA presente em diversas espécies do grupo das *Xanthomonas*. Em *Xanthomonas oryzae* pv. oryzae (*Xoo*), LipA foi caracterizada como uma proteína degradante da parede celular e como fator de virulência importante na patogênese bacteriana. No curso deste estudo, reunimos uma série de evidências de que a proteína LipA esteja diretamente envolvida na patogênese da PD. Tais evidências nos levou à proposição de um novo modelo para a doença, no qual a fitotoxina LipA está diretamente ligada aos sintomas comumente observados, diferentemente da hipótese amplamente difundida de que os mesmos sejam causados pelo estresse hídrico resultante do bloqueio dos vasos do xilema por agregados bacterianos.

CAPÍTULO I

FUNDAMENTAÇÃO TEÓRICA

1. O fitopatógeno *Xylella fastidiosa*

1.1. Características Gerais

Xylella fastidiosa é uma gama-proteobactéria da ordem Xanthomonadales e o agente causador de diversas doenças em plantas, com um amplo espectro de hospedeiros de grande importância econômica (2). *X. fastidiosa* é uma bactéria Gram-negativa, de crescimento lento, estritamente aeróbica, não possui flagelo e apresenta formato de bastonete, medido de 0,25-0,5 μm de diâmetro e 1-4 μm de comprimento (Figura 1) (3, 4).

X. fastidiosa é transmitida por insetos que se alimentam da seiva bruta pertencentes às famílias Cicadellidae (*sharpshooters*) e Cercopidae (*spittlebugs*), popularmente conhecidos como cigarrinhas (Figura 2), como também por enxertia (5-7). *X. fastidiosa* possui uma característica única em relação aos demais fitopatógenos transmitidos por vetores, que é a transmissão persistente sem a necessidade de um período de latência, além de não acumular-se na hemolinfa do inseto transmissor. A transmissão *de X. fastidiosa* é o resultado de três eventos: a aquisição da bactéria pelo vetor em uma planta infectada, a ligação bacteriana à porção anterior do tubo digestivo do inseto e o desligamento e inoculação das mesmas em outra planta hospedeira. O sucesso da transmissão depende de múltiplos ciclos de multiplicação bacteriana após a inoculação. As cigarrinhas permanecem infectivas por longos períodos, sendo necessárias poucas bactérias presentes na porção anterior do intestino do vetor para que a transmissão ocorra. A bactéria multiplica-se e se adere ao canal alimentar (precibário), à câmara de bombeamento (cibário), à entrada do esôfago e às regiões da parte anterior do intestino do inseto, formando um biofilme no tubo intestinal pela ligação polar à cutícula. Este padrão de ligação permite a formação de uma camada única em contato direto com o fluido xilemático, o que aparentemente potencializa a quantidade de nutrientes circulantes dentro do biofilme bacteriano (5, 7-10).

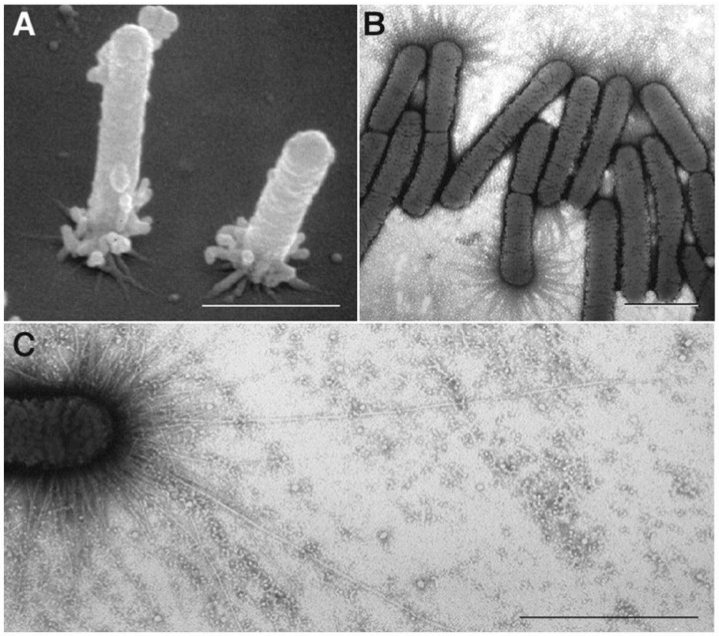

Figura 1: *Xylella fastidiosa*. Micrografia eletrônica de varredura (A) e de transmissão (B e C) mostrando células bacterianas aderidas ao substrato (A). Destaque aos pílus curtos (B) e longos (C) em uma das extremidades do bastonete. Barras: 1 μm. Fonte: Modificado de Meng, Y. *et al.,* 2005 (11).

Diferentemente de outras bactérias patogênicas, que podem espalhar pelos tecidos vegetais utilizando-se dos vasos do xilema, *X. fastidiosa* é exclusivamente limitada ao mesmo, sobrevivendo em suas células ou em elementos traqueais (12). O desenvolvimento das doenças causadas por *X. fastidiosa* dependem da habilidade deste patógeno em multiplicar-se a partir do ponto de inoculação e espalhar-se sistemicamente na planta infectada. A capacidade do patógeno em espalhar-se pelos vasos em espécies suscetíveis é, presumivelmente, essencial para que a doença se desenvolva. Espécies vegetais resistentes à *X. fastidiosa* são capazes de restringir a população bacteriana ao ponto de inoculação, onde a bactéria sobrevive endofiticamente sem desencadear nenhuma doença (12, 13).

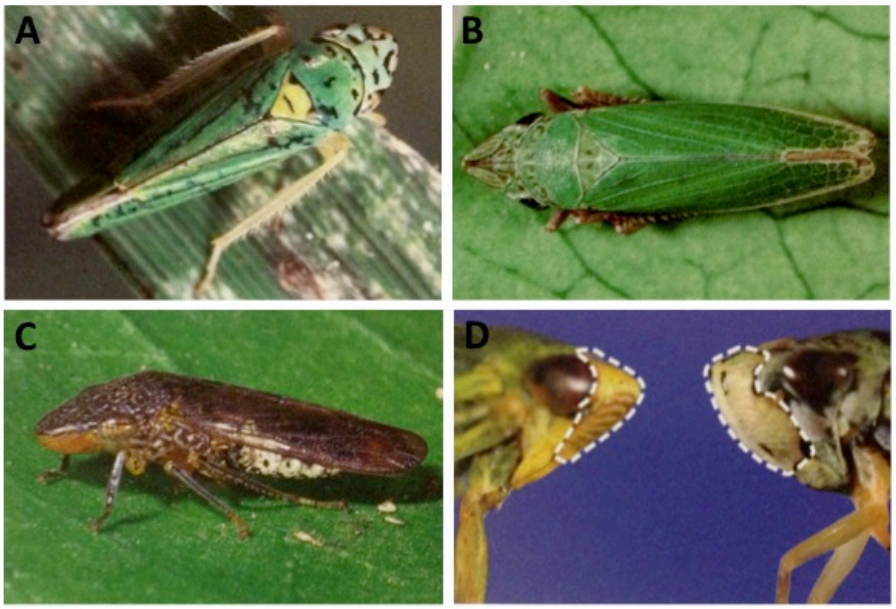

Figura 2: Insetos transmissores da bactéria *X. fastidiosa*. (**A**) *Graphocephala atropunctata* (*blue-green sharpshooter*). (**B**) *Draeculacephala minerva* (*green sharpshooter*). (**C**) *Homalodisca coagulata* (*glassy-winged sharpshooter*). (**D**) As cigarrinhas do tipo *sharpshooter* podem ser distinguidas de outros insetos semelhantes (que também se alimentam da seiva bruta) pelo formato da extremidade da cabeça (destacada pela linha pontilhada). Visão lateral de um inseto que se alimenta da seiva de gramíneas (*Thamnotettix zeleri*; esquerda) e *Graphocephala atropunctata* (direita). Fonte: modificado de Varela, L. G. *et al*., 2001 (14).

As doenças mais importantes causadas por *X. fastidiosa* são a Doença de Pierce (PD, do inglês *Pierce's Disease*) da videira (*Vittis* spp.) e a Clorose Variegada dos Citros (CVC), entretanto, este patógeno possui uma ampla gama de hospedeiros, incluindo membros de pelo menos 28 famílias de plantas mono e dicotiledôneas, como a amendoeira, cafeeiro, pessegueiro, entre muitas outras (12, 13, 15-20).

X. fastidiosa é geneticamente diversa, sendo dividida em quatro subespécies: subespécie *pauca*, causadora da CVC e CLS (*Coffee Leaf Scorch*) na América do Sul; subespécie *sandyi*, agente etiológico da OLS (*Oleander Leaf Scorch*) na América do Norte; subespécie *multiplex*, causadora de várias doenças

em frutíferas comerciais, tais como amendoeira, pessegueiro, entre outras; e subespécie *fastidiosa*, agente causador da PD em videira (21, 22).

A Doença de Pierce foi descrita após a infecção, na década de 1880, de 14.000 hectares de videira na região do Condado de Orange (CA), nos Estados Unidos. O declínio da indústria da uva na década de 1890 na Flórida, nos Estados Unidos, também foi associado à mesma doença. A PD foi então descrita em 1982 pelo fitopatologista Newton Pierce, recebendo o seu nome posteriormente (22).

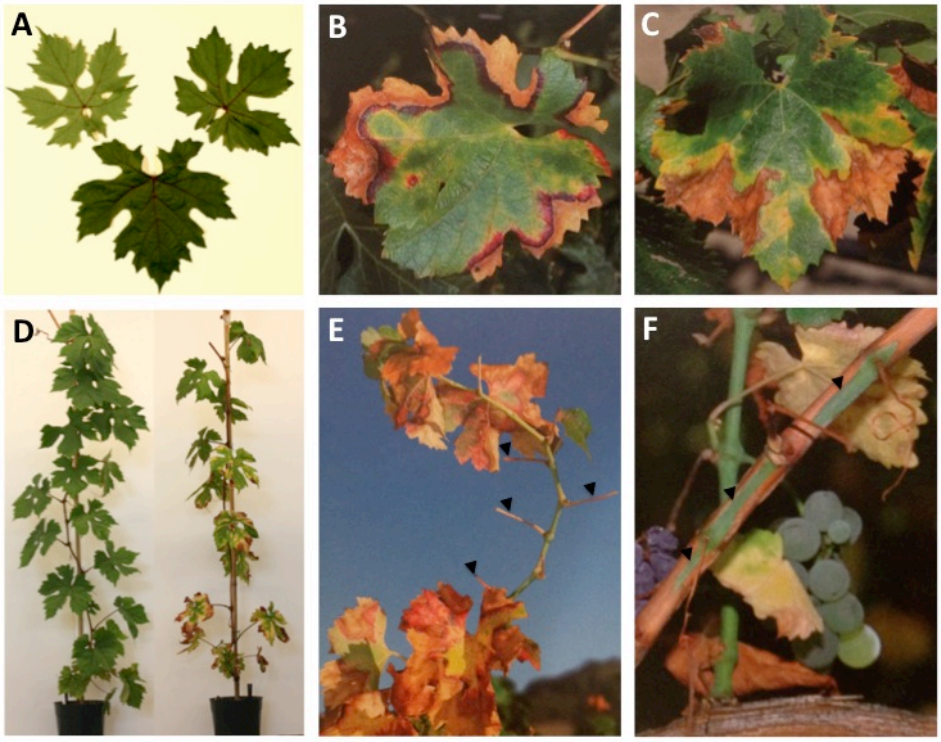

Figura 3: Sintomas da Doença de Pierce em *Vitis vinifera* L. (**A**) Folhas saudáveis de videira não infectadas por *X. fastidiosa*. (**B-C**) Folhas sintomáticas mostrando o desenvolvimento progressivo do descoloramento e queima marginal (*leaf scorch*). (**D**) Planta não infectada (esquerda) e infectada (direita) por *X. fastidiosa* Temecula 1, mostrando a progressão dos sintomas da porção inferior, onde a bactéria foi inoculada, para a parte superior da planta. (**E**) Sintoma característico da Doença de Pierce (*matchstick*) no qual os pecíolos (setas pretas) permanecem ligados ao caule mesmo após o desprendimento da lâmina foliar. (**F**) Lignificação irregular do caule, produzindo ilhas de tecido imaturo (setas pretas) circundadas por tecido maduro lignificado (marrom). Fonte: as imagens em B, C, E e F foram modificadas de Varela, L. G. *et al*., 2001 (14).

Na década de 1940, os insetos transmissores da doença (*sharpshooters* e *spittlebugs*) foram identificados (23). Entretanto, até o início da década de 1970, o agente causador da PD, bem como da doença em pessegueiros (*Phony Peach Disease*), foi erroneamente assumido como sendo de origem viral (24). Em 1978, Davis, M. J. e colaboradores descreveram a bactéria *X. fastidiosa* como sendo o agente etiológico da PD (4). Wells, J. M. e colaboradores (1987) sugeriram, após análises ultra-estruturais, que tal bactéria seria similar às bactérias pertencentes às famílias Rickettsiaceae e Legionellaceae (25). Posteriormente, Hopkins, D. L. (1989) descreveu o mesmo patógeno como "bactéria limitada ao xilema" (XLB). Análises comparativas do rRNA 16S revelou a proximidade filogenética de *X. fastidiosa* com o grupo das bactérias Xanthomonadaceas, excluindo qualquer relação da mesma com a família Rickettsiaceae (13).

A PD é capaz de destruir plantações inteiras de uva e têm causado grandes perdas econômicas no Sudoeste dos Estados Unidos, especialmente no estado da Califórnia. A recente invasão, na região Sul deste estado, de uma nova espécie de inseto transmissor (*glassy-winged sharpshooter* - *Homalodisca vitripennis*), que possui maior capacidade de dispersão que as espécies nativas, resultou em um aumento rápido da ocorrência da PD e têm afetado severamente a cultura da videira na região (7).

A PD é tipicamente caracterizada pela queima de porções da lâmina foliar bem como a colonização extensiva dos vasos do xilema (Figura 3). Tais características aparecem algumas semanas após a infecção por *X. fastidiosa* e são mais proeminentes no final do verão, quando a máxima demanda por água não é suprida pelos vasos parcialmente ocluídos pela bactéria (26). Os vasos do xilema são interconectados por canais que permitem a passagem da seiva bruta mas bloqueia a passagem de objetos maiores em função da presença das membranas de pontoação (*pit membranes*) (27). O movimento das células bacterianas no xilema, crucial para a colonização sistêmica da planta, parece ser dependente da capacidade da bactéria em degradar os polissacarídeos componentes dessas membranas (28), entretanto, o movimento passivo de poucas células bacterianas pelo xilema foi demonstrado (29).

Três possíveis hipóteses têm sido propostas para explicar o desenvolvimento e a progressão dos sintomas na PD: i) proliferação sistêmica da bactéria e o bloqueio dos vasos do xilema por agregados de células bacterianas e pelo material secretado pelas mesmas, bem como por tiloses, o que levaria à redução do fluxo de água e ao estresse hídrico (26, 30-36); ii) reação sistêmica do hospedeiro em reposta à infecção bacteriana como, por exemplo, desequilíbrio nos reguladores de crescimento; e iii) fitotoxina(s) produzida(s) por *X. fastidiosa* (2). A hipótese da oclusão baseia-se na observação do bloqueio de vasos do xilema em plantas infectadas por *X. fastidiosa* (13). Geralmente, espécies de plantas que apresentam os sintomas mais severos da PD são aquelas que possuem a maior proporção de vasos colonizados pela bactéria, suportando a hipótese da oclusão (12, 37, 38). O reduzido potencial hídrico, bem como a diminuição da condutância hidráulica e a alta resistência estomática foram correlacionados com os sintomas da PD (30). Entretanto, a avaliação se a deficiência hídrica resultaria no desenvolvimento dos sintomas da PD levou à conclusão de que outros fatores, além do estresse hídrico, estão envolvidos no desenvolvimento da PD, uma vez que o déficit de água não produziu os mesmos sintomas observados na doença (39). Embora a hipótese da oclusão seja amplamente considerada, os sintomas causados pelo estresse hídrico e a PD não são similares e parecem ser aditivos em efeito (32). Além disso, o acúmulo de *X. fastidiosa* em folhas de videiras infectadas não possui correlação direta com os sintomas, favorecendo a hipótese da resposta sistêmica (40). A ausência de correlação entre os sintomas da PD e concentrações de *X. fastidiosa*, bem como o baixo índice de oclusão de vasos em plantas infectadas (2-4%) (41) sugerem que a hipótese de estresse hídrico como principal causa dos sintomas observados na PD deva ser reexaminada (2, 39, 42).

1.2. Os Genomas

O genoma completo da linhagem 9a5c de *X. fastidiosa* (Xf-CVC), causadora da CVC e originalmente isolada no Estado de São Paulo, no Brasil, foi o primeiro fitopatógeno a ter o seu genoma seqüenciado e anotado (43). Em seguida, o genoma das linhagens Ann-1 e Dixon, isoladas da planta ornamental oleandro (*Nerium oleander*) e da amendoeira, respectivamente, foi parcialmente seqüenciado e anotado (44). As sequências completas dos genomas de outras duas linhagens de *X. fastidiosa*, M12 e M23, ambas isoladas de amendoeiras no estado da Califórnia, nos Estados Unidos, foram publicadas em 2010. A linhagem M12 de *X. fastidiosa* tem um cromossomo principal composto por 2.475.130 pares de base (pb) e nenhum plasmídeo. Um total de 2.368 ORFs (do inglês *Open Reading Frames*) foi predito no cromossomo principal. A linhagem M23 tem um cromossomo principal com 2.535.690 pb e um plasmídeo de 38.297 pb. Um total de 2.280 ORFs foi predito no cromossomo principal (45).

O genoma de Xf-CVC é composto por um cromossomo circular de 2,679305 pb (52,7% rico em GC) e por dois plasmídeos, sendo um megaplasmídeo de 51,158 pb (pXF51) e um miniplasmídeo de 1285 pb (pXF1.3). Das 2904 ORFs preditas, 47% possui alta homologia com proteínas conhecidas, o que permitiu a anotação de funções hipotéticas de grande parte do genoma (43, 46). Dentre as diferentes categorias funcionais anotadas, 147 proteínas foram associadas à patogenicidade, virulência e adaptação. Interessantemente, os genes *avr* (genes de avirulência, cujos produtos interagem com proteínas de resistência do hospedeiro), responsáveis pela especificidade planta-patógeno e geralmente encontrados em bactérias fitopatogênicas, não foram encontrados no genoma de *X. fastidiosa* (43).

O senquenciamento completo do genoma de *X. fastidiosa* Temecula 1 (Xf-PD), linhagem causadora da Doença de Pierce e originalmente isolada no condado de Temecula, na Califórnia (EUA), foi concluído em 2003 (47). Ao contrário do que ocorre na linhagem Xf-CVC, Xf-PD carrega apenas um miniplasmídeo (pXFPD1.3) de 1.345 pb. Das 2.066 ORFs identificadas em Xf-PD, 2.025 (98%) também estão presentes em Xf-CVC, sendo que 94,5% das ORFs compartilhadas entre essas linhagens apresentam ao menos 80% de identidade

entre seus resíduos de aminoácidos, com uma média geral de 95,7% de identidade. Apenas 41 ORFs (1,9%) são específicas a Xf-PD, enquanto 152 ORFs (6,8%) são exclusivas a Xf-CVC. A maior discrepância observada entre os genomas de Xf-CVC e Xf-PD é a diferença de tamanho em 159.503 pb e a ausência do megaplasmídeo pXF51 em Xf-PD (47).

Os genes envolvidos no metabolismo e nas funções básicas da célula estão entre os genes mais conservados em Xf-CVC e Xf-PD. Dentre os genes que apresentam maior divergência, alguns estão possivelmente envolvidos na interação planta-patógeno, como os genes codificantes para as fimbrias e hemaglutininas (envolvidos na agregação celular), colicinas, hemolisinas, bacteriocinas, proteínas de resistência a drogas e enzimas de restrição e modificação do DNA. Alguns genes presentes nas linhagens Xf-CVC e Xf-PD possuem alterações na leitura (*frameshift*) ou apresentam códons de parada e podem ser, portanto, não funcionais. Um exemplo deles é o gene precursor da poligalacturonase, que possui um códon de parada *in-frame* em Xf-CVC mas está intacto em Xf-PD. Esse gene é essencial para a expressão de enzimas de degradação da parede celular e na migração do patógeno nos vasos do xilema e não é, aparentemente, essencial para a patogenicidade da linhagem 9a5c em citros. A ausência de uma cópia funcional do gene *pglA* em Xf-CVC poderia explicar o longo período de incubação observado deste patógeno em citros, bem como sua menor virulência em comparação à Xf-PD (47, 48).

Recentemente, foram publicadas as sequências do genoma da linhagem EB92-1, isolada em 1992 por D. L. Hopkins do sabugueiro do Canadá (*elderberry*) (49). Esta linhagem infecta e coloniza videiras, sobrevivendo por muitos anos na planta hospedeira, entretanto, não causa sintomas e é capaz de promover um efetivo biocontrole contra a PD. O genoma incompleto desta linhagem é composto por 2.478.730 pb e por um plasmídeo de 1.346 pb e é bastante similar ao genoma da linhagem Temecula 1, entretanto, 10 genes potencialmente envolvidos na virulência bacteriana estão ausentes. A incapacidade desta linhagem em causar sintomas foi associada à ausência destes potenciais efetores de patogenicidade. Dentre os genes ausentes, dois codificam para enzimas secretadas pelo sistema de secreção do tipo II, sendo elas a serina-protease PD0956 e a lipase/esterase

LipA (PD1703), além de dois genes que codificam as toxinas Zot (PD0928 e PD0915), que são importantes fatores de virulência secretados por *Vibrio cholerae,* e seis genes de hemaglutininas (PD0986, PD1792, PD2108, PD2110, PD2116 e PD2118) (50).

1.3. Os proteomas

Embora as análises genômicas tenham produzido uma grande quantidade de informações sobre as diferentes linhagens de *X. fastidiosa*, os proteomas deste patógeno foram, até o presente momento, pouco caracterizados.

Recentemente, Silva, M. S. *et al.* (51) caracterizaram o proteoma da linhagem 9a5c de *X. fastidiosa* em estágio de biofilme maduro, no qual *X. fastidiosa* apresenta maior virulência e alta resistência a substância tóxicas como antibióticos e detergentes. A análise comparativa demonstrou diferenças fenotípicas entre células do biofilme em comparação às células planctônicas, especialmente no padrão da expressão de proteínas envolvidas no metabolismo, mobilidade, adesão e resposta ao estresse. Proteínas envolvidas na formação da fímbria (XF0615 e PilT), na adesão celular (XF0389), no metabolismo de carbono e aminoácidos e biossíntese de cofatores, na percepção de quorum (*quorum-sensing*), tais como as proteínas XF1605, XF1186 e peptidilprolil *cis-trans* isomerases, bem como a proteína de membrana externa MopB (XF0343), foram identificadas como estando superexpressas no estágio de biofilme maduro. Semelhantemente, proteínas envolvidas na produção de toxinas (XF1137), fatores de virulência (XF0389), bem como proteínas envolvidas na adaptação e repostas ao estresse (XF0615 e XF1213) foram reguladas da mesma maneira. Interessantemente, as proteínas expressas no estágio de biofilme em *X. fastidiosa* não diferiram das proteínas expressas por *P. aeruginosa* e *E. coli,* corroborando a idéia de que proteínas associadas à adaptação e competição são fatores importantes na manutenção do biofilme (51).

Dentre os diversos subproteomas de um microorganismo bacteriano, o secretoma pode ser definido como sendo o conjunto de proteínas secretadas pela célula (52). Tais proteínas são usualmente conhecidas como proteínas

excretórias/secretórias (ES) e são, em muitos casos, relevantes fatores de virulência no processo patogênico (53). Em função do papel crucial desempenhado pelas proteínas extracelulares na interação planta-patógeno, faz-se necessário o conhecimento deste subproteoma em *X. fastidiosa*. A caracterização das proteínas extracelulares e associadas à superfície de *X. fastidiosa* foi primeiramente descrita na linhagem 9a5c, causadora da CVC (54). No presente trabalho, encontra-se a primeira caracterização do secretoma, bem como dos proteomas da superfície (*surfaceome*) e da membrana externa de *X. fastidiosa* Temecula 1, causadora da PD.

1.3.1. Os Sistemas de Secreção e o Secretoma

Proteínas secretadas por bactérias desempenham diversas funções importantes, tais como a disponibilização de nutrientes, comunicação célula-célula, desintoxicação do ambiente e eliminação de potenciais competidores. Mais especificamente, proteínas extracelulares de bactérias patogênicas são, muitas vezes, fatores cruciais responsáveis pela virulência bacteriana. A intimidade da associação entre fitopatógenos bacterianos e o hospedeiro vegetal acontece na interação de bactérias que se multiplicam nos tecidos vegetais como, por exemplo, nos vasos do xilema e floema, ou mesmo dentro de células vivas do hospedeiro. A comunicação por meio da secreção de proteínas e metabólitos, que são absorvidos pelo hospedeiro ou detectados na superfície celular, desempenha papel importante na determinação do resultado do processo interativo (55, 56).

Células bacterianas, como todos os outros tipos celulares, interagem com o seu ambiente externo. Essa interação, muitas vezes, é realizada por meio de moléculas secretadas por diferentes mecanismos. A secreção desses fatores permite que tais organismos possam influenciar o ambiente externo, muitas vezes inacessível devido à impossibilidade de locomoção ou restrições de crescimento impostas pelo ambiente. Bactérias Gram-negativas possuem uma membrana externa que dificulta a internalização e secreção de solutos e polipeptídeos. Para superar essa barreira, tais bactérias desenvolveram diversas estratégias, algumas específicas às espécies patogênicas, que permitem o acesso de fatores de

virulência ao ambiente extracelular. A maioria da bioquímica celular é catalisada por proteínas citoplasmáticas separadas do meio externo por membranas semi-permeáveis. Entretanto, muitos polipeptídeos residem e funcionam em espaços extra-citoplasmáticos e sub-compartimentos organelares. Algumas dessas proteínas são canais e bombas que podem ocupar 20 ± 40% da capacidade codificante de um genoma. As demais proteínas, que compõem o secretoma, são enzimas hidrolíticas, adesinas e toxinas e residem no periplasma bacteriano ou são secretadas para o espaço extracelular. Tais proteínas podem representar 10 ± 20% do proteoma de um organismo (57, 58).

Embora a disponibilidade de sequências completas de diversos genomas bacterianos tenha permitido a predição *in silico* da localização sub-celular de diversos proteomas bacterianos, a verificação experimental de tais predições têm produzido diversos resultados inesperados. A localização extracelular inesperada de tais proteínas poderiam ser o resultado da atividade de sistemas de secreção bacterianos ainda desconhecidos, ou mesmo o produto da lise de parte da população celular, que resultaria na liberação das proteínas citoplasmáticas mais abundantes (59).

As bactérias secretam proteínas por meio de diversos sistemas especializados de secreção. Embora os componentes de tais sistemas estejam presentes em diversos microorganismos, os mesmos são melhor compreendidos em bactérias Gram-negativas (60, 61). A maioria das proteínas extracelulares bacterianas são secretadas pelo sistema de secreção Sec (*general secretory Sec pathway*), embora existam outros sistemas especializados em secreção (62-64). Para ser reconhecida pelo sistema de secreção Sec, uma proteína é marcada na porção N-terminal por uma sequência conhecida por peptídeo sinal ou sinal de retenção. Imediatamente após esta sequência, encontra-se um sítio de clivagem reconhecido por uma enzima peptidase, que clivará o peptídeo sinal e encaminhará a proteína ao complexo Sec localizado na membrana citoplasmática (65).

Outras classes de proteínas que ainda não tiveram seus mecanismos de secreção elucidados são as chamadas proteínas *Sec-attached*, que são aparentemente retidas na membrana citoplasmática mesmo na ausência de sinais

de retenção conhecidos, bem como as proteínas de superfície sem ancoragem (*anchorless surface proteins*), que são proteínas que desempenham papéis de manutenção celular no citoplasma mas que são exportadas para a superfície celular por mecanismos ainda desconhecidos. Tais proteínas não possuem peptídeo sinal, domínios hidrofóbicos de ancoragem à membrana ou motivos conhecidos de transporte à parede celular. Interessantemente, tais proteínas têm sido funcionalmente caracterizadas como facilitadoras do processo de colonização, persistência e invasão de tecidos hospedeiros por bactérias patogênicas (66, 67).

Dentre os sistema de secreção bacterianos mais estudados, encontram-se os sistema dos tipos I a VI. Os sistemas de secreção dos tipos II e V funcionam por um mecanismo composto por dois passos, no qual proteínas são primeiramente transportadas ao espaço periplasmático através da membrana interna (IM, do inglês *inner membrane*) e então enviadas ao espaço extracelular pela membrana externa (OM, do inglês *outer membrane*) (68, 69). Na secreção por meio dos sistemas do tipo I (composto pelos transportadores do tipo ABC), e tipos III e IV, o material é transportado diretamente ao espaço externo ou inserido na célula hospedeira. O sistema de secreção do tipo III é especificamente utilizado na secreção de fatores de virulência por bactérias patogênicas e é utilizado na supressão da resposta imune do hospedeiro, que é iniciada pela planta em resposta à detecção dos padrões moleculares associados a patógenos (PAMP, do inglês *Pathogen-Associated Molecular Patterns*), também conhecidos como padrões moleculares associados a micróbios (MAMP, do inglês *Microbe-Associated Molecular Patterns*) (70, 71). O sistema de secreção do tipo IV é primariamente envolvido na mobilização de DNA entre bactérias ou entre células bacterianas e vegetais, embora uma toxina de *B. pertussis* e o antígeno CagA de *Helicobacter pylori* sejam transportados por este sistema (72, 73).

A análise genômica de diversas cepas de *X. fastidiosa* revelaram a ausência de genes codificadores para a maquinaria necessária à secreção pelo sistema do tipo III, bem como a ausência de moléculas efetoras do mesmo tipo, o que poderia refletir o estilo de vida deste patógeno, que coloniza células mortas lignificadas do xilema (43, 44, 47, 74). *X. fastidiosa* possui diversos genes

similares aos genes codificadores de hemolisinas e componentes do sistema de secreção do tipo I, que é composto neste patógeno por pelo menos 23 sistemas contendo 46 proteínas pertencentes à superfamília ABC (do inglês *ATP Binding Cassette*) (75). De modo geral, o sistema de secreção do tipo I está envolvido na resistência a drogas e secreção de hemolisinas e consiste de duas proteínas pareadas que estão localizadas na membrana interna, além de um terceiro componente que é, geralmente, a proteína TolC, que conecta as membranas interna (IM) e externa (OM) (76). *X. fastidiosa* possui apenas um homólogo da proteína TolC, que demonstrou-se essencial à patogenicidade da bactéria no processo infectivo em videira bem como à sobrevivência do patógeno no xilema (77).

Diversas evidências suportam a importância do sistema de secreção do tipo II na patogênese bacteriana. Os genes codificadores dos componentes deste sistema estão presentes em diversos organismos patogênicos de hospedeiros animais e vegetais. A natureza hidrolítica das enzimas secretadas por esse sistema sugere que o mesmo promova a degradação das células e tecidos hospedeiros (78-86). Em alguns casos, exoenzimas secretadas pelo sistema de secreção do tipo II contribuem diretamente para a virulência bacteriana, tais como em *E. coli*, *V. Cholerae*, *P. aeruginosa*, entre outras (79). Mutações em genes específicos deste sistema levaram à atenuação da virulência bacteriana em diferentes modelos animais e vegetais (85, 87, 88).

O sistema de secreção do tipo II é essencial à virulência de diversas bactérias fitopatogênicas, incluindo os patógenos do gênero *Xanthomonas*. O sistema de secreção do tipo II em *Xanthomonas* é amplamente envolvido na secreção de enzimas extracelulares necessárias à hidrólise de componentes da parede celular vegetal (89). A grande similaridade do sistema de secreção do tipo II em *Xanthomonas* e *X. fastidiosa* sugere que esse sistema possa desempenhar também um papel importante na virulência de *X. fastidiosa*. A análise comparativa dos genomas de *X. fastidiosa* e de diferentes patovares de *Xanthomonas* revelou que *X. fastidiosa* possui todos os genes necessários à montagem e funcionamento do sistema de secreção do tipo II (43, 89).

Dentre as diversas classes de proteínas secretadas pelo sistema de secreção do tipo II e abundantemente encontradas nos secretomas de microorganismos fitopatogênicas, destacam-se as enzimas degradantes da parede celular vegetal (CWDEs, do inglês *Cell Wall Degrading Enzymes*). As CWDEs são utilizadas na digestão dos componentes da parede celular e têm sido descritas como importantes fatores de virulência em diversas bactérias e fungos fitopatogênicos, incluindo *X. fastidiosa* (28, 90-104).

A parede celular vegetal é composta por celulose, hemicelulose e pectina - e no caso de plantas lenhosas, lignina - e oferece uma barreira à entrada de fitopatógenos. Com o intuito de ultrapassar essa barreira, bactérias secretam CWDEs, dentre as quais encontram-se as celulases, xilanases, pectinases, proteases e lipases, que são abundantemente secretadas por bactérias fitopatogênicas. O genoma de *X. fastidiosa* contêm diversos genes similares a genes codificadores de CWDEs, incluindo lipases/esterases, proteases, xilanases, celulases, as enzimas poligalacturonase (PG) e endo-1,4-β-glucanase (EGase), além de genes similares ao sistema *Xps* (do inglês *Xanthomonas protein secretion*), envolvidos na secreção de CWDEs pelo sistema do tipo II em *Xanthomonas* (43, 54, 89-91, 105). Interessantemente, PG e EGase possuem, em conjunto, a capacidade de degradar a membrana de pontoação das células do xilema, permitindo o movimento da bactéria entre os vasos do xilema da videira, uma vez que os poros das membranas de pontoação são muito pequenos para permitirem a passagem passiva das células bacterianas (28). Por esse motivo, têm sido proposto que *X. fastidiosa* secrete CWDEs para digerir os polissacarídeos das membranas de pontoação e espalhar-se sistemicamente, assim como é feito por outros fungos e bactérias patogênicas (33, 106, 107). Análises microscópicas suportaram essa hipótese mostrando a passagem de *X. fastidiosa* pela membrana de pontoação em videira infectadas (108). *X. fastidiosa* com o gene pglA (codificante da poligalacturonase) mutado possui crescimento limitado quando inoculada em videira, indicando que a degradação da pectina (principal componente das membranas de pontoação) pela PG não é apenas importante para o movimento das células no xilema, mas é também um mecanismo utilizado na liberação de polissacarídeos da parede celular que

possam ser utilizados como fonte de carbono e que suplementariam a baixa quantidade de nutrientes disponíveis no xilema (48).

Smolka, M. B. e colaboradores (2003) foram os primeiros a caracterizar as proteínas extracelulares da linhagem 9a5c de *X. fastidiosa* com o intuito de descrever as proteínas secretadas, dentre as quais incluem-se potenciais CWDEs, bem com as proteínas de adesão possivelmente envolvidas na virulência bacteriana (54). Diversas proteínas envolvidas na formação do pílus tipo IV (PilY1: XF0032 e XF1224), na adesão (Hsf: XF1981) e mobilidade (*twitching motility*) celular (PilT: XF1633), foram identificadas. Interessantemente, a proteína OprF (XF0343) foi identificada como a proteína de membrana externa mais abundante, em contraste com a descrição da proteína MopB como sendo a proteína de membrana externa mais abundante em *X. fastidiosa* Temecula 1 (54, 109). Dentre as proteínas localizadas na fração extracelular, as proteínas envolvidas na adesão, proteólise, defesa, toxicidade e metabolismo do ferro representaram as classes funcionais mais abundantes. A secreção de proteases (XF0816, XF1026 e XF1851) foi descrita como tendo um possível papel na aquisição de nutrientes bem como na degradação da membrana de pontoação, que permitiria a movimentação da bactéria pelos vasos do xilema. Duas proteínas do tipo hemolisina (XF2407 e XF0668/XF1011) que pertencem à família das toxinas RTX e que estão aparentemente envolvidas na virulência bacteriana, foram encontradas. Quatro enzimas com atividade antioxidante (XF2614, XF1530, XF2232 e XF1827) foram também localizadas na porção extracelular da cultura de *X. fastidiosa*. Considerando que tais enzimas sejam ativas fora da célula bacteriana, acredita-se que as mesmas estejam envolvidas na proteção contra radicais livres produzidos pela planta, um mecanismo conhecido de defesa vegetal contra microorganismos. Diversas outras proteínas com funções diversas, como lipase (XF1253), malato desidrogenase (XF1211), fosforilase polinucleotídica (XF0239) e anidrase carbônica (XF2095) foram também encontradas na porção extracelular (54).

Outro sistema de secreção amplamente utilizado por bactérias é o sistema do “tipo VI”, mediado pelas vesículas de membrana externa (OMVs, do inglês *Outer Membrane Vesicles*) (Figura 4). A secreção de fatores de virulência por

bactérias Gram-negativas é dificultado pelo envelope bacteriano, que é composto por duas membranas lipídicas, a membrana interna ou membrana citoplasmática e a membrana externa, separadas pelo espaço periplasmático e pela camada de peptidoglicanos (110). Na maioria das bactérias Gram-negativas, a porção externa da membrana externa é composta por lipopolisacarídeos (LPS) enquanto ambas as partes da membrana interna são compostas por fosfolipídeos. O espaço periplasmático, composto por um conteúdo protéico viscoso, possui aproximadamente 13 nm de largura e ocupa 7-40% do volume celular (111). Um dos mecanismos desenvolvidos pelas bactérias Gram-negativas para superar essa barreira foi o sistema de secreção no qual parte do conteúdo periplasmático contendo moléculas com atividade biológica é envolvida pela membrana externa bacteriana e então liberada por OMVs, que são esferas compostas pela membrana lipídica, um conteúdo luminal eletro-denso e possuem um diâmetro médio de 50-250 nm, dependendo da espécie bacteriana (112). Ao contrário de outros mecanismos de secreção, as OMVs permitem a secreção de moléculas insolúveis junto ou complexadas a moléculas solúveis. Proteínas solúveis são associadas às OMVs pelo conteúdo periplasmático ou externamente como material aderente. OMVs secretadas podem disseminar longe das células bacterianas e desempenhar funções importantes no ambiente bem como em outras células, inclusive na modulação da patogênese, na comunicação célula-célula, na aquisição de nutrientes e na transferência horizontal de genes (113-117).

As OMVs são secretadas por bactérias patogênicas e não patogênicas e já foram descritas em muitas espécies bacterianas, tais como *Escherichia coli* (118-121), *Shigella* spp. (122, 123), *Neisseria* spp. (124-126), *Pseudomonas aeruginosa* (127-129), *Helicobacter pylori* (130-133), *Salmonella* spp. (134-136), *Brucella melitensis* (137, 138), *Xanthomonas campestris* pv. campestris (139) e muitas outras (1, 140). Recentemente, a secreção mediada por OMVs foi descrita em *X. fastidiosa*. Neste estudo, descreveu-se a secreção do autotransportador XatA do tipo AT-1 (codificado pelo gene PD0528), que também está associado à membrana externa bacteriana e envolvido na adesão e migração celular, produção de biofilme e virulência (141).

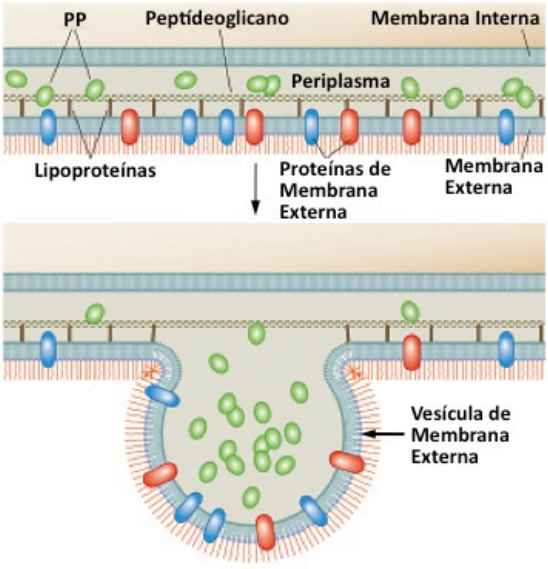

Figura 4: Modelo proposto para a formação das vesículas de membrana externa (OMVs). As OMVs são liberadas contendo proteínas periplasmáticas (PP), proteínas de membrana externa (OMPs) e lipídeos, incluindo padrões moleculares associados a patógenos (PAMPs) e outros fatores de virulência. Embora o mecanismo não seja completamente conhecido, acredita-se que a liberação das OMVs ocorra em locais onde a ligação lipoprotéica entre a membrana externa e a camada de peptídeoglicanos esteja ausente ou desfeita. Fonte: modificado de Ellis, T. N., *et al.* (2010) (1).

Dentre os sistemas de secreção presentes em *X. fastidiosa* e em outros fitopatógenos, o sistema do tipo II, responsável pela secreção de enzimas hidrolíticas, e o sistema do tipo VI, mediado pelas vesículas de membrana externa, parecem desempenhar importantes papéis na virulência bacteriana (2, 141). Dentre as enzimas amplamente secretadas por estes sistemas, encontram-se as lipases extracelulares. Tais enzimas catalisam reações de hidrólise e, em alguns casos, funcionam como CWDEs, desempenhando importante papel na patogênese de diversas doenças animais e vegetais (142).

1.3.1.1. Lipases Extracelulares

Lipases são triacilglicerol hydrolases (E.C. 3.1.1.3) que catalisam a hidrólise de triglicerídeos, produzindo ácidos graxos, diacilgliceróis, monoacilgliceróis e glicerol como produtos, além de catalisarem a hidrólise e transesterificação de ésteres e exibirem propriedades enantio-seletivas. Tais enzimas são únicas devido à sua natureza interfacial, catalisando a reação na interface água-lipídeo. As lipases fazem parte da superfamília das α/β hidrolases e geralmente possuem o motivo pentapeptídico Gly-X-Ser-X-Gly conservado e não exigem cofatores para que a catálise enzimática aconteça. As lipases agem

em ésteres de glicerol de cadeia longa insolúveis em água, enquanto as esterases agem em ésteres de glicerol de cadeia curta solúveis em água. Dois critérios têm sido utilizados para classificar enzimas lipolíticas como lipases “verdadeiras”: (a) a enzima deve apresentar ativação interfacial, ou seja, deve ser ativada pela presença de uma interface, tendo sua atividade aumentada rapidamente assim que o substrato (triacilglicerídio) formar uma emulsão; (b) a enzima deve conter um tampa cobrindo o sítio ativo, que é então movimentada em contato com a interface. Entretanto, tais critérios têm se mostrado ineficientes na classificação das lipases, uma vez que diversas enzimas contendo a tampa, mas que não apresentam a ativação interfacial, têm sido descritas. Por esse motivo, as lipases podem ser simplesmente definidas como carboxilesterases que catalisam a hidrólise e síntese de acilgliceróis de cadeia longa (143-149).

Quando as primeiras lipases bacterianas foram estruturalmente elucidadas, logo observou-se que tais enzimas apresentavam um padrão de enovelamento comum, mesmo na ausência de similaridade em suas sequências de aminoácidos. Comparações estruturais mais detalhadas de lipases com outras enzimas, tais como acetilcolinesterases e serina caboxipeptidases, confirmou a existência deste padrão, que foi então denominado α/β hidrolase, uma vez que tais enzimas catalisam reações de hidrólise (144, 146, 150-152).

O padrão canônico de enovelamento das α/β hidrolases é encontrado em muitas enzimas hidrolíticas com especificidades a diferentes substratos, incluindo as lipases e esterases, e constitui um dos padrões mais promíscuos conhecidos (145). Este padrão consiste em uma fita central contendo 8 folhas-β paralelas e uma fita antiparalela (Figura 5). As folhas paralelas β3 a β8 são conectadas por α-hélices. A curvatura das folhas-β bem como as posições espaciais de α-hélices topologicamente equivalentes podem variar consideravelmente entre as diversas enzimas. O sítio ativo das α/β hidrolases é composto por três resíduos catalíticos, sempre nesta ordem: um resíduo nucleofílico (serina, cisteína ou aspartato), um resíduo ácido catalítico (aspartato ou glutamato) e um resíduo de histidina. Essa ordem é diferente daquelas observadas em outras proteínas que também possuem tríades catalíticas (145, 146, 150-154).

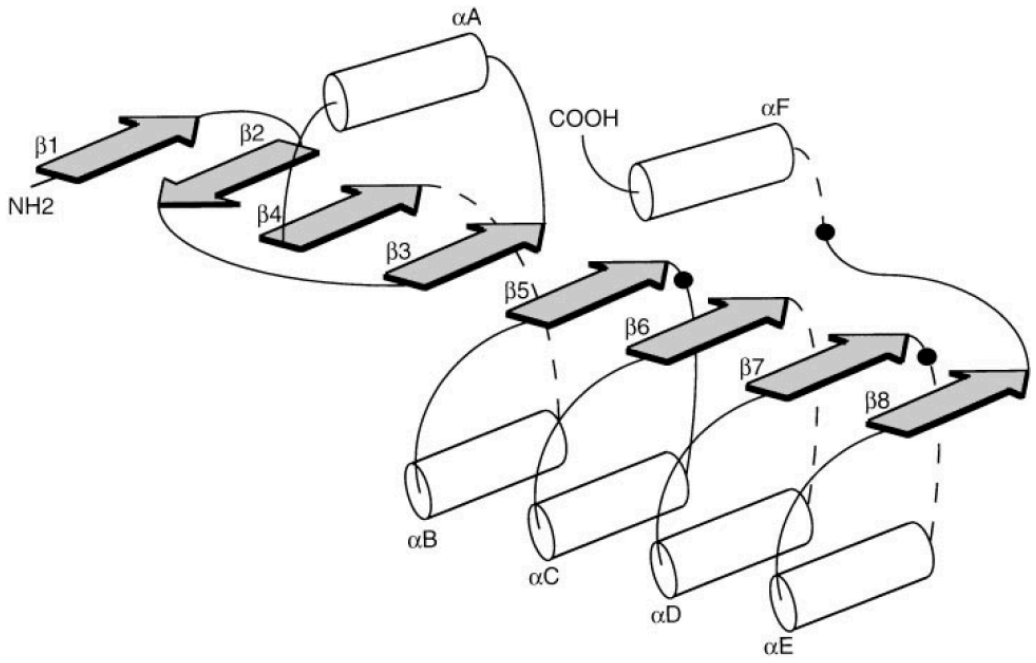

Figura 5: Estrutura comum das α/β hidrolases. Estruturas em α-hélices e folhas-β estão representadas por cilindros e setas (cinza), respectivamente. A posição topológica do sítio ativo (tríade catalítica) está indicada por círculos sólidos, sendo o resíduo nucleofílico localizado após a folha β5, e os resíduos Asp/Glu e His localizados após β7 e entre β8 e αF, respectivamente.

As lipases se tornaram um importante grupo de enzimas com importância industrial uma vez que catalisam uma ampla variedade de reações como hidrólise, esterificação, transesterificação e interesterificação, além de possuírem alta estabilidade em solventes orgânicos (147, 155). O alto nível de produção destes catalisadores biológicos requer o conhecimento dos mecanismos reguladores da expressão gênica, do enovelamento e da secreção protéica. Em bactérias, a transcrição de genes codificadores de lipases pode ser regulada pela comunicação célula-célula, sendo a secreção protéica realizada pelo caminho secretório dependente da proteína Sec ou pelos transportadores do tipo ABC. Diversos genes bacterianos codificadores de lipases têm sido clonados, mas os mecanismos moleculares responsáveis pela regulação da expressão de tais genes permanecem, na sua maioria, ainda desconhecidos (147-149, 156-158).

Dentre os possíveis papéis desempenhados pelas lipases microbianas extracelulares, incluem-se a digestão de lipídeos para a aquisição de nutrientes, adesão às células e tecidos hospedeiros, interações sinérgicas com outras enzimas, hidrólise não específica em função de atividade fosfolipolítica adicional, iniciação do processo inflamatório e defesa mediada pela lise da microflora no processo competitivo (159). Lipases extracelulares têm sido encontradas em diversos patógenos bacterianos, tais como *Staphylococcus aureus* (160), *Staphylococcus epidermidis* (161), *Propionibacterium acnes* (162) e *Pseudomonas aeruginosa* (163, 164), bem como em fungos patogênicos, tais como *Malassezia furfur* (165) e *Candida albicans* (159). Interessantemente, lipases têm sido descritas como fatores de virulência importantes na patogênese de diversas doenças humanas, animais e vegetais, tais como nas patologias causadas por *Candida parapsilosis* (166), *Staphylococcus aureus* (167), *Candida albicans* (168), *Fusarium graminearum* (169, 170) e na doença de Marek causada pelo vírus MDV (171). Recentemente, a lipase/esterase LipA foi descrita nas bactérias fitopatogênicas *Xanthomonas oryzae* pv. oryzae e *X. campestris* pv. vesicatoria e funcionalmente caracterizada como importante fator de virulência requerido para a patogênese em arroz e tomate, respectivamente (88, 142, 172, 173).

1.3.1.1.1. A Proteína LipA

LipA é uma enzima do tipo α/β hidrolase de 42 kDa que foi primeiramente identificada em *Xanthomonas oryzae* pv. oryzae (*Xoo*), um importante patógeno do arroz (172). LipA possui um domínio LIP, comumente encontrado em lipases secretadas, mas possui baixa homologia com lipases bacterianas comumente conhecidas. Proteínas ortólogas de LipA estão presentes em diversas bactérias Gram-negativas, incluindo todas as espécies de *Xanthomonas* com genoma seqüenciado (142).

Estudos funcionais em *Xoo* mostraram que LipA é secretada pelo sistema de secreção do tipo II e parece funcionar cooperativamente com xilanases na promoção da virulência deste patógeno (172). Mutantes de *Xoo* para o sistema de

secreção do tipo II, que é conhecido por secretar CWDEs, são severamente deficientes em virulência (174). *Xoo* mutantes para o gene *lipA*, bem como para o gene *clsA*, codificante de uma celulase, apresentaram reduzida virulência, entretanto, mutantes para ambos os genes (mutantes duplos) apresentaram uma redução substancial na patogenicidade quando comparados aos mutantes únicos, indicando a existência de uma redundância funcional em relação aos papéis desempenhados por essas enzimas na virulência de *Xoo* (88). Interessantemente, o tratamento de folhas e raízes de arroz com LipA induziram resposta imune vegetal, resultando na deposição de calose e em morte celular programada. Acredita-se que a resposta imune seja ativada por moléculas solúveis resultantes da degradação da parece celular, e não pelo reconhecimento direto da proteína por receptores celulares na planta, como acontece com outras CWDEs de fungos previamente descritas (88, 175).

A caracterização estrutural da proteína LipA de *Xoo* realizada por Aparna, G. *et al.* (2009) mostrou que LipA é uma α/β hidrolase com nove cadeias centrais em estrutura folhas-beta circundadas por alfa-hélices em uma topologia típica de α/β hidrolase, além de uma sequência N-terminal (144, 153). Os resíduos canônicos da tríade catalítica (Ser-176, His-377 e Asp-336) (Figura 6A) estão localizados em posições semelhantes às observadas em outras hidrolases. O aminoácido nucleofílico Ser-176 posiciona-se no motivo G-X-S-X-G, que é conservado em hidrolases (176).

Uma característica distinta da estrutura da LipA é a presença de um domínio de 108 aminoácidos presente como uma inserção entre as fitas β6 e β7 que corresponde topologicamente à posição de inserção da tampa em triacilglicerol lipases (Figura 6B). Esse domínio de inserção consiste em sete alfa-hélices e uma 3_{10}-hélice (142).

LipA possui baixa similaridade de sequência (≤20%) com outras hidrolases caracterizadas, entretanto, possui alta similaridade estrutural com a lipase CalA de *Candida antarctica* (177, 178). CalA também possui um domínio em tampa equivalente ao domínio observado em LipA. A superimposição dos mesmos

(Figura 7B) indicou uma similaridade conformacional considerável entre ambas regiões (142).

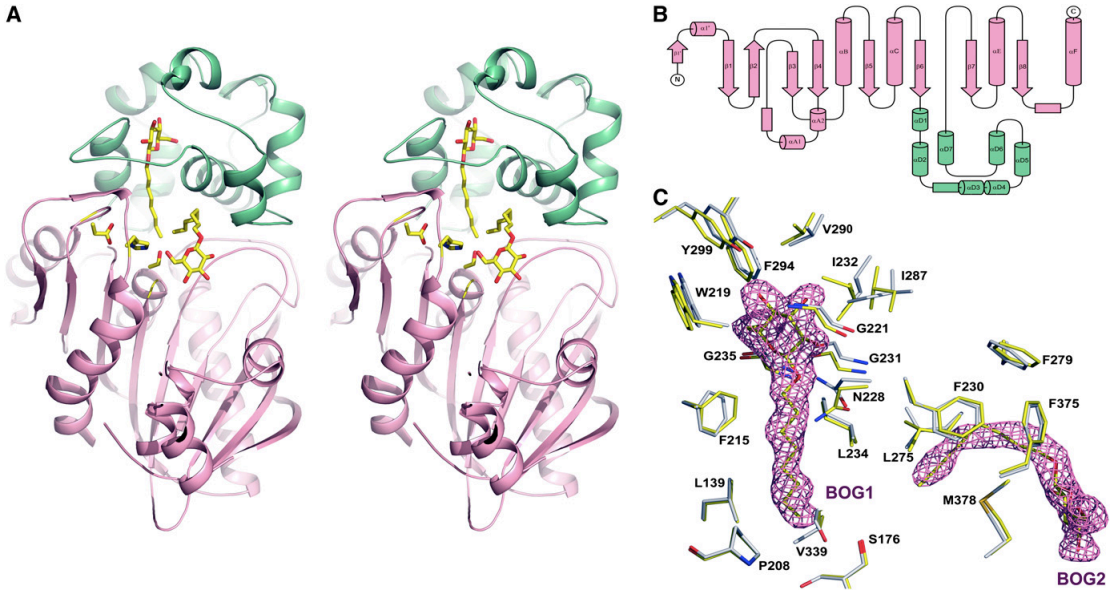

Figura 6: Estrutura tridimensional da proteína LipA de *Xoo*. (**A**) Estrutura da LipA mostrando a ligação de duas moléculas de β-octil glicosídeo (BOG) e a tríade catalítica. O domínio hidrolase está mostrado em rosa e o domínio ligante em verde. Os aminoácidos ligantes Ser-176, Asp-336 e His-377 estão representados em amarelo. (**B**) Diagrama topológico da proteína LipA. As sequências em estrutura folhas-beta estão representados por setas, enquanto as α-hélices e 3_{10}-hélices estão representados por cilindros e retângulos, respectivamente. O grupo de hélices αD compõe o domínio de ligação (verde). (**C**) Resíduos de aminoácidos mostrando o túnel de ligação ao BOG. Aminoácidos estão representados em amarelo. O sitio ativo Ser-176 está em destaque. Os resíduos da estrutura da proteína LipA sem a ligação do BOG está superimposta e mostrada em cinza. Fonte: modificado de Aparna, G. *et al.*, 2009 (142).

A análise do ligante de LipA indicou a co-cristalização da proteína com o detergente β-octil glicosídeo (BOG). A estrutura do co-cristal mostrou duas moléculas de BOG ligantes a LipA (Figura 7A). BOG1 mostrou-se mais rigidamente ligado, enquanto BOG2 liga-se mais frouxamente à proteína. Um mapa de densidade eletrônica ao redor dos ligantes está representado na Figura 7C. Análises por Calorimetria de Titulação Isotérmica confirmaram as predições estruturais de ligação da proteína LipA aos substratos (142).

Análises comparativas por alinhamento de sequências das proteínas LipA provenientes de diversas espécies de *Xanthomonas* e *X. fastidiosa* (linhagem 9a5c) indicaram o agrupamento dessas sequências com altos índices de confiabilidade. Apenas um pequeno sub-grupo dentre as proteínas LipA com alta similaridade - provenientes do grupo das *Xanthomonas* e os organismos no grupo em azul mostrado na Figura 8, que inclui *X. fastidiosa* - contêm o domínio de ligação ao substrato do tipo LipA. Interessantemente, apesar da alta conservação dos resíduos de aminoácidos ao redor do túnel identificado nas proteínas do tipo LipA, aparentemente apenas as proteínas pertencentes ao grupo das *Xanthomonas* possuem a capacidade de ligação ao carboidrato. Essa preposição baseia-se na análise estrutural que indica o resíduo Gly-231 como sendo crucial para o posicionamento do anel do açúcar e de que qualquer substituição nessa posição aboliria a ligação ao carboidrato. Esse resíduo é invariante em todas as proteínas LipA de *Xanthomonas*, com a exceção de uma delas, como mostrado na Figura 7D (142).

O movimento da tampa em lipases é um mecanismo envolvido na ativação interfacial em resposta a triacilglicerídeos altamente hidrofóbicos (179). As esterases agem em substratos menos hidrofóbicos e geralmente não possuem um domínio em tampa, que pode estar ausente também em certas lipases (149, 180). A presença de um domínio não usual no lugar do domínio em tampa na proteína LipA de *Xoo* indicou que a mesma poderia apresentar atividade esterásica (142). A associação do domínio catalítico de hidrolases com domínios não catalíticos especializados na ligação específica a um determinado substrato foi previamente descrita em outras enzimas, incluindo esterases (181, 182). Análises da atividade enzimática revelaram que LipA de *Xoo* degrada triacilglicerídeos de cadeia curta mas não apresenta atividade em triacilglicerídeos de cadeia longa, além de apresentar atividade em ésteres, indicando sua classificação como lipase não verdadeira (142).

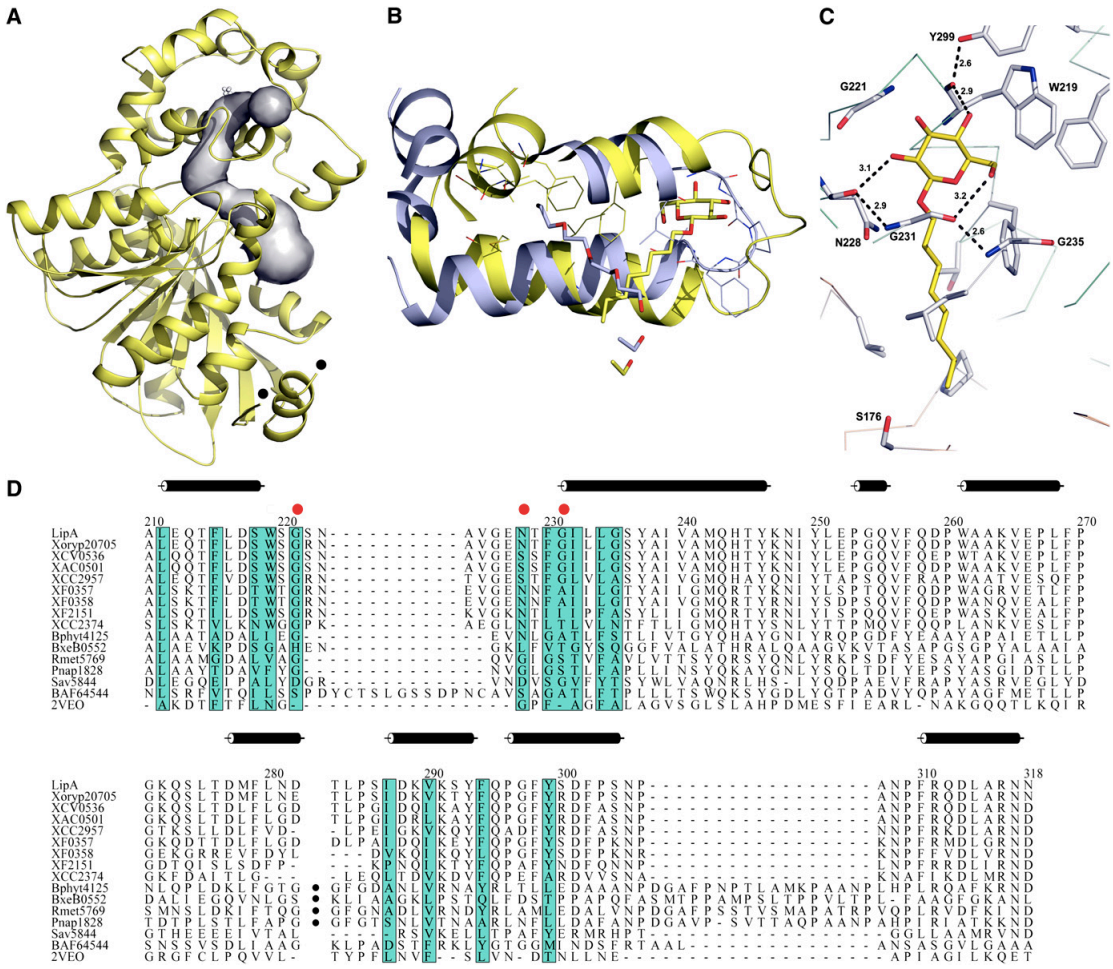

Figura 7: O túnel de ligação da proteína LipA possui um sítio de ancoragem a carboidrato. (**A**) Representação tridimensional do túnel de ligação da proteína LipA. Os dois círculos pretos representam a sequência entre os aminoácidos 28 e 36 na qual a densidade eletrônica está faltando. (**B**) Superimposição dos domínios tampas das proteínas LipA (amarelo) e CalA (azul). BOG e PEG estão representados em bastões amarelo e azul, respectivamente. Os resíduos de Ser dos sítios ativos das proteínas LipA e CalA também estão mostrados em amarelo e azul, respectivamente. (**C**) Interações específicas importantes do BOG1 no domínio de ligação ao carboidrato de LipA estão mostradas por linhas pontilhadas (distância em Å). (**D**) Alinhamento múltiplo do domínio de ligação de LipA com regiões homólogas em outras bactérias. Resíduos em verde são aminoácidos que se alinham ao túnel e os pontos em vermelho indicam os resíduos do domínio de ligação ao carboidrato que foram mutagenizados. Os pontos pretos representam os aminoácidos (39-45) presentes nas sequências das proteínas correspondentes mas que não estão mostrados na figura. Os cilindros pretos indicam alfa-hélices. Fonte: modificado de Aparna, G. *et al.,* 2009 (142).

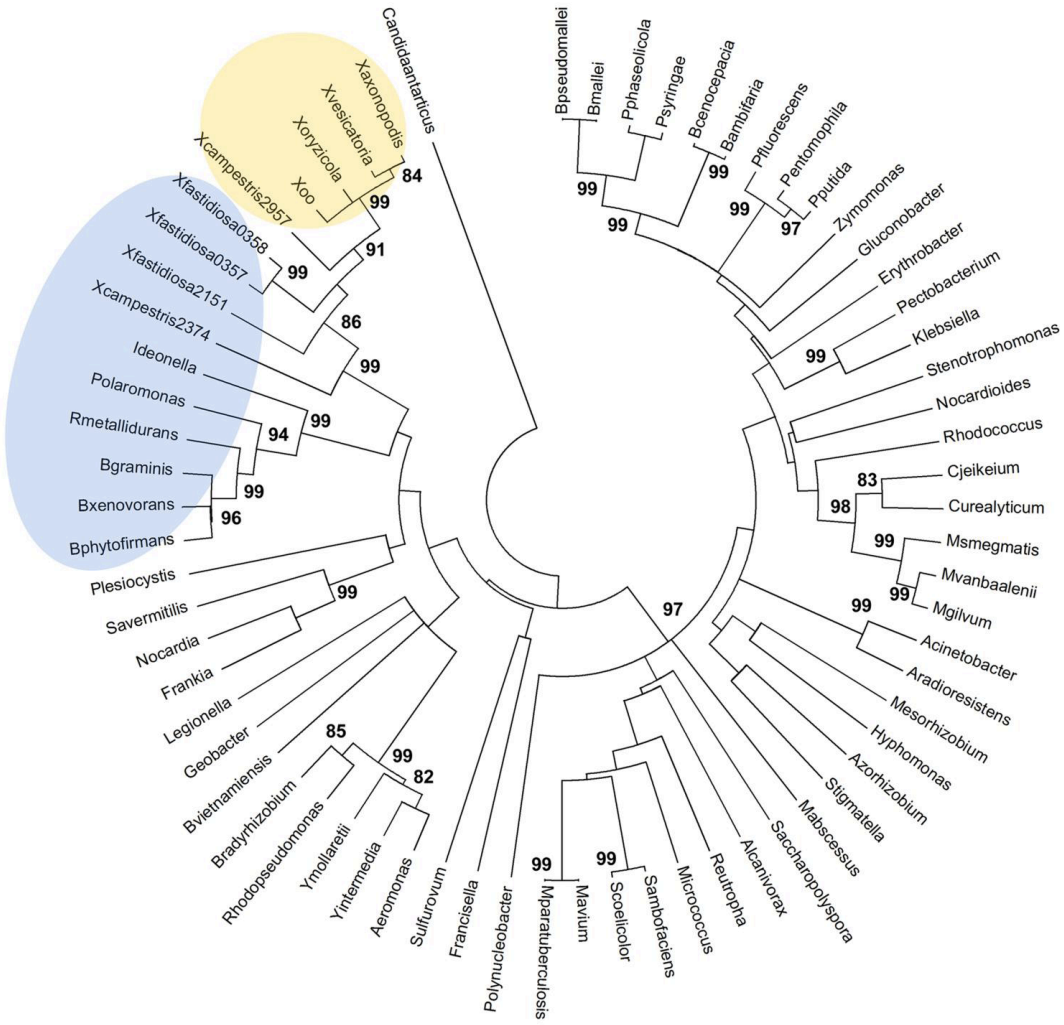

Figura 8: Análise filogenética das sequências homólogas a LipA. As proteínas de Xanthomonas (grupo em amarelo) agrupam-se no dendrograma filogenético dos homólogos de LipA depositados no banco de dados do NCBI. Os agrupamentos em amarelo e azul contêm as proteínas que foram escolhidas em buscas por homologia utilizando apenas a sequência do domínio de ligação ao substrato da LipA. O grupo em amarelo contêm: *Xanthomonas oryzicola* (Xoryp20705); *X. campestris* pv. vesicatoria (XCV0536); *X. axonopodis* pv. citrii (XAC0501); *X. campestris* pv. campestris str. ATCC33913 (XCC2957) e a LipA de Xoo. O grupo em azul contêm, entre outras, as proteínas XF0358, XF0357 e XF2151 de *X. fastidiosa* 9a5c (Xf-CVC) que são proteínas homologas às proteínas PD1703, PD1702 e PD1211 de *X. fastidiosa* Temecula 1 (Xf-PD), respectivamente. Fonte: modificado de Aparna, G. *et al.*, 2009 (142).

Análises estruturais demonstraram que o domínio em tampa da proteína LipA de *Xoo* foi funcionalmente convertido em um domínio de ligação a carboidrato que confere à esta proteína a propriedade de degradação da parede celular vegetal. O domínio de ligação ao substrato de LipA pode ter sido adquirido por um ancestral comum não patogênico de *Xanthomonas* e *Xylella* e então alterado para atuar em ésteres carboxílicos ligados a carboidratos. Diversos complexos de polissacarídeos esterificados a diversos compostos fenólicos e alifáticos dominam o ambiente da interface planta/solo, provavelmente induzindo a evolução destas estruturas especializadas encontradas em hidrolases bacterianas (142).

2. Referências

1. Ellis TN, Kuehn MJ (2010) Virulence and immunomodulatory roles of bacterial outer membrane vesicles. *Microb Molec Bio Rev: MMBR* **74**(1):81-94.

2. Chatterjee S, Almeida RP, Lindow S (2008) Living in two worlds: the plant and insect lifestyles of Xylella fastidiosa. *Ann Rev Phyto* **46**:243-271.

3. Mollenhauer HH, Hopkins DL (1974) Ultrastructural study of Pierce's disease bacterium in grape xylem tissue. *J Bacteriology* **119**(2):612-618.

4. Davis MJ, Purcell AH, Thomson SV (1978) Pierce's disease of grapevines: isolation of the causal bacterium. *Science* **199**(4324):75-77.

5. Alves E*, et al.* (2008) Retention sites for Xylella fastidiosa in four sharpshooter vectors (Hemiptera: Cicadellidae) analyzed by scanning electron microscopy. *Curr Microb* **56**(5):531-538.

6. Purcell AH, Finlay AH, McLean DL (1979) Pierce's disease bacterium: mechanism of transmission by leafhopper vectors. *Science* **206**(4420):839-841.

7. Redak RA*, et al.* (2004) The biology of xylem fluid-feeding insect vectors of Xylella fastidiosa and their relation to disease epidemiology. *Ann Rev Entomol* **49**:243-270.

8. Brlansky RH, Damsteegt VD, Hartung JS (2002) Transmission of the citrus variegated chlorosis bacterium Xylella fastidiosa with the sharpshooter oncometopia nigricans. *Plant Dis* **86**(11):1237-1239.

9. Backus EA, Morgan DJ (2011) Spatiotemporal colonization of Xylella fastidiosa in its vector supports the role of egestion in the inoculation mechanism of foregut-borne plant pathogens. *Phytopat* **101**(8):912-922.

10. Almeida RPP, Purcell AH (2006) Patterns of Xylella fastidiosa colonization on the precibarium of sharpshooter vectors relative to transmission to plants. *Ann Entomol Soc Amer* **99**(5):884-890.

11. Meng Y*, et al.* (2005) Upstream migration of Xylella fastidiosa via pilus-driven twitching motility. *J Bacter* **187**(16):5560-5567.

12. Purcell AH, Hopkins DL (1996) Fastidious xylem-limited bacterial plant pathogens. *Ann Rev Phytopat* **34**:131-151.

13. Hopkins DL (1989) Xylella Fastidiosa: Xylem-limited bacterial pathogen of plants. *Ann Rev Phytopat* **27**(1):271-290.

14. Varela LG, Smith RJ, Phillips PA (2001) Pierce's Disease. (University of California, Agriculture and Natural Resources).

15. Costa HS*, et al.* (2004) *Plant hosts of Xylella fastidiosa in and near southern California vineyards*. *Plant Dis* **88**(11):1255-1261.

16. Hernandez-Martinez R, de la Cerda KA, Costa HS, Cooksey DA, Wong FP (2007) Phylogenetic relationships of Xylella fastidiosa strains isolated from landscape ornamentals in southern California. *Phytopat* **97**(7):857-864.

17. Montero-Astua M*, et al.* (2008) Isolation and molecular characterization of Xylella fastidiosa from coffee plants in Costa Rica. *J Microb* **46**(5):482-490.

18. Huang Q, Sherald JL (2004) Isolation and phylogenetic analysis of Xylella fastidiosa from its invasive alternative host, porcelain berry. *Curr Microb* **48**(1):73-76.

19. Schuenzel EL, Scally M, Stouthamer R, Nunney L (2005) A multigene phylogenetic study of clonal diversity and divergence in North American strains of the plant pathogen Xylella fastidiosa. *Appl Environ Microb* **71**(7):3832-3839.

20. Hopkins DL, Purcell AH (2002) Xylella fastidiosa: cause of Pierce's disease of grapevine and other emergent diseases. *Plant Dis* **86**(10):1056-1066.

21. Schaad NW, Postnikova E, Lacy G, Fatmi M, Chang CJ (2004) Xylella fastidiosa subspecies: X. fastidiosa subsp. [correction] fastidiosa [correction] subsp. nov., X. fastidiosa subsp. multiplex subsp. nov., and X. fastidiosa subsp. pauca subsp. nov. *System Appl Microb* **27**(3):290-300.

22. Nunney L*, et al.* (2010) Population genomic analysis of a bacterial plant pathogen: novel insight into the origin of Pierce's disease of grapevine in the U.S. *PloS one* **5**(11):e15488.

23. Almeida RPP, Blua MJ, Lopes JRS, Purcell AH (2005) Vector transmission of Xylella fastidiosa: applying fundamental knowledge to generate disease management strategies. *Ann Entomo Soc Amer* **98**(6):775-786.

24. Hewitt WB, Houston BR, et al. (1946) Leafhopper transmission of the virus causing Pierce's disease of grape and dwarf of alfalfa. *Phytopat* **36**:117-128.

25. Wells JM*, et al.* (1987) Xylella fastidiosa: gram-negative, xylem-limited, fastidious plant bacteria related to Xanthomonas spp. *Intern J Syst Bacter* **37**(2):136-143.

26. McElrone AJ, Sherald JL, Forseth IN (2001) Effects of water stress on symptomatology and growth of Parthenocissus quinquefolia infected by Xylella fastidiosa. *Plant Dis* **85**(11):1160-1164.

27. Berlyn GP (1983) Plant structures: xylem structure and the ascent of sap. *Science* **222**(4623):500-501.

28. Perez-Donoso AG*, et al.* (2010) Cell wall-degrading enzymes enlarge the pore size of intervessel pit membranes in healthy and Xylella fastidiosa-infected grapevines. *Plant Phys* **152**(3):1748-1759.

29. Chatelet DS, Matthews MA, Rost TL (2006) Xylem structure and connectivity in grapevine (Vitis vinifera) shoots provides a passive mechanism for the spread of bacteria in grape plants. *Ann Botany* **98**(3):483-494.

30. Goodwin PH, DeVay JE, Meredith CP (1988) Roles of water stress and phytotoxins in the development of Pierce's disease of the grapevine. *Physiol Mol Plant Path* **32**(1):1-15.

31. Goodwin PH, DeVay JE, Meredith CP (1988) Physiological responses of Vitis vinifera cv. “Chardonnay” to infection by the Pierce's disease bacterium. *Physiol Mol Plant Path* **32**(1):17-32.

32. McElrone AJ, Sherald JL, Forseth IN (2003) Interactive effects of water stress and xylem-limited bacterial infection on the water relations of a host vine. *J Exper Bot* **54**(381):419-430.

33. Newman KL, Almeida RP, Purcell AH, Lindow SE (2004) Cell-cell signaling controls Xylella fastidiosa interactions with both insects and plants. *Proc Nat Acad Sci USA* **101**(6):1737-1742.

34. Mollenhauer HH, Hopkins DL (1976) Xylem morphology of Pierce's disease-infected grapevines with different levels of tolerance. *Phys Plant Path* **9**(1):95-100.

35. Stevenson JF, Matthews MA, Rost TL (2004) Grapevine susceptibility to Pierce's disease I: relevance of hydraulic architecture. *Amer J Enol Vitic* **55**(3):228-237.

36. Stevenson JF, Matthews MA, Greve LC, Labavitch JM, Rost TL (2004) Grapevine susceptibility to Pierce's disease II: progression of anatomical symptoms. *Amer J Enol Vitic* **55**(3):238-245.

37. Baccari C, Lindow SE (2011) Assessment of the process of movement of Xylella fastidiosa within susceptible and resistant grape cultivars. *Phytopat* **101**(1):77-84.

38. Chatelet DS, Wistrom CM, Purcell AH, Rost TL, Matthews MA (2011) Xylem structure of four grape varieties and 12 alternative hosts to the xylem-limited bacterium Xylella fastidious. *Ann Botany* **108**(1):73-85.

39. Thorne ET, Stevenson JF, Rost TL, Labavitch JM, Matthews MA (2006) Pierce’s disease symptoms: comparison with symptoms of water deficit and the impact of water deficits. *Amer J Enol Vitic* **57**(1):1-11.

40. Gambetta GA, Fei J, Rost TL, Matthews MA (2007) Leaf scorch symptoms are not correlated with bacterial populations during Pierce's disease. *J Exper Bot* **58**(15-16):4037-4046.

41. Newman KL, Almeida RP, Purcell AH, Lindow SE (2003) Use of a green fluorescent strain for analysis of Xylella fastidiosa colonization of Vitis vinifera. *Appl Envirl Microb* **69**(12):7319-7327.

42. Choat B, Gambetta GA, Wada H, Shackel KA, Matthews MA (2009) The effects of Pierce's disease on leaf and petiole hydraulic conductance in Vitis vinifera cv. Chardonnay. *Phys Plantar* **136**(4):384-394.

43. Simpson AJ*, et al.* (2000) The genome sequence of the plant pathogen Xylella fastidiosa. The Xylella fastidiosa Consortium of the Organization for Nucleotide Sequencing and Analysis. *Nature* **406**(6792):151-159.

44. Bhattacharyya A*, et al.* (2002) Whole-genome comparative analysis of three phytopathogenic Xylella fastidiosa strains. *Proc Nat Acad Sci USA* **99**(19):12403-12408.

45. Chen J*, et al.* (2010) Whole genome sequences of two Xylella fastidiosa strains (M12 and M23) causing almond leaf scorch disease in California. *J Bacter* **192**(17):4534.

46. Simpson AJ, Perez JF (1998) ONSA, the Sao Paulo Virtual Genomics Institute. Organization for Nucleotide Sequencing and Analysis. *Nature Biotech* **16**(9):795-796.

47. Van Sluys MA*, et al.* (2003) Comparative analyses of the complete genome sequences of Pierce's disease and citrus variegated chlorosis strains of Xylella fastidiosa. *J Bacter* **185**(3):1018-1026.

48. Roper MC, Greve LC, Warren JG, Labavitch JM, Kirkpatrick BC (2007) Xylella fastidiosa requires polygalacturonase for colonization and pathogenicity in Vitis vinifera grapevines. *Mol Plant-Mic Inter: MPMI* **20**(4):411-419.

49. Hopkins, DL (2005) Biological control of Pierce's disease in the vineyard with strains of Xylella fastidiosa benign to grapevine. *Plant Dis* **89**(12):1348-1352.

50. Zhang S*, et al.* (2011) The Xylella fastidiosa biocontrol strain EB92-1 genome is very similar and syntenic to Pierce's disease strains. *J Bacter* **193**(19):5576-5577.

51. Silva MS, De Souza AA, Takita MA, Labate CA, Machado MA (2011) Analysis of the biofilm proteome of Xylella fastidiosa. *Proteo Sci* **9**:58.

52. Skach WR (2007) The expanding role of the ER translocon in membrane protein folding. *The J Cell Bio* **179**(7):1333-1335.

53. Tjalsma H, Bolhuis A, Jongbloed JD, Bron S, van Dijl JM (2000) Signal peptide-dependent protein transport in Bacillus subtilis: a genome-based survey of the secretome. *Microb Mol Bio Rev: MMBR* **64**(3):515-547.

54. Smolka MB*, et al.* (2003) Proteome analysis of the plant pathogen Xylella fastidiosa reveals major cellular and extracellular proteins and a peculiar codon bias distribution. *Proteomics* **3**(2):224-237.

55. Lei B, Mackie S, Lukomski S, Musser JM (2000) Identification and immunogenicity of group A Streptococcus culture supernatant proteins. *Infect Immunity* **68**(12):6807-6818.

56. Jungblut PR*, et al.* (1999) Comparative proteome analysis of Mycobacterium tuberculosis and Mycobacterium bovis BCG strains: towards functional genomics of microbial pathogens. *Mol Microb* **33**(6):1103-1117.

57. Greenbaum D, Luscombe NM, Jansen R, Qian J, Gerstein M (2001) Interrelating different types of genomic data, from proteome to secretome: 'oming in on function. *Geno Resear* **11**(9):1463-1468.

58. Antelmann H*, et al.* (2001) A proteomic view on genome-based signal peptide predictions. *Geno Resear* **11**(9):1484-1502.

59. Economou A (2002) Bacterial secretome: the assembly manual and operating instructions. *Mol Memb Bio* **19**(3):159-169.

60. Saier MH, Jr. (2006) Protein secretion and membrane insertion systems in gram-negative bacteria. *The J Membr Bio* **214**(2):75-90.

61. Dalbey RE, Kuhn A (2000) Evolutionarily related insertion pathways of bacterial, mitochondrial, and thylakoid membrane proteins. *Ann Rev Cell Developm Bio* **16**:51-87.

62. Lee PA, Tullman-Ercek D, Georgiou G (2006) The bacterial twin-arginine translocation pathway. *Ann Rev Microb* **60**:373-395.

63. De Buck E, Lammertyn E, Anne J (2008) The importance of the twin-arginine translocation pathway for bacterial virulence. *Tren In Microb* **16**(9):442-453.

64. Muller M, Klosgen RB (2005) The Tat pathway in bacteria and chloroplasts. *Mol Membr Bio* **22**(1-2):113-121.

65. Economou A (1999) Following the leader: bacterial protein export through the Sec pathway. *Tren In Microb* **7**(8):315-320.

66. Henningham A*, et al.* (2012) Conserved anchorless surface proteins as group A streptococcal vaccine candidates. *J Mol Med* **90**(10):1197-1207.

67. Glowalla E, Tosetti B, Kronke M, Krut O (2009) Proteomics-based identification of anchorless cell wall proteins as vaccine candidates against Staphylococcus aureus. *Infect Immunity* **77**(7):2719-2729.

68. Henderson IR, Navarro-Garcia F, Desvaux M, Fernandez RC, Ala'Aldeen D (2004) Type V protein secretion pathway: the autotransporter story. *Microb Molec Bio Rev: MMBR* **68**(4):692-744.

69. Korotkov KV, Sandkvist M, Hol WG (2012) The type II secretion system: biogenesis, molecular architecture and mechanism. *Nature Rev. Microb* **10**(5):336-351.

70. Loquet A*, et al.* (2012) Atomic model of the type III secretion system needle. *Nature* **486**(7402):276-279.

71. Souza DP*, et al.* (2011) A component of the Xanthomonadaceae type IV secretion system combines a VirB7 motif with a N0 domain found in outer membrane transport proteins. *PLoS Pathogens* **7**(5):e1002031.

72. Burns DL (1999) Biochemistry of type IV secretion. *Curr Opinion In Microb* **2**(1):25-29.

73. Odenbreit S*, et al.* (2000) Translocation of Helicobacter pylori CagA into gastric epithelial cells by type IV secretion. *Science* **287**(5457):1497-1500.

74. Bhattacharyya A*, et al.* (2002) Draft sequencing and comparative genomics of Xylella fastidiosa strains reveal novel biological insights. *Geno Resear* **12**(10):1556-1563.

75. Meidanis J, Braga MD, Verjovski-Almeida S (2002) Whole-genome analysis of transporters in the plant pathogen Xylella fastidiosa. *Microb Mol Bio Rev: MMBR* **66**(2):272-299.

76. Lubelski J, Konings WN, Driessen AJ (2007) Distribution and physiology of ABC-type transporters contributing to multidrug resistance in bacteria. *Microb Mol Bio Rev: MMBR* **71**(3):463-476.

77. Reddy JD, Reddy SL, Hopkins DL, Gabriel DW (2007) TolC is Required for Pathogenicity of Xylella fastidiosa in Vitis vinifera Grapevines. *Mol Plant-Micro Interac* **20**(4):403-410.

78. Bell KS*, et al.* (2004) Genome sequence of the enterobacterial phytopathogen Erwinia carotovora subsp. atroseptica and characterization of virulence factors. *Proc Nat Acad Sci USA* **101**(30):11105-11110.

79. Sandkvist M (2001) Type II secretion and pathogenesis. *Infect Immunity* **69**(6):3523-3535.

80. Tauschek M, Gorrell RJ, Strugnell RA, Robins-Browne RM (2002) Identification of a protein secretory pathway for the secretion of heat-labile enterotoxin by an enterotoxigenic strain of Escherichia coli. *Proc Nat Acad Sci USA* **99**(10):7066-7071.

81. Buell CR*, et al.* (2003) The complete genome sequence of the Arabidopsis and tomato pathogen Pseudomonas syringae pv. tomato DC3000. *Proc Nat Acad Sci USA* **100**(18):10181-10186.

82. da Silva AC*, et al.* (2002) Comparison of the genomes of two Xanthomonas pathogens with differing host specificities. *Nature* **417**(6887):459-463.

83. Lee HM*, et al.* (2004) Functional dissection of the XpsN (GspC) protein of the Xanthomonas campestris pv. campestris type II secretion machinery. *J Bacter* **186**(10):2946-2955.

84. Iwobi A*, et al.* (2003) Novel virulence-associated type II secretion system unique to high-pathogenicity Yersinia enterocolitica. *Infect Immunity* **71**(4):1872-1879.

85. Rossier O, Starkenburg SR, Cianciotto NP (2004) Legionella pneumophila type II protein secretion promotes virulence in the A/J mouse model of Legionnaires' disease pneumonia. *Infect Immunity* **72**(1):310-321.

86. Riekki R*, et al.* (2000) Members of the amylovora group of Erwinia are cellulolytic and possess genes homologous to the type II secretion pathway. *Mol & Gener Genet: MGG* **263**(6):1031-1037.

87. Paranjpye RN, Strom MS (2005) A Vibrio vulnificus type IV pilin contributes to biofilm formation, adherence to epithelial cells, and virulence. *Infect Immunity* **73**(3):1411-1422.

88. Jha G, Rajeshwari R, Sonti RV (2007) Functional interplay between two Xanthomonas oryzae pv,. oryzae secretion systems in modulating virulence on rice. *Mol Plant-Micro Interac: MPMI* **20**(1):31-40.

89. Jha G, Rajeshwari R, Sonti RV (2005) Bacterial type two secretion system secreted proteins: double-edged swords for plant pathogens. *Mol Plant-Micro Interac: MPMI* **18**(9):891-898.

90. Wulff NA, Carrer H, Pascholati SF (2006) Expression and purification of cellulase Xf818 from Xylella fastidiosa in Escherichia coli. *Curr Microb* **53**(3):198-203.

91. Maria Fedatto L*, et al.* (2006) Detection and characterization of protease secreted by the plant pathogen Xylella fastidiosa. *Microb Resear* **161**(3):263-272.

92. Jaroszuk-Scisel J, Kurek E, Slomka A, Janczarek M, Rodzik B (2011) Activities of cell wall degrading enzymes in autolyzing cultures of three Fusarium culmorum isolates: growth-promoting, deleterious and pathogenic to rye (Secale cereale). *Mycologia* **103**(5):929-945.

93. King BC*, et al.* (2011) Arsenal of plant cell wall degrading enzymes reflects host preference among plant pathogenic fungi. *Biotech Biofuels* 4:4.

94. Sipos B*, et al.* (2010) Characterisation of specific activities and hydrolytic properties of cell-wall-degrading enzymes produced by Trichoderma reesei Rut C30 on different carbon sources. *Appl Biochem Biotech* **161**(1-8):347-364.

95. Roncero MI*, et al.* (2000) Role of cell wall-degrading enzymes in pathogenicity of Fusarium oxysporum. *Rev. Iberoamer Micologia* **17**(1):S47-53.

96. Wilson DB (2004) Studies of Thermobifida fusca plant cell wall degrading enzymes. *Chem Rec* **4**(2):72-82.

97. Jayasinghe CK, Wijayaratne SC, Fernando TH (2004) Characterization of cell wall degrading enzymes of Thanatephorus cucumeris. *Mycopathologia* **157**(1):73-79.

98. Carden DE, Felle HH (2003) The mode of action of cell wall-degrading enzymes and their interference with Nod factor signalling in Medicago sativa root hairs. *Planta* **216**(6):993-1002.

99. Norman-Setterblad C, Vidal S, Palva ET (2000) Interacting signal pathways control defense gene expression in Arabidopsis in response to cell wall-degrading enzymes from Erwinia carotovora. *Mol Plant-Micro Interac: MPMI* **13**(4):430-438.

100. Norman C, Vidal S, Palva ET (1999) Oligogalacturonide-mediated induction of a gene involved in jasmonic acid synthesis in response to the cell-wall-degrading enzymes of the plant pathogen Erwinia carotovora. *Mol Plant-Micro Interac: MPMI* **12**(7):640-644.

101. Dean RA, Timberlake WE (1989) Production of cell wall-degrading enzymes by Aspergillus nidulans: a model system for fungal pathogenesis of plants. *The Plant Cell* **1**(3):265-273.

102. Szczesny R*, et al.* (2010) Functional characterization of the Xcs and Xps type II secretion systems from the plant pathogenic bacterium Xanthomonas campestris pv vesicatoria. *The New Phytologist* **187**(4):983-1002.

103. Wang L, Rong W, He C (2008) Two Xanthomonas extracellular polygalacturonases, PghAxc and PghBxc, are regulated by type III secretion regulators HrpX and HrpG and are required for virulence. *Mol Plant-Micro Interact : MPMI* **21**(5):555-563.

104. Thieme F*, et al.* (2005) Insights into genome plasticity and pathogenicity of the plant pathogenic bacterium Xanthomonas campestris pv. vesicatoria revealed by the complete genome sequence. *J Bacteriol* **187**(21):7254-7266.

105. Sun QH*, et al.* (2005) Type-II secretion pathway structural gene xpsE, xylanase- and cellulase secretion and virulence in Xanthomonas oryzae pv. oryzae. *Plant Pathol* **54**(1):15-21.

106. Barras F, van Gijsegem F, Chatterjee AK (1994) Extracellular Enzymes and Pathogenesis of Soft-Rot Erwinia. *Ann Rev Phytopat* **32**(1):201-234.

107. Kikot GE, Hours RA, Alconada TM (2009) Contribution of cell wall degrading enzymes to pathogenesis of Fusarium graminearum: a review. *J Basic Microbio* **49**(3):231-241.

108. Ellis EA, McEachern GR, Clark S, Cobb BG (2010) Ultrastructure of pit membrane dissolution and movement of Xylella fastidiosa through pit membranes in petioles of Vitis vinifera. *Botany* **88**(6):596-600.

109. Dandekar AM*, et al.* (2012) An engineered innate immune defense protects grapevines from Pierce disease. *Proc Nat Acad Sci USA* **109**(10):3721-3725.

110. Bos MP, Robert V, Tommassen J (2007) Biogenesis of the gram-negative bacterial outer membrane. *Ann Rev Microbio* **61**:191-214.

111. Koch AL (1998) The biophysics of the gram-negative periplasmic space. *Crit Rev Microbio* **24**(1):23-59.

112. Beveridge TJ (1999) Structures of gram-negative cell walls and their derived membrane vesicles. *J Bacteriol* **181**(16):4725-4733.

113. Mashburn LM, Whiteley M (2005) Membrane vesicles traffic signals and facilitate group activities in a prokaryote. *Nature* **437**(7057):422-425.

114. Mayrand D, Grenier D (1989) Biological activities of outer membrane vesicles. *Canad J Microbio* **35**(6):607-613.

115. Renelli M, Matias V, Lo RY, Beveridge TJ (2004) DNA-containing membrane vesicles of Pseudomonas aeruginosa PAO1 and their genetic transformation potential. *Microbiology* **150**(Pt 7):2161-2169.

116. Grenier D, Mayrand D (1987) Functional characterization of extracellular vesicles produced by Bacteroides gingivalis. *Infect Immunity* **55**(1):111-117.

117. Kolling GL, Matthews KR (1999) Export of virulence genes and Shiga toxin by membrane vesicles of Escherichia coli O157:H7. *App Environ Microbio* **65**(5):1843-1848.

118. Roy K, Hamilton DJ, Munson GP, Fleckenstein JM (2011) Outer membrane vesicles induce immune responses to virulence proteins and protect against colonization by enterotoxigenic Escherichia coli. *Clin Vacc Immun: CVI* **18**(11):1803-1808.

119. Lee EY*, et al.* (2007) Global proteomic profiling of native outer membrane vesicles derived from Escherichia coli. *Proteomics* **7**(17):3143-3153.

120. Balsalobre C*, et al.* (2006) Release of the type I secreted alpha-haemolysin via outer membrane vesicles from Escherichia coli. *Mol Microbio* **59**(1):99-112.

121. Wai SN, Takade A, Amako K (1995) The release of outer membrane vesicles from the strains of enterotoxigenic Escherichia coli. *Microbio Immunol* **39**(7):451-456.

122. Mitra S*, et al.* (2012) Outer membrane vesicles of Shigella boydii type 4 induce passive immunity in neonatal mice. *FEMS Immunol Medical Microbio* **66**(2):240-250.

123. Camacho AI*, et al.* (2011) Mucosal immunization with Shigella flexneri outer membrane vesicles induced protection in mice. *Vaccine* **29**(46):8222-8229.

124. Mirlashari MR, Hoiby EA, Holst J, Lyberg T (2002) Outer membrane vesicles from Neisseria meningitidis. *APMIS : Acta Patholo, Microbio Immuno Scandin* **110**(3):193-204.

125. Santos S*, et al.* (2012) Outer membrane vesicles (OMV) production of Neisseria meningitidis serogroup B in batch process. *Vaccine* **30**(42):6064-6069.

126. Vida A*, et al.* (2011) Neutralization of Neisseria meningitidis outer membrane vesicles. *Inflamm Res: Offic J Europ Histam Res Soc... [et al.]* **60**(9):801-805.

127. Choi DS*, et al.* (2011) Proteomic analysis of outer membrane vesicles derived from Pseudomonas aeruginosa. *Proteomics* **11**(16):3424-3429.

128. Ellis TN, Leiman SA, Kuehn MJ (2010) Naturally produced outer membrane vesicles from Pseudomonas aeruginosa elicit a potent innate immune response via combined sensing of both lipopolysaccharide and protein components. *Infect Immunity* **78**(9):3822-3831.

129. Bomberger JM*, et al.* (2009) Long-distance delivery of bacterial virulence factors by Pseudomonas aeruginosa outer membrane vesicles. *PLoS Pathogens* 5(4):e1000382.

130. Parker H, Keenan JI (2012) Composition and function of Helicobacter pylori outer membrane vesicles. *Microb Infection / Inst Pasteur* **14**(1):9-16.

131. Parker H, Chitcholtan K, Hampton MB, Keenan JI (2010) Uptake of Helicobacter pylori outer membrane vesicles by gastric epithelial cells. *Infect Immunity* **78**(12):5054-5061.

132. Yonezawa H*, et al.* (2009) Outer membrane vesicles of Helicobacter pylori TK1402 are involved in biofilm formation. *BMC Microbiol* **9**:197.

133. Mullaney E*, et al.* (2009) Proteomic and functional characterization of the outer membrane vesicles from the gastric pathogen Helicobacter pylori. *Proteomics. Clin Applicat* **3**(7):785-796.

134. Yoon H, Ansong C, Adkins JN, Heffron F (2011) Discovery of Salmonella virulence factors translocated via outer membrane vesicles to murine macrophages. *Infect Immunity* **79**(6):2182-2192.

135. Muralinath M, Kuehn MJ, Roland KL, Curtiss R, 3rd (2011) Immunization with Salmonella enterica serovar Typhimurium-derived outer membrane vesicles delivering the pneumococcal protein PspA confers protection against challenge with Streptococcus pneumoniae. *Infect Immunity* **79**(2):887-894.

136. Nakae T (1975) Outer membrane of Salmonella typhimurium: reconstitution of sucrose-permeable membrane vesicles. *Biochem Biophys Res Communic* **64**(4):1224-1230.

137. Jain-Gupta N*, et al.* (2012) Pluronic P85 enhances the efficacy of outer membrane vesicles as a subunit vaccine against Brucella melitensis challenge in mice. *FEMS Immunol Medic Microbio* **66**(3):436-444.

138. Avila-Calderon ED*, et al.* (2012) Characterization of outer membrane vesicles from Brucella melitensis and protection induced in mice. *Clin & Developm Immunol* 2012:352493.

139. Sidhu VK, Vorholter FJ, Niehaus K, Watt SA (2008) Analysis of outer membrane vesicle associated proteins isolated from the plant pathogenic bacterium Xanthomonas campestris pv. campestris. *BMC Microbio* **8**:87.

140. Kulp A, Kuehn MJ (2010) Biological functions and biogenesis of secreted bacterial outer membrane vesicles. *Ann Rev Microbio* **64**:163-184.

141. Matsumoto A, Huston SL, Killiny N, Igo MM (2012) XatA, an AT-1 autotransporter important for the virulence of Xylella fastidiosa Temecula1. *MicrobiologyOpen* **1**(1):33-45.

142. Aparna G, Chatterjee A, Sonti RV, Sankaranarayanan R (2009) A cell wall-degrading esterase of Xanthomonas oryzae requires a unique substrate recognition module for pathogenesis on rice. *The Plant Cell* **21**(6):1860-1873.

143. Marchot P, Chatonnet A (2012) Enzymatic activity and protein interactions in alpha/beta hydrolase fold proteins: moonlighting versus promiscuity. *Prot Pept Lett* **19**(2):132-143.

144. Holmquist M (2000) Alpha/Beta-hydrolase fold enzymes: structures, functions and mechanisms. *Curr Prot & Pept Sci* **1**(2):209-235.

145. Ollis DL*, et al.* (1992) The alpha/beta hydrolase fold. *Prot Engineer* **5**(3):197-211.

146. Carr PD, Ollis DL (2009) Alpha/beta hydrolase fold: an update. *Prot Pept Lett* **16**(10):1137-1148.

147. Gupta R, Gupta N, Rathi P (2004) Bacterial lipases: an overview of production, purification and biochemical properties. *Appl Microbio Biotech* **64**(6):763-781.

148. Jaeger KE*, et al.* (1994) Bacterial lipases. *FEMS Microbio Rev* **15**(1):29-63.

149. Jaeger KE, Dijkstra BW, Reetz MT (1999) Bacterial biocatalysts: molecular biology, three-dimensional structures, and biotechnological applications of lipases. *Ann Rev Microbiol* **53**:315-351.

150. Jochens H*, et al.* (2011) Protein engineering of alpha/beta-hydrolase fold enzymes. *Chembioc: a Europ J Chemic Biol* **12**(10):1508-1517.

151. Lazniewski M, Steczkiewicz K, Knizewski L, Wawer I, Ginalski K (2011) Novel transmembrane lipases of alpha/beta hydrolase fold. *FEBS Lett* **585**(6):870-874.

152. Schrag JD, Cygler M (1997) Lipases and alpha/beta hydrolase fold. *Meth Enzymol* **284**:85-107.

153. Nardini M, Dijkstra BW (1999) Alpha/beta hydrolase fold enzymes: the family keeps growing. *Curr Opin Struct Biol* **9**(6):732-737.

154. Marchot P, Chatonnet A (2012) Hydrolase versus other functions of members of the alpha/beta-hydrolase fold superfamily of proteins. *Prot Pept Lett* **19**(2):130-131.

155. Singh AK, Mukhopadhyay M (2012) Overview of fungal lipase: a review. *Appl Biochem Biotech* **166**(2):486-520.

156. Angkawidjaja C, Kanaya S (2006) Family I.3 lipase: bacterial lipases secreted by the type I secretion system. *Cell Mol Life Sci: CMLS* **63**(23):2804-2817.

157. Rosenau F, Jaeger K (2000) Bacterial lipases from Pseudomonas: regulation of gene expression and mechanisms of secretion. *Biochimie* **82**(11):1023-1032.

158. Severina LO (1984) Extracellular and intracellular bacterial lipases. *Izvest Akad Nauk SSSR. Ser Biologich* (4):594-603.

159. Schaller M, Borelli C, Korting HC, Hube B (2005) Hydrolytic enzymes as virulence factors of Candida albicans. *Mycoses* **48**(6):365-377.

160. Tyski S, Tylewska S, Hryniewicz W, Jeljaszewicz J (1987) Induction of human neutrophils chemotaxis by staphylococcal lipase. *Zentralblatt fur Bakteriologie, Mikrobiologie, und Hygiene. Ser A, Me Microbiol, Infect Dis, Virol, Parasitol* **265**(3-4):360-368.

161. Longshaw CM, Farrell AM, Wright JD, Holland KT (2000) Identification of a second lipase gene, gehD, in Staphylococcus epidermidis: comparison of sequence with those of other staphylococcal lipases. *Microbiology* **146**(Pt 6):1419-1427.

162. Miskin JE, Farrell AM, Cunliffe WJ, Holland KT (1997) Propionibacterium acnes, a resident of lipid-rich human skin, produces a 33 kDa extracellular lipase encoded by gehA. *Microbiology* **143**(Pt 5):1745-1755.

163. Chihara-Siomi M*, et al.* (1992) Purification, molecular cloning, and expression of lipase from Pseudomonas aeruginosa. *Arch Biochem Biophys* **296**(2):505-513.

164. Martinez A, Ostrovsky P, Nunn DN (1999) LipC, a second lipase of Pseudomonas aeruginosa, is LipB and Xcp dependent and is transcriptionally regulated by pilus biogenesis components. *Mol Microbio* **34**(2):317-326.

165. Brunke S, Hube B (2006) MfLIP1, a gene encoding an extracellular lipase of the lipid-dependent fungus Malassezia furfur. *Microbiology* **152**(Pt 2):547-554.

166. Gacser A, Trofa D, Schafer W, Nosanchuk JD (2007) Targeted gene deletion in Candida parapsilosis demonstrates the role of secreted lipase in virulence. *The J Clin Investig* **117**(10):3049-3058.

167. Hu C, Xiong N, Zhang Y, Rayner S, Chen S (2012) Functional characterization of lipase in the pathogenesis of Staphylococcus aureus. *Biochem Biophys Res Commun* **419**(4):617-620.

168. Gacser A*, et al.* (2007) Lipase 8 affects the pathogenesis of Candida albicans. *Infect Immunity* **75**(10):4710-4718.

169. Feng J, Liu G, Selvaraj G, Hughes GR, Wei Y (2005) A secreted lipase encoded by LIP1 is necessary for efficient use of saturated triglyceride lipids in Fusarium graminearum. *Microbiology* **151**(Pt 12):3911-3921.

170. Voigt CA, Schafer W, Salomon S (2005) A secreted lipase of Fusarium graminearum is a virulence factor required for infection of cereals. *The Plant J: Cell Mol Biol* 42(3):364-375.

171. Kamil JP*, et al.* (2005) vLIP, a viral lipase homologue, is a virulence factor of Marek's disease virus. *J Virology* **79**(11):6984-6996.

172. Rajeshwari R, Jha G, Sonti RV (2005) Role of an in planta-expressed xylanase of Xanthomonas oryzae pv. oryzae in promoting virulence on rice. *Mol Plant-Micro Interact: MPMI* 18(8):830-837.

173. Tamir-Ariel D, Rosenberg T, Navon N, Burdman S (2012) A secreted lipolytic enzyme from Xanthomonas campestris pv. vesicatoria is expressed in planta and contributes to its virulence. *Mol Plant Pathol* **13**(6):556-567.

174. Ray SK, Rajeshwari R, Sonti RV (2000) Mutants of Xanthomonas oryzae pv. oryzae deficient in general secretory pathway are virulence deficient and unable to secrete xylanase. *Mol Plant-Micro Interact: MPMI* **13**(4):394-401.

175. Ron M, Avni A (2004) The receptor for the fungal elicitor ethylene-inducing xylanase is a member of a resistance-like gene family in tomato. *The Plant Cell* **16**(6):1604-1615.

176. Jaeger K-E, Dijkstra BW, Reetz MT (1999) Bacterial biocatalysts: molecular biology, three-dimensional structures, and biotechnological applications of lipases. *Ann Rev Microbio* **53**(1):315-351.

177. Holm L, Sander C (1998) Dictionary of recurrent domains in protein structures. *Proteins* **33**(1):88-96.

178. Ericsson DJ*, et al.* (2008) X-ray structure of Candida antarctica lipase A shows a novel lid structure and a likely mode of interfacial activation. *J Mol Biol* **376**(1):109-119.

179. Verger R (1997) Interfacial activation of lipases: facts and artifacts. *Tren Biotech* **15**(1):32-38.

180. van Pouderoyen G, Eggert T, Jaeger KE, Dijkstra BW (2001) The crystal structure of Bacillus subtilis lipase: a minimal alpha/beta hydrolase fold enzyme. *J Mol Biol* **309**(1):215-226.

181. Wei Y*, et al.* (1999) Crystal structure of brefeldin A esterase, a bacterial homolog of the mammalian hormone-sensitive lipase. *Nature Struct Biol* **6**(4):340-345.

182. Szeltner Z, Polgar L (2008) Structure, function and biological relevance of prolyl oligopeptidase. *Curr Prot & Pept Sci* **9**(1):96-107.

CAPÍTULO II

*The Type II Secreted Lipase/Esterase LipA is a Key Virulence Factor Required for Xylella fastidiosa Pathogenesis in Grapevines**

*Este capítulo está formatado de acordo com as normas do periódico *Proceedings of the National Academy of Sciences*, *PNAS*.

The Type II Secreted Lipase/Esterase LipA is a Key Virulence Factor Required for *Xylella fastidiosa* Pathogenesis in Grapevines

Rafael Nascimento[1,5], Hossein Gouran[1], Aye Tu[1], Sandeep Chakraborty[4], Basuthkar J. Rao[4], Paul A. Feldstein[2], George Bruening[2], Luiz R. Goulart[3,5], and Abhaya M. Dandekar[1,*].

[1]Plant Sciences Department, [2]Plant Pathology Department, [3]Medical Microbiology and Immunology Department, University of California, Davis, 1 Shields Ave, Davis CA 95616.
[4]Department of Biological Sciences, Tata Institute of Fundamental Research, Mumbai, India.
[5]Institute of Genetics and Biochemistry, Federal University of Uberlândia, Av. Amazonas, Bloco 2E, Campus Umuarama, 38400-902, Uberlândia MG, Brazil.

*Corresponding author:
Abhaya M. Dandekar
Dept. of Plant Sciences
University of California - Davis, CA 95616, USA
E-mail: amdandekar@ucdavis.edu

Resumo

A Doença de Pierce (PD) em videiras (*Vitis vinifera* L.) é causada pela bactéria *Xylella fastidiosa* (*Xf*), uma gama-proteobactéria responsável por diversas doenças em plantas economicamente importantes. Um sintoma característico da PD é a queimadura, caracterizado por zonas de clorose progredindo em necrose nas margens da lâmina foliar. O processo resultante da oclusão dos elementos do xilema por células bacterianas e pelo biofilme associados às mesmas, bem como o consequente bloqueio do fluxo da seiva, têm sido hipotetizado como a principal causa dos sintomas comumente observados na PD. Embora tal hipótese seja suportada por algumas evidências, o mecanismo de virulência de *Xf* não foi totalmente compreendido. A análise do secretoma de *Xf* Temecula 1 revelou que uma lipase/esterase (PD1703) é abundantemente secretada *in vitro*. Esta proteína foi caracterizada como ortóloga à proteína LipA presente em bactérias do grupo das Xanthomonas e funcionalmente caracterizada como degradante da parede celular neste grupo. A proteína LipA foi associada à matriz extracelular filamentosa e análises proteômicas adicionais revelaram sua presença nas vesículas de membrana externa. O acúmulo da proteína LipA em folhas de plantas infectadas foi positivamente associado aos sintomas da PD e inversamente correlacionado com o título bacteriano. LipA induziu resposta de hipersensibilidade em videiras e foi regulada por sinalização célula-célula, mecanismo conhecido por modular a patogênese bacteriana. Com base em tais evidências, propomos que a secreção da proteína LipA mediada pelas vesículas de membrana externa e sua liberação e acúmulo em margens foliares, onde leva ao desenvolvimento dos sintomas comumente observados na doença, seja um mecanismo essencial à patogênese de *X. fastidiosa* na PD.

Palavras-chave: *Xylella fastidiosa*, Doença de Pierce, lipase, esterase, LipA.

Abstract

Pierce's Disease (PD) of grapevines is caused by the bacterium *Xylella fastidiosa* (*Xf*), a xylem-limited gamma-proteobacterium that is responsible for several economically important diseases in many plants. A characteristic symptom of PD is leaf scorching, with regions of chlorosis progressing into necrotic zones at the peripheral margins of infected leaves. The occlusion of xylem elements and interference with water transport by *Xf* and its associated biofilm have been hypothesized as the main cause of PD symptom development; however, *Xf* virulence mechanism has not been elucidated. The analysis of *Xf* Temecula 1 secretome revealed a putative lipase/esterase (PD1703) that was abundantly secreted in the bacterial culture supernatant, and was characterized as a protein ortholog of the cell wall degrading enzyme LipA of *Xanthomonas* strains. The LipA was secreted and associated with a biofilm filamentous network and additional proteomic analysis revealed its abundant presence in outer membrane vesicles (OMVs). Accumulation of LipA in leaf regions was positively associated with PD symptoms and inversely correlated with bacterial titer. The lipase/esterase was found to elicit a hypersensitive response in grapevine and was regulated by quorum-sensing signaling, which is known to modulate bacterial pathogenesis. We propose that *Xff* pathogenesis is caused by LipA secretion mediated by OMV cargos, and its release and accumulation in leaf margins leads to the observed PD symptoms development.

Key-words: *Xylella fastidiosa*, Pierce's Disease, lipase, esterase, LipA.

Introduction

Xylella fastidiosa (*Xf*) is a fastidious, xylem-limited gamma-proteobacterium that causes several economically important diseases in many plants, including grapevine, citrus, periwinkle, almond, oleander, and coffee (1, 2). *Xf* is obligately vector-transmitted by various xylem sap-feeding sharpshooter insects (3, 4). The *Xf* subspecies *fastidiosa* (*Xff*), as exemplified by the California strain Temecula 1, causes Pierce Disease (PD) in grapevine, a disease that poses a great threat to the wine-growing regions in California (5). The *Xf* life cycle and virulence mechanism are not entirely understood (6). A characteristic PD symptom is marginal leaf chlorosis progressing to necrosis (leaf scorch). Three general explanations for PD symptom development have been proposed: occlusion of xylem elements and interference with water transport by *Xf* and its associated biofilm, plant systematic response, e.g., growth regulator imbalance, and *Xf*-generated phytotoxin (5). The occlusion hypothesis extends from early observations of xylem element blockage in PD (7). Generally plant species and regions of the plant body that show the most severe symptoms are those that have the greatest proportion of colonized vessels (3, 8-12), in agreement with the occlusion hypothesis. PD and other *Xf* diseases are associated with decreased leaf water potential (13) and altered carbon isotope incorporation (14), consistent with water stress. Although the occlusion hypothesis is widely considered to be supported, wilting and PD symptoms are not similar and appear to be additive in effect (15), and *Xf* accumulation in grapevine leaves is not correlated with PD symptom severity, favoring the hypothesis of plant systemic response (16). In contrast, our results, presented here, strongly support the third hypothesis of *Xf*-generated phytotoxin.

The secretion of virulence factors by pathogens has been shown to be an important mechanism by which many plant diseases are triggered. Unlike its closely related pathogens from genus Xanthomonas, *Xff* does not possess the type III secretion system (T3SS) (17); however, they share a similar type II secretion system (T2SS) that secretes a battery of important extracellular enzymes, which are responsible for the virulence of both pathogens (18). In *Xff*, genes encoding for plant cell wall degrading enzymes (CWDEs) such as

polygalacturonase, cellulase, lipase/esterase and several proteases have been identified (19). These enzymes may play a role in *Xff* migration inside the xylem vessels through the degradation of the pit membrane and also in the release of carbohydrates necessary for the bacterial survival. The degradation of the cell wall by CWDEs releases oligosaccharides as products, which can induce potent innate immune responses of plants. The plant defense responses include the production of phytoalexins, fortification of cell walls through the deposition of callose, oxidative burst, and induction of programmed cell death (20-22).

A type II secreted lipase named LipA has been characterized in the rice pathogen *Xanthomonas oryzae* pv. *oryzae* (*Xoo*). LipA is a 42-kDa α/β hydrolase fold protein with lipase/esterase function and is present in all xanthomonads whose genome has been sequenced and in many other gram-negative bacteria. Mutations in the LipA gene caused partial loss of *Xoo* virulence in rice. Immune defense responses in rice leaves and roots were elicited upon treatment with LipA, which induced callose deposition and programmed cell death. Recently, LipA from *Xoo* was characterized as a cell wall degrading enzyme with a carbohydrate-binding domain, which was determined to be essential for the protein virulence function (23). In addition, LipA was identified to be required for wild-type levels of virulence of *Xanthomonas campestris* pv. vesicatoria (*Xcv*) on tomato. Moreover, LipA has been shown to be expressed *in planta* by *Xcv* from the early stages of infection of tomato leaves (24).

We report here our analysis of the *Xff* Temecula1 (PD strain) secretome, including comparison with bacterial surfaceome, outer membrane and outer membrane vesicles proteome. The uncharacterized protein PD1703 was identified as the most abundant secreted protein. *In silico* analysis revealed PD1703 to be a *Xff* ortholog of the type II secreted and cell wall degrading protein LipA from xanthomonads. *Xff* LipA also was found in the cargo of outer membrane vesicles (OMVs), which is known for many pathogenic bacteria as a mechanism to deliver virulence factors (25). Further analysis revealed that LipA is also present in the infected grapevine leaf proteome and to be spatially associated with PD symptoms. Virulence assays on grapevine leaves showed the ability of *Xff* LipA to

induce hypersensitive response-like symptoms, demonstrating that LipA very likely plays an important role in *Xff* pathogenesis in PD.

Results

Lipases are highly abundant component of the *Xff* secretome.

The bacterial proteome was investigated following the workflow described in Fig. 1A in order to characterize the subcellular localization of *Xff* proteins. The identities of soluble supernatant proteins (SSPs) in culture medium were assessed after removing bacterial cells and cell fractions from the media by a series of ultracentrifugation and concentration steps. A total of 24 SSPs were identified by LC-MS/MS in the culture supernatant (Table 1), which includes many potential cell wall degrading enzymes such as lipases/esterases (PD1703, PD1702 and PD1211), proteases (PspB, PD0657, PD0950, PD0956 and PD1850) and cellulase (GuxA). SSPs potentially related to cell adhesion (PspA and XadA), bacterial toxicity (FrpC), and pathogenesis (PD1506 and VirK) were also identified. The separation of SSPs proteins by one-dimensional SDS-PAGE (Fig. 1B) revealed a prominent 40-50 KDa band, indicating that few proteins were highly abundant in *Xff* secretome. Followed by in-gel digestion, the mass spectrometry analysis of this particular band was carried out and two 42KDa (PD1703, PD1702) and one 46 KDa (PD1211) putative uncharacterized proteins were identified. The high amino acid sequence homology of these three proteins (Fig. S1) allowed us to estimate their relative abundance by their number of assigned spectra obtained in our proteomic analysis, which revealed that PD1703 (64.5%; 783) is relatively more abundant in the secretome when compared to PD1702 (34.2%; 268) and PD1211 (1.3%; 10) (Fig. 1B). *In silico* analysis revealed that PD1703 was predicted to be a secreted lipase/esterase protein and shared high degree of sequence similarity with the cell wall-degrading enzyme LipA from *Xanthomonas oryzae* pv. oryzae (*Xoo*) (23) and *Xanthomonas campestris* pv. vesicatoria (*Xcv*) (24), which suggests that *Xff* PD1703 is an ortholog of LipA-like proteins found in many *Xanthomonas* strains. In order to confirm the lipase/esterase functions of this highly abundant protein found in the secretome, we evaluated the enzymatic activity of *Xff* SSPs on short- and long-chain triacylglycerides. As reported for *Xoo* LipA (23), *Xff* secreted proteins can degrade smaller chain length triacylglycerides like tributyrin (C4) but has no activity on long-chain triacylglycerides like tricaprin (C10) (Fig. S2A). Similarly to *Xoo* LipA, *Xff* SSPs also show esterase activity on p-nitrophenyl butyrate (pNP-C4) (Fig. S2B).

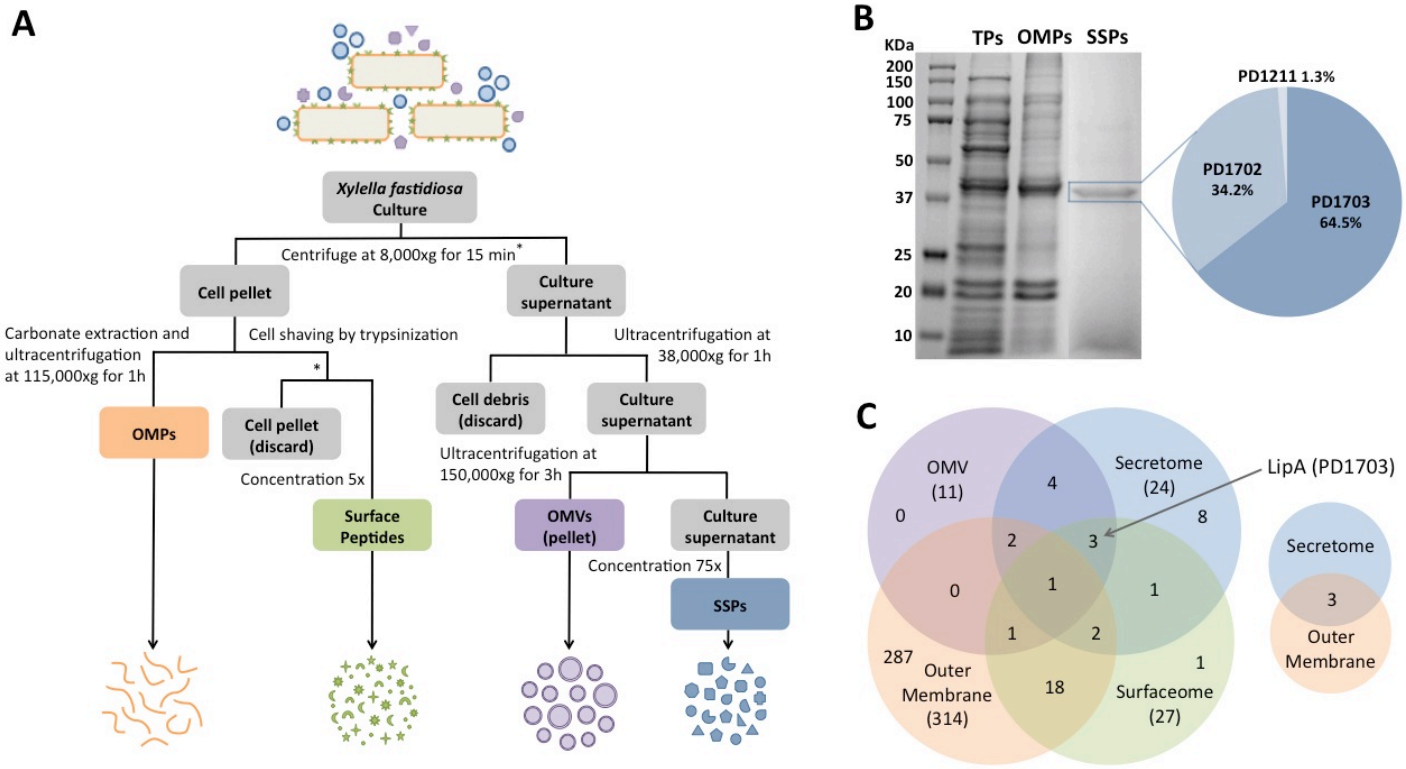

Fig.1: *X. fastidiosa* subcellular proteomic analysis. (**A**) Workflow describing the procedures used for the isolation of *X. fastidiosa* Temecula 1 outer membrane proteins (OMPs), outer membrane vesicles (OMVs), surface peptides (surfaceome) and soluble supernatant proteins (SSPs). Outer membrane proteins were extracting using 0.1 M sodium carbonate (pH 11.0) buffer followed by mass spectrometry. For the isolation of surface peptides, cells ($4x10^8$ cells/mL) were harvested from a culture (4-6 days old) and subjected to tryptic digestion (cell shaving). Peptides were concentrated (5x) and directly subjected to LC/MSMS. OMVs were purified from the culture supernatant following two ultracentrifugation steps (38,000 x *g* for 1h to pellet cell debris followed by 150,000 x *g* for 3h for OMVs precipitation). The remaining supernatant was concentrated (~75-100x) using Amicon Ultra-15 3K filters units for the identification of the SSPs by mass spectrometry. (**B**) SDS-PAGE 12% resolution of 10 μg of *Xff* total protein (TP), OMP (Table S2) and SSPs (Table 1). Three putative lipase/esterases (PD1703, PD1702, and PD1211) were identified in the highlighted band, which is mostly composed by PD1703 (LipA) and PD1702. (**C**) Venn diagram quantifying the number of proteins identified in each subcellular proteome. The major outer membrane protein MopB was found in all samples, although it is scarcely present in the secretome. The lipase/esterase LipA (*) was found in the secretome, surfaceome and OMV proteome.

Table 1: List of *X. fastidiosa* Temecula 1 soluble supernatant proteins (SSPs) identified in the secretome.

Accession number[1]	Protein description	Gene name	OMV	Surface	OM	Prot. local.[2]	Theor. Mw[3]	Signal Pept.[4]	SecP score[5]	Seq. coverage	Matched peptides
Q87AW0	Putative uncharacterized protein	PD1703	√	√	-	U	42.4	-	0.889430	78.80%	102
Q87AW1	Putative uncharacterized protein	PD1702	√	-	-	U	42.7	-	0.885983	83.90%	36
Q87DF4	Outer membrane protein XadA	xadA	√	√	-	U	97.5	-	0.963014	34.80%	28
Q87BM1	Bacteriocin	frpC	√	√	-	EC	150.3	-	0.605475	19.20%	21
Q87EJ4	Serine protease	pspB	√	-	-	OM	101.3	26|27	-	22.10%	20
Q87DM5	Putative uncharacterized protein	PD0657	-	-	-	EC	34.1	29|30	-	37.00%	7
Q87C82	Putative uncharacterized protein	PD1211	√	-	-	U	46.4	-	0.939004	30.20%	13
Q87AL6	Outer membrane protein	ompW	√	-	√	OM	23.1	23|24	-	36.70%	12
Q87AV4	Outer membrane protein	mopB	√	√	√	OM	42.3	-	0.939696	24.40%	7
Q87BF0	Hemolysin-type calcium binding protein	PD1506	√	-	-	EC	164.2	-	0.728400	7.23%	5
Q87CV6	Serine protease	PD0950	-	-	-	OM	96.0	-	0.914469	7.26%	4
Q87E92	Chorismate mutase	pheA	-	-	-	P	21.4	-	0.115485	34.00%	6
Q87CV2	Putative uncharacterized protein	PD0956	-	-	√	U	37.2	-	0.890737	21.60%	6
Q87BZ7	Putative uncharacterized protein	PD1299	-	√	-	U	55.7	-	0.898888	11.10%	6
Q87D31	VirK protein	PD0855	-	-	-	U	16.0	22|23	-	24.80%	4
Q87AH5	Peptidase (M20/M25/M40 family)	PD1850	-	-	-	U	57.7	-	0.582143	7.94%	4
Q87EI9	Putative uncharacterized protein	PD0318	-	-	√	OM	110.9	33|34	-	3.87%	4
Q87E00	Cellulose 1,4-beta-cellobiosidase	guxA	-	-	-	OM	67.7	-	0.883389	7.31%	3
Q87AN1	Hemagglutinin-like protein	pspA	-	-	-	OM	355.2	-	0.957381	0.95%	3
Q87BN7	Aminotransferase	aspC	-	-	-	C	46.3	-	0.092435	3.06%	2

Q87DY9	Putative uncharacterized protein	PD0540	-	√	√	U	15.2	-	0.903987	18.0%	2
Q87D30	Peptidyl-dipeptidase	dcp	-	√	√	C	77.5	-	0.798642	2.62%	2
Q87CK4	Putative uncharacterized protein	PD1063	-	-	√	OM	21.1	20|21	-	13.7%	2
Q87C13	TonB-dependent receptor	PD1283	√	-	√	OM	102.7	31|32	-	2.82%	2

1: Protein accesion number at UniProt Knowledgebase (UniProtKB; http://www.uniprot.org/);

2: Protein localization as prediceted by PSORTb v. 3.0.2 Subcellular Localization Prediction Tool (http://www.psort.org/psortb/; C: Cytoplasmic; OM: Outer Membrane; P: Periplasmic; EC: Extracellular; U: Unknown);

3: Theoretical protein molecular weight shown in KDa;

4: Position of signal peptide cleavage site as predicted by SignalP 4.0 Server (http://www.cbs.dtu.dk/services/SignalP/);

5: Prediction of non-classical protein secretion by SecretomeP 2.0 Server (http://www.cbs.dtu.dk/services/SecretomeP/) used for proteins without signal peptide. Score >0.5 indicates non-classical secretion.

Xff secretes LipA as cargo in outer membrane vesicles.

Gram-negative bacteria produce outer membrane vesicles (OMVs) that contain biologically active proteins and perform diverse biological processes (25, 26). The production of OMVs by *Xff* was recently reported elsewhere (27). However, the complete OMV protein cargo was not investigated, as described for many other gram-negative bacteria species (25), including the *Xff* closely related pathogen *Xanthomonas campestris* pv. campestris (*Xcc*) (28). The transmission electron microscopy (TEM) analysis of the negatively stained material resultant from the OMV purification process (Fig. 1A) revealed that *Xff* releases OMVs (Fig. 2A). Our investigation of OMV protein cargo by LC-MS/MS allowed us to identify 11 proteins (Table 2). Interestingly, the most abundant SSP, LipA (PD1703), was also found as part of the OMV cargo. Immunoblot analysis confirmed the localization of *Xff* LipA in the secretome as well OMV proteome (Fig. 2C). In addition to LipA, the secreted proteins PD1702, XadA and bacteriocin were also identified as part of the OMV cargo, indicating that the delivery of these proteins in the host could also be mediated by OMVs. Four outer membrane proteins (MopB, OmpW, serine protease PspB and TonB-dependent receptor PD1283) were also identified as part of the *Xff* OMV proteome. MopB, which was previously identified by us as the major *Xff* OMP (29), OmpW and the TonB-dependent receptor PD1283 were also found in our OM preparation (Table S2). The presence of MopB in both the *Xff* OM and OMV was confirmed by immunoblot (Fig. 2D). Although MopB was found in the secreted proteomic analysis (LC-MS/MS) (Table 1), it was not detected by immunoblot analysis of the same sample (Fig. 2D), indicating that its residual presence might be the result of contamination due to its high abundance in the cell outer membrane. Interestingly, the elongation factor Tu (EF-Tu), which is known to be a PAMP in many gram-negative bacteria (30, 31), was abundantly found in *Xff* outer membrane, but was not identified in *Xff* secretome or as part of the OMV cargo (Table S2; Fig. 2E).

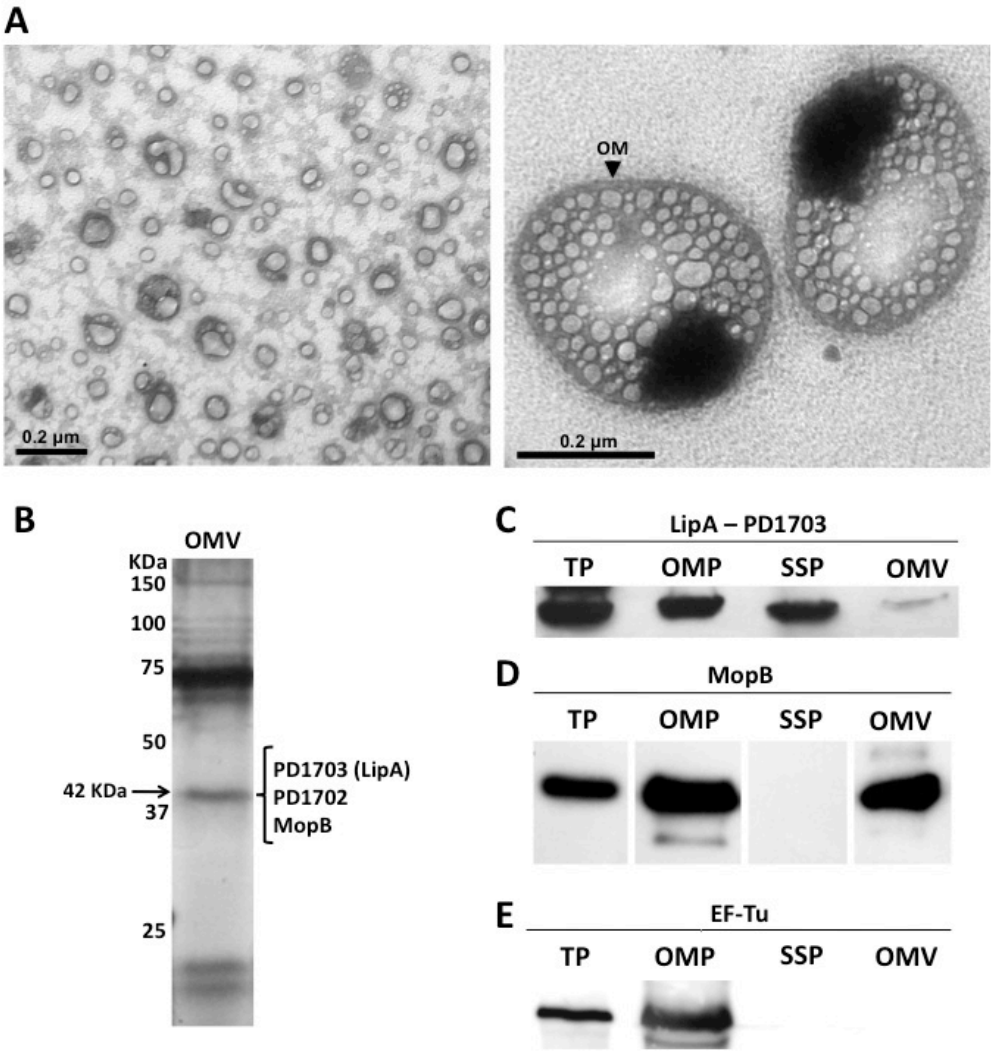

Fig. 2: *X. fastidiosa* outer membrane vesicles (OMVs) visualization and protein cargo analysis. (**A**) Electron micrograph of negatively stained outer membrane vesicles extracted from the *Xff* Temecula 1 cell free supernatant. Both small (left; <200 nm diameter) and large (right; up to 400 nm diameter) OMVs were identified. The black arrow indicates the outer membrane, which was released from the bacterial cell to pack the periplasmic content and to produce the OMV. Large OMVs appear to contain an electrodense material of unknown composition that is not seen in small OMVs. (**B**) Silver-stained SDS-PAGE 12% separation of OMV cargo showing the three 42 KDa proteins (LipA, PD1702 and MopB) found in the OMV proteomic analysis (Table S1). (**C-E**) Immunoblot detection of LipA, MopB, and EF-Tu in *Xff* total proteins (TP), outer membrane proteins (OMP), soluble supernatant proteins (SSP), and outer membrane vesicle proteins (OMV). For TP, OMP and SSP, 10 μg of proteins were loaded in the gel; however, only 2 μg of proteins were loaded in OMV due to the high non-protein content of this sample, which might explain the weak detection of LipA, as shown in C.

Table 2: List of proteins identified in *X. fastidiosa* Temecula 1 outer membrane vesicles (OMVs) proteomic analysis.

Accession number[1]	Protein description	Gene name	SSP	Surface	OM	Prot. local.[2]	Theor. Mw[3]	Sequence coverage	Matched peptides
Q87DF4	Outer membrane protein XadA	xadA	√	√	-	U	97.5	55.0%	61
Q87AW0	Putative uncharacterized protein	PD1703	√	√	-	U	42.4	67.0%	22
Q87AW1	Putative uncharacterized protein	PD1702	√	-	-	U	42.7	63.0%	11
Q87AL6	Outer membrane protein ompW	ompW	√	-	√	OM	23.1	19%	6
Q87AV4	Outer membrane protein mopB	mopB	√	√	√	OM	42.3	15%	5
Q87AA4	Fimbrial protein	pilA	-	√	√	EC	15.3	15%	2
Q87BM1	Bacteriocin	frpC	√	√	-	EC	150.3	8%	7
Q87EJ4	Serine protease	pspB	√	-	-	OM	101.3	4%	4
Q87C13	TonB-dependent receptor	PD1283	√	-	√	OM	102.7	4%	3
Q87C82	Putative uncharacterized protein	PD1211	√	-	-	U	46.4	6%	2
Q87BF0	Hemolysin-type calcium binding protein	PD1506	√	-	-	EC	164.2	4%	2

1: Protein accesion number at UniProt Knowledgebase (UniProtKB; http://www.uniprot.org/);

2: Protein localization as prediceted by PSORTb v. 3.0.2 Subcellular Localization Prediction Tool (http://www.psort.org/psortb/; OM: Outer Membrane; EC: Extracellular; U: Unknown);

3: Theoretical protein molecular weight shown in KDa.

LipA is localized in the secreted filamentous network.

To visualize *Xff* secreted material distribution pattern, we examined bacteria cells in culture by means of scanning and transmission electronic microscopy (SEM and TEM). Negatively stained cell clusters show that *Xff* produces cell aggregates embedded in a dense secreted material (Fig. 3A) possibly composed of EPS and proteins that are weakly attached to the bacterial surface. Fig. 3B shows the same dense material surrounding planktonic cells. SEM analysis of the bacterial culture revealed that *Xff* secretes a filamentous network (Fig. 3C and D) of unknown composition similar to the matrix seen surrounding cells aggregates in the xylem vessels of infected grapevines (32). TEM analysis of the secreted matrix revealed its close localization to the *Xff* cells *in vitro* (Fig. 3E). Immunogold labeling and TEM revealed that LipA is embedded in the *Xff* secreted network as shown in Fig. 3F.

LipA accumulates abundantly in leaf regions having minimal *Xff* titer and is associated with PD symptoms.

Although LipA was found to accumulate in both OMVs and the secreted matrix of *Xff* cells, its localization in *Xff*-infected host tissue was unknown. In order to search for LipA as well as for other potential secreted virulence factors in the host, we evaluated the total leaf proteome of *Xff* infected and non-infected grapevines. A total of 524 proteins were found, out of which 6 proteins were of *Xff* origin (Table 3). Interestingly, LipA (i.e., the most abundantly secreted protein) and MopB (i.e., the most abundant protein in the outer membrane) were also identified in the host tissue. The surface protein Hsf was found in the infected grapevine leaves, even though it was not previously identified in our secretome analysis, which suggests that both expression and secretion of Hsf might be triggered during the infection/colonization process. As expected, no *Xff* protein was found in the non-infected grapevine leaves.

The accumulation of LipA in the host tissue followed by *Xff* infection confirmed our hypothesis that LipA is highly expressed and secreted not only *in*

vitro but also during the *Xff* infection/colonization process in the host. We postulated that LipA could be playing an important role in *Xff* pathogenesis in grapevines as observed for *Xoo* LipA, which is known to elicit callose deposition and programmed cell death in rice (23, 33). In an effort to test our hypothesis, we evaluated whether the presence and abundance of LipA correlates with Pierce's Disease symptoms in infected (12 wpi) grapevine leaves. First, we analyzed the distribution of the bacterial population inside the host followed by the division of the tested leaves in three major areas (inside, middle and outside), as shown in Fig. 4A. The number of *Xff* cells present in each portion of the leaf was determined to be significantly different. *Xff* was abundantly found in the inside portion of the infected leaves closely associated with the petiole, and its population decreased significantly in the middle and outside areas specially closer to the edges (Fig 4B). Interestingly, the clearest PD symptom in grapevines – which is characterized by the marginal leaf necrosis (often called leaf scorch) – shows a gradient of abundance that is opposite to that of *Xff* cells, indicating that PD symptoms are not associated with the presence of *Xff* in the symptomatic lesions, as previously observed (16). We postulated that *Xff* could be releasing from its colonized region near the petiole either or both of LipA-containing OMVs or SSP. These could result in LipA accumulation, causing PD symptoms. In order to test our hypothesis, we detected LipA using a polyclonal antibody in the three divided areas described above. Interestingly, LipA was found to be slightly more abundant in the leaf edges when compared to the middle and inside portions, as shown in Fig. 4C. However, when the amount of LipA per *Xff* cell was calculated, a difference of ~100-fold ($p<0.05$) was observed (Fig. 4D).

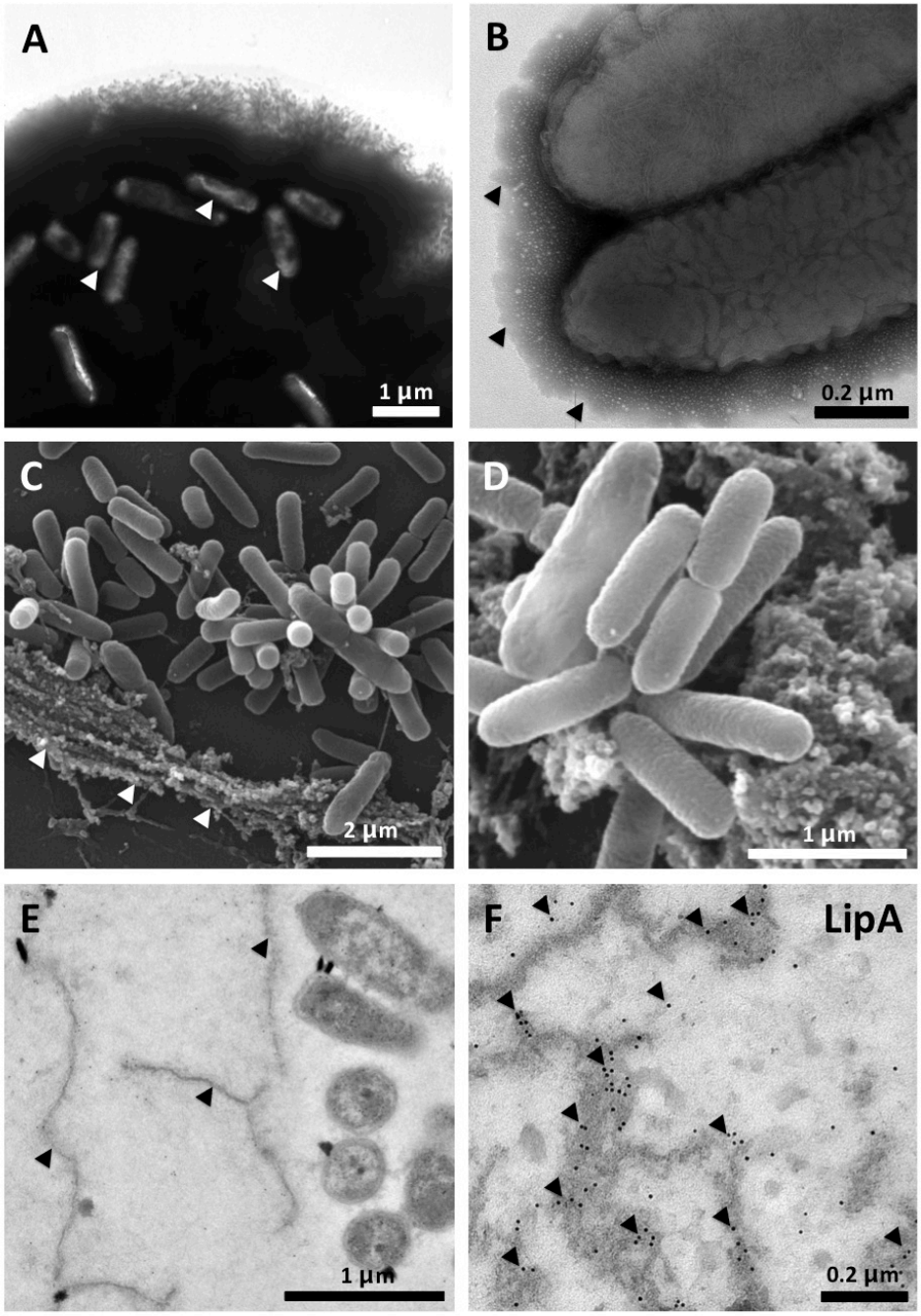

Fig. 3: Electron microscopy analysis of *Xff* cells and the secreted filamentous network. (**A**) Negative staining of *Xff* aggregates showing the abundant secreted material in which bacterial cells (white arrow) are imbedded. (**B**) Closer look at the secreted material surrounding *Xff* cells isolated from the same culture shown in A. (**C-D**) Scanning electron microscopy of *Xff* showing bacterial cells surrounded by the secreted filamentous network (white arrows). (**E-F**) Immunogold detection of LipA in the secreted filamentous network (black arrows) surrounding *Xff* cells (E). LipA was found in abundance in the secreted network as shown in F (black arrows).

Table 3: List of *X. fastidiosa* Temecula 1 proteins found in infected grapevine leaf proteomic analysis.

Accession number[1]	Protein description	Gene name	SSP	Surface	OMV	OM	Prot. local.[2]	Theor. Mw[3]	Sequence coverage	Matched peptides
Q87AW0	Putative uncharacterized protein	PD1703	√	√	√	-	U	42.4	19.6%	7
Q87AV4	Outer membrane protein	mopB	√	√	√	√	OM	42.3	11.1%	3
Q87BC0	60 kDa chaperonin	groL	-	√	-	√	C	57.7	6.2%	2
Q87B34	Glyceraldehyde-3-phosphate dehydrogenase	gapA	-	-	-	√	C	36.0	5.0%	2
P63774	10 kDa chaperonin	groS	-	√	-	√	C	10.0	25.3%	2
Q87DE1	Surface protein	hsf	-	-	-	-	U	203.1	1.46%	2

1: Protein accesion number at UniProt Knowledgebase (UniProtKB; http://www.uniprot.org/);

2: Protein localization as prediceted by PSORTb v. 3.0.2 Subcellular Localization Prediction Tool (http://www.psort.org/psortb/; C: Cytoplasmic; OM: Outer Membrane; U: Unknown);

3: Theoretical protein molecular weight shown in KDa.

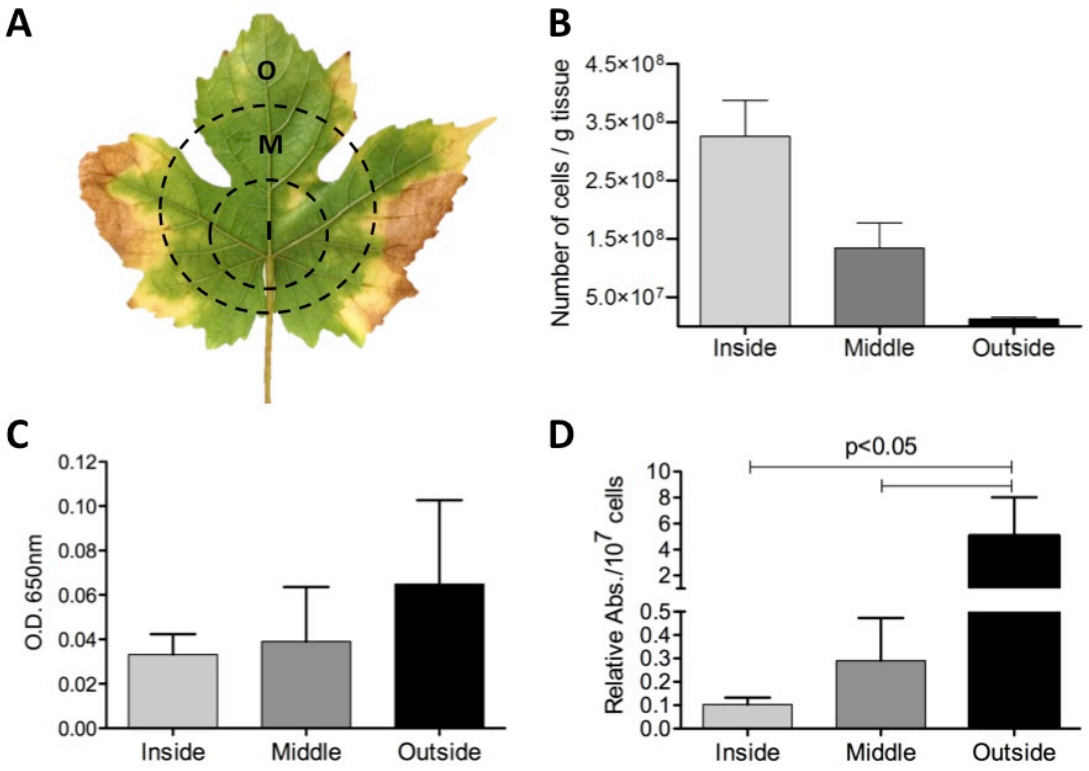

Fig. 4: LipA movement detection in grapevine leaves. (**A**) Grapevine leaf showing the three (1-2 cm long) segments used for detection of LipA: I (inside), M (middle) and O (outside). (**B**) The titration of *Xff* cells in which leaf segment (n=3) revealed the reduction (about 10-fold) of the bacterial population in the leaf edges (outside) when compared to the center (inside). The bacterial titration was carried out using a standard curve of *Xff* dilutions (5 dilutions; R^2=0.9817; p<0.01). (**C-D**) The amount of LipA detected in grapevine leaves differ slightly in the different segments (C), however, the relative abundance of LipA per number of *Xff* cells (D) present is significantly higher in the outside area when compared to middle and inside segments (n=3; p<0.05), indicating that the secreted LipA is moving from the *Xff*-crowded area to the leaf symptomatic extremities where the bacteria is scarcely present. This experiment was conducted twice with similar results.

Wild-type *Xff* and its quorum-sensing mutants have distinct patterns of expression for LipA and other secreted proteins.

Cell–cell signaling plays an important role in the virulence of many plant pathogenic bacteria. *Xff* produces the quorum-sensing signaling molecule designated DSF (diffusible signaling factor), which is known to regulate bacterial pathogenesis. In *Xanthomonas campestris* pv. campestris (*Xcc*) and *Xanthomonas*

oryzae pv. oryzae (*Xoo*), DSF-deficient mutants have reduced virulence (34, 35). However, *Xff* rpfF mutants that are deficient in DSF production possess a hypervirulent phenotype when inoculated in grapevines (32). The rpfF gene is required for DSF production in both *Xff* and Xanthomonas species. Interestingly, *Xff rpfC* mutants have been shown to overproduce DSF, to have a hyperattachment phenotype, and to be deficient in virulence and movement in the xylem vessels of grapevines (36). For specific virulence-related genes, messenger RNA accumulation for *rpfC* and *rpfF* mutants relative to wildtype was assessed by RT-PCR (Fig. 5). The three most abundant secreted lipases (PD1703, PD1702 and PD1211), as well as other putative virulence factors (the serine protease PD0950 and the uncharacterized secreted protein PD0657), were down-regulated in the *rpfC* mutant, which has been shown to be non-pathogenic. *Xff* genes coding for hemolysin-type calcium binding protein PD1506, and the outer membrane proteins PspA, PspB, and MopB are up-regulated in the *rpfC* mutant strain.

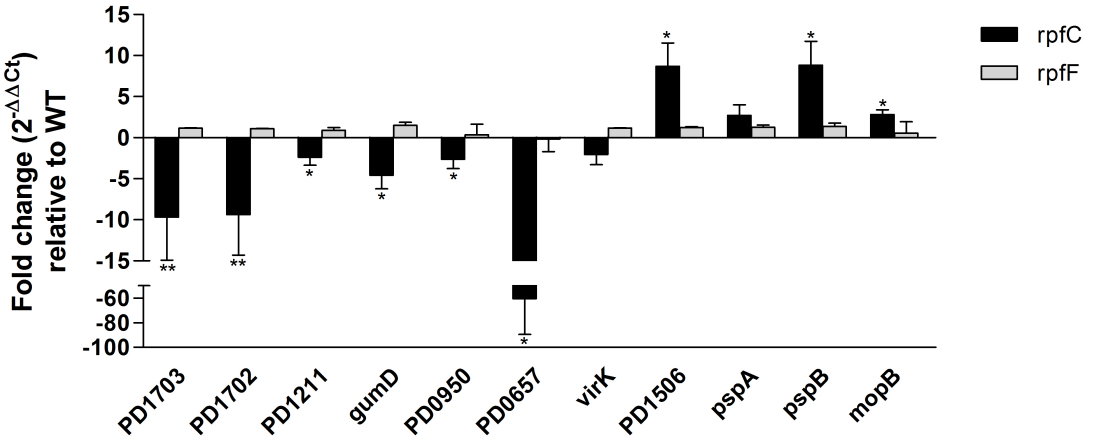

Fig. 5: LipA is down-regulated in a *Xff* virulence deficient, quorum-sensing mutant. Comparison of RNA accumulation for mutants and wildtype by RT-PCR revealed that the three most abundant secreted lipases (LipA-PD1703, PD1702 and PD1211) as well as other putative virulence factors are regulated by *rpfC*. RNA was extracted from *Xff* cells grown in PD3 medium (3 flasks/condition; 10^7-10^8 cells/mL) at 28°C and 120 rpm. The 16S rRNA gene was used as endogenous control. Unpaired t test with Welch's correction was used for statistical analysis (One-tailed p value; *p<0.05; **p<0.01).

LipA elicits a hypersensitive response in grapevine.

LipA from *Xoo* has been shown to elicit innate immune response mediated by the cell wall degradation and also to induce callose deposition and trigger programmed cell death on rice (23, 33). In addition, LipA has been shown to be required for wild-type levels of virulence of *Xcv* on tomato (24). The analysis of the high-resolution crystal structure of *Xoo* LipA revealed that the canonical catalytic triad residues Ser-176, Asp-336 and His-377 forms the Gly-X-Ser-X-Gly motif that is conserved in hydrolases. Moreover, mutation in the residue Ser-176 resulted in the reduction of the virulence of *Xoo* when inoculated on rice, confirming that the enzymatic activity of LipA is essential for optimal levels of virulence (23). Our *in silico* analyses revealed that both *Xff* LipA catalytic triad from Temecula 1 (PD1703) and 9a5c (XF0357) strains is located in the residues Ser-165, Asp-325 and His-367 (Fig. S1). In order to test whether LipA contributes to *Xff* virulence in grapevine, we pressure-infiltrated leaves with protein extract from *E. coli* bearing both LipA- and ΔS165LipA-expressing plasmids or its empty vector control. Heterologous expression was confirmed by immunoblot detection of both LipA and ΔS165LipA in the total protein sample and culture supernatant (data not shown). The LipA, but not the control (Fig. 6A-B), extract induced necrosis in the infiltrated area, indicating that LipA may be contributing to *Xff* pathogenesis in grapevines. Interestingly, *Xff* LipA mutated in the Ser-165 elicited reduced HR-like symptoms when infiltrated in grapevine leaves (Fig. 6C), indicating that enzymatic activity of *Xff* LipA is essential for optimal levels of virulence, essentially as observed for *Xoo* LipA.

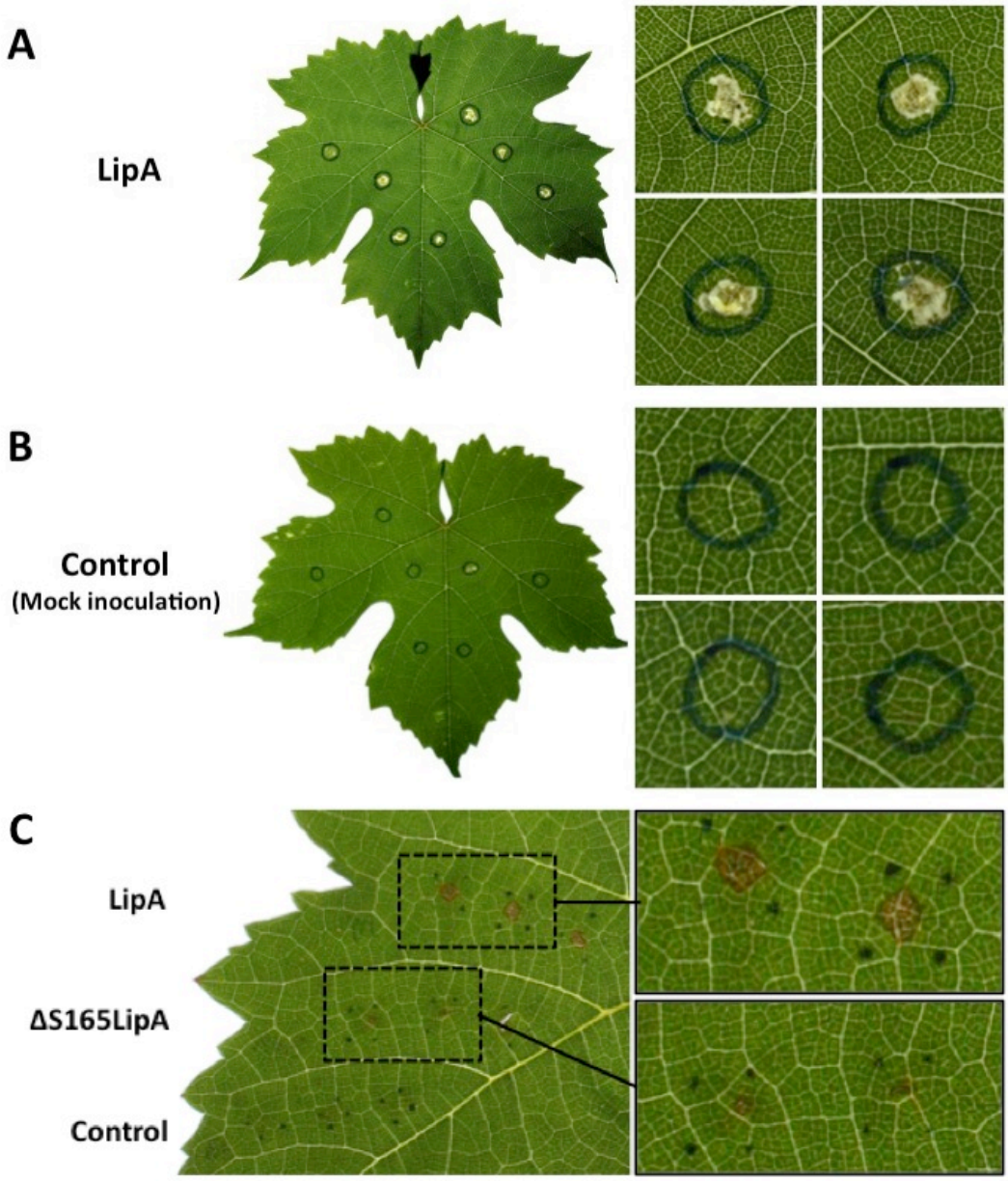

Fig. 6: LipA elicits HR-like symptoms in grapevine leaves. Crude protein from LipA-expressing *E. coli* was isolated and syringe-infiltrated in grapevine leaves of greenhouse-grown plants. (**A**) HR-like symptoms appeared in 24 hours after infiltration. (**B**) No reaction was observed for the infiltration of crude protein from *E. coli* expressing the empty vector (pJexpress 401). (**C**) Reduction of HR-like symptoms caused by ΔS165LipA, in which the residue Ser-165 from *Xff* LipA catalytic triad was mutated. Wildtype LipA caused the same level of necrosis as shown in A.

Supplementary Figures

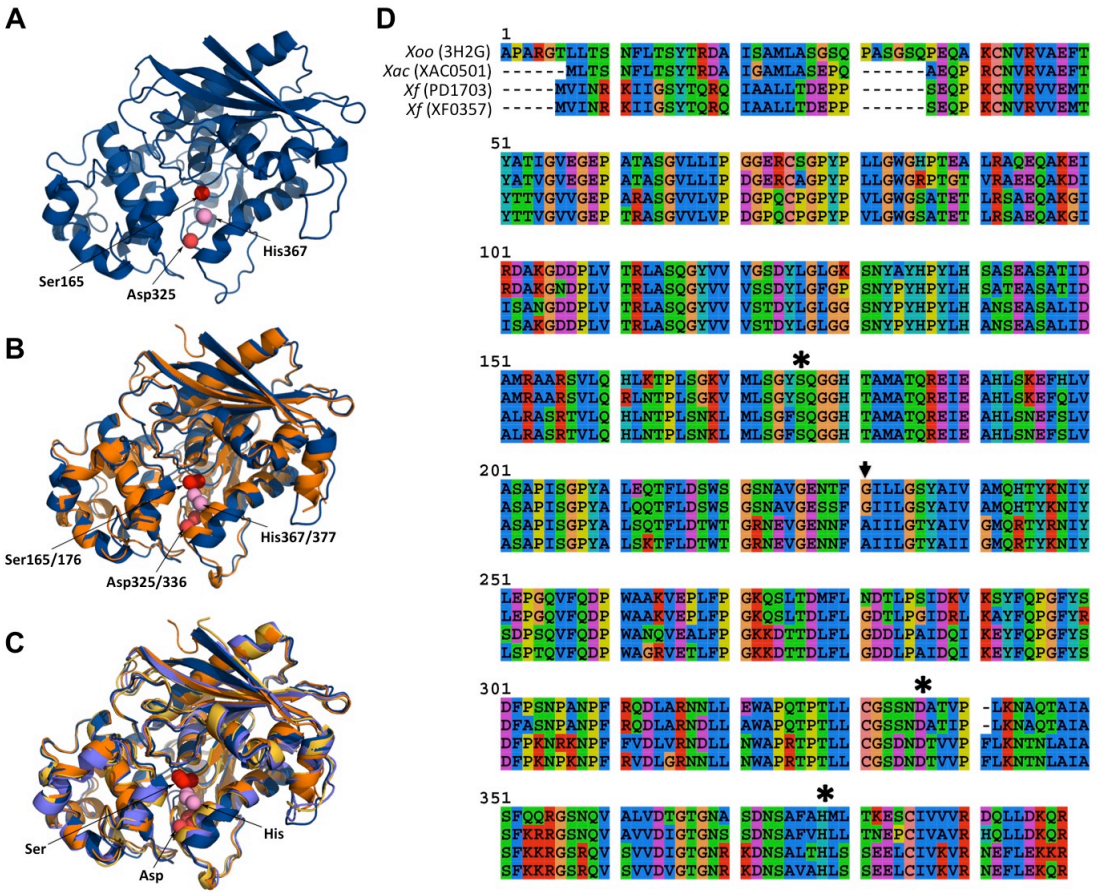

Fig. S1: *In silico* analysis of LipA. The structures for PD1703 (*X. fastidiosa* Temecula 1), XF0357 (*X. fastidiosa* 9a5c) and XAC0501 (*Xac*, *Xanthomonas axonopodis* pv. citri) were predicted using GENO3D (37). (**A**) The catalytic active triad in PD1703. The multiple superimpositions of these structures were obtained using MUSTANG (38). (**B**) The alignment of 3H2G (*Xoo*, *Xanthomonas oryzae* pv. oryzae) and PD1703 (colored orange and blue, respectively) (**C**) The alignment of all four structures - 3H2G, PD1703, XF0357 and XAC0501 (colored orange, blue, slate and yellow, respectively). (**D**) The multiple sequence alignment for these proteins was generated using Clustal W (39). The catalytic triad Ser-Asp-His is indicated by asterisks. In *Xf* strains, the residue Ala replaces the residue Gly-231 (indicated by a black arrow), which is required for the sugar ring positioning of the LipA-like carbohydrate-binding domain in *Xoo* (23). The alignment image was generated using Seaview (40).

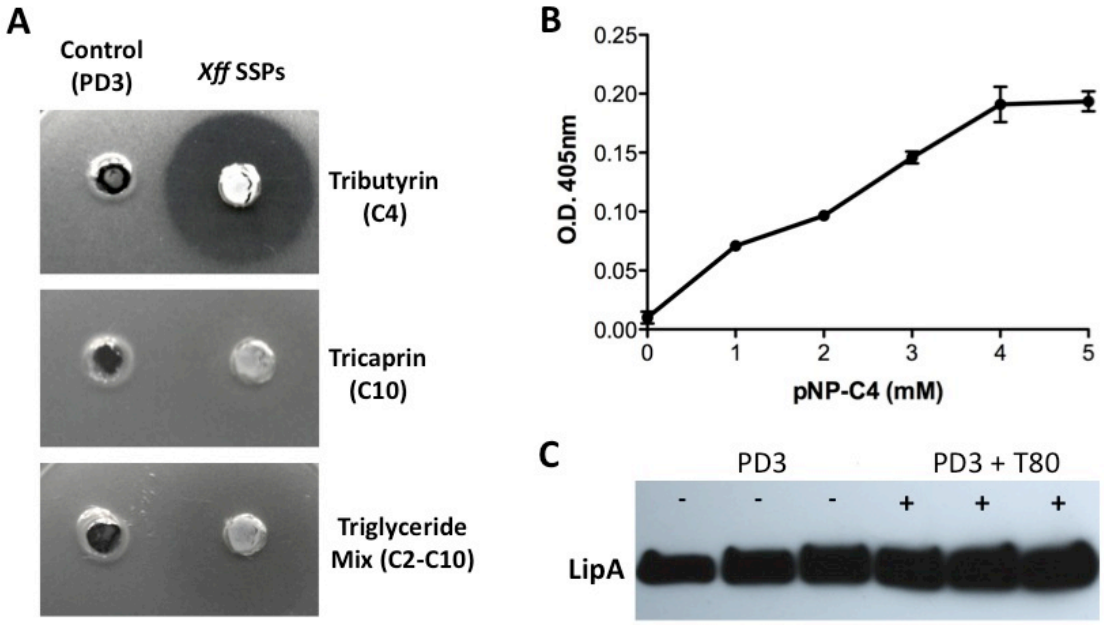

Fig. S2: *Xff* SSPs exhibit lipase/esterase activities. Triglycerides were incorporated into an agarose gel layer. Holes on the left received PD3 medium (control); holes on the right received *Xff* SSPs. (**A**) Presence of a zone of clearance indicates LipA activity on short-chain triacylglycerides (C4-Tributyrin), while no activity is seen on long-chain triacylglycerides (C10-Tricaprin). Weak activity is seen on a mixture of triglycerides that contains short- and long-chain triacylglycerides (C2-C10). (**B**) Esterase activity of *Xff* SPPs towards p-nitrophenol butyrate (pNP-C4) at 37°C in Tris-HCl, pH 7.5. A_{405} was measured after a 10 min incubation with increasing concentrations of the substrate. (**C**) Induction *in vitro* of LipA protein expression by Tween 80 was accessed after growing *Xff* in PD3 cultures supplemented with 0.1% (v/v) Tween 80 (3 flasks/condition; growth until $3x10^8$ cells/mL) followed by LipA immunoblot detection.

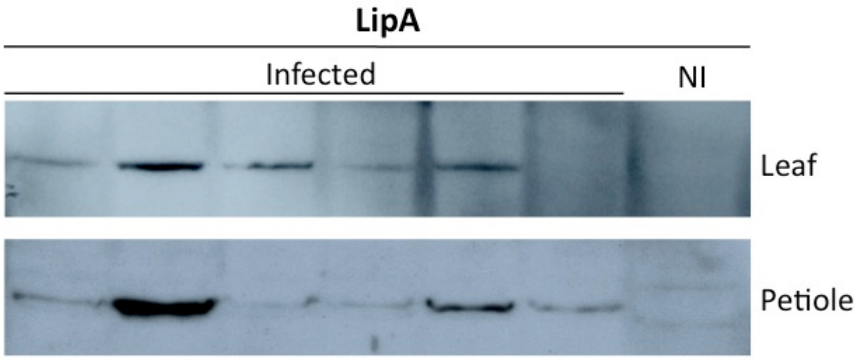

Fig. S3: *In planta* detection of LipA. Leaf and petiole proteins extracted from *Xff*-infected (12 wpi) and non-infected (NI) plants were used for detection of LipA (42kDa).

Supplementary Tables

Table S1: List of *X. fastidiosa* Temecula 1 proteins identified in the surfaceome (cell shaving) analysis.

Accession number[1]	Protein description	Gene name	SSP	OMV	OM	Prot. local.[2]	Theor. Mw[3]	Sequence coverage	Matched peptides
Q87DF4	Outer membrane protein XadA	xadA	√	√	-	U	97.5	12.10%	12
Q87BD1	Peptidyl-prolyl cis-trans isomerase	PD1525	-	-	√	OM	25.0	25.40%	6
Q87AW0	Putative uncharacterized protein	PD1703	√	√	-	U	42.4	20.40%	9
Q87BC0	60 kDa chaperonin	groL	-	-	√	C	57.7	9.32%	6
Q87DY9	Putative uncharacterized protein	PD0540	√	-	√	U	15.2	11.60%	2
Q87A98	Succinyl-CoA ligase [ADP-forming] subunit beta	sucC	-	-	√	C	41.0	10.60%	4
Q87BM1	Bacteriocin	frpC	√	√	-	EC	150.3	2.55%	4
Q87BZ7	Putative uncharacterized protein	PD1299	√	-	-	U	55.7	5.73%	3
Q87A38	Temperature acclimation protein B	PD1993	-	-	√	C	8.0	38.40%	3
Q87BK3	UTP-glucose-1-phosphate uridylyltransferase	gtaB	-	-	√	C	32.6	5.74%	2
P66380	30S ribosomal protein S12	rpsL	-	-	√	C	13.6	14.50%	2
Q87A29	50S ribosomal protein L1	rplA	-	-	√	C	24.3	9.48%	2
Q87D30	Peptidyl-dipeptidase	dcp	√	-	√	C	77.6	4.51%	3
Q87AA4	Fimbrial protein	pilA	-	√	√	EC	15.3	7.43%	2

P66349	30S ribosomal protein S10	rpsJ	-	-	√	C	11.5	10.70%	2
Q87D28	Putative uncharacterized protein	PD0858	-	-	-	U	18.5	12.20%	2
P66605	30S ribosomal protein S6	rpsF	-	-	√	C	16.4	6.29%	1
P63774	10 kDa chaperonin	groS	-	-	√	C	10.0	15.80%	2
Q87ER8	Putative uncharacterized protein	PD0230	-	-	√	U	12.5	9.09%	1
Q87A33	DNA-directed RNA polymerase subunit beta'	rpoC	-	-	√	C	155.8	1.56%	2
Q87A00	Oxidoreductase	PD2039	-	-	√	U	80.5	2.08%	2
Q87A31	50S ribosomal protein L7/L12	rplL	-	-	√	U	12.7	14.80%	2
Q87AV4	Outer membrane protein mopB	mopB	√	√	√	OM	42.3	3.08%	1
Q877P8	Elongation factor Tu	tufA	-	-	√	C	42.9	1.52%	1
Q87CB5	Peptidyl-prolyl cis-trans isomerase	PD1168	-	-	√	OM	24.8	6.90%	1
Q87E60	30S ribosomal protein S4	rpsD	-	-	√	C	23.4	4.33%	1
Q87E05	Phosphoenolpyruvate synthase	ppsA	-	-	√	C	87.3	1.00%	1

1: Protein accesion number at UniProt Knowledgebase (UniProtKB; http://www.uniprot.org/);

2: Protein localization as prediceted by PSORTb v. 3.0.2 Subcellular Localization Prediction Tool (http://www.psort.org/psortb/; C: Cytoplasmic; OM: Outer Membrane; EC: Extracellular; U: Unknown);

3: Theoretical protein molecular weight shown in KDa.

Table S2: List of *X. fastidiosa* Temecula 1 proteins identified in the outer membrane proteomic analysis.

Accession number[1]	Protein description	Gene name	Prot. local.[2]	Theor. Mw[3]	Sequence coverage	Matched peptides
28199417	60 kDa chaperonin	groL	C	58	97.8	66
28199862	Elongation factor Tu	tufA	C	43	86.1	32
28199584	Outer membrane protein	mopB	OM	42	49.3	25
28199254	Chaperone protein	dnaK	C	68	58.3	32
28198761	Peptidyl-dipeptidase	dcp	C	78	48.7	26
28199866	DNA-directed RNA polymerase subunit beta'	rpoC	C	156	41.3	41
28199169	TonB-dependent receptor	PD1283	OM	103	42.9	27
28199863	Elongation factor G	fusA	C	78	44.2	21
28199337	30S ribosomal protein S1	rpsA	C	62	46.2	17
28199830	Outer membrane export factor	tolC	OM	49	55.5	20
28199867	DNA-directed RNA polymerase subunit beta	rpoB	C	155	24.5	20
28198797	Outer membrane protein P6 precursor	PD0895	OM	21	44.3	11
28198239	Putative uncharacterized protein	PD0318	OM	111	23.0	18
28198193	Polyphosphate-selective porin O	oprO	OM	44	41.6	15
28198133	ATP-dependent RNA helicase	deaD	C	68	43.0	16
28198042	Leucyl aminopeptidase	pepA	C	52	43.1	13
28199166	Low molecular weight heat shock protein	hspA	U	18	73.7	9

28198164	Bifunctional aconitate hydratase 2	acnB	C	94	27.5	16
28199416	10 kDa chaperonin	groS	C	10	85.2	10
28199827	30S ribosomal protein S2	rpsB	C	29	50.0	11
28198356	50S ribosomal protein L2	rplB	C	30	41.8	10
28199449	Metallopeptidase	PD1570	P	78	32.7	14
28198247	Outer membrane antigen	oma	OM	88	21.0	13
28199468	TonB-dependent receptor	btuB	OM	114	31.9	17
28198925	Putative uncharacterized protein	PD1028	U	25	51.8	7
28199864	30S ribosomal protein S7	rpsG	C	17	49.6	13
28198126	Polynucleotide phosphorylase/polyadenylase	pnp	C	76	24.8	14
28199507	HflK protein	hflk	U	41	45.1	11
28198196	Heat shock protein 90	htpG	C	72	31.7	12
28199868	50S ribosomal protein L7/L12	rplL	U	13	57.3	11
28198158	Putative uncharacterized protein	PD0230	U	13	91.7	9
28198376	30S ribosomal protein S4	rpsD	C	23	58.6	10
28198666	Alpha-ketoglutarate decarboxylase	odhA	C	105	23.3	13
28198122	Translation initiation factor IF-2	infB	C	97	30.6	19
28199900	Oxidoreductase	PD2039	U	81	24.0	11
28198665	Dihydrolipoamide acetyltransferase	sucB	C	42	28.9	10
28199714	Fructose-bisphosphate aldolase	PD1845	C	36	41.6	8
28198359	30S ribosomal protein S3	rpsC	C	27	49.0	10

28199904	Protease IV	sppA	CM	69	23.5	10
28199497	Serine/threonine protein kinase	PD1620	OM	43	40.5	9
28198377	DNA-directed RNA polymerase subunit alpha	rpoA	C	37	44.3	13
28199574	OmpA family protein	ompA	OM	26	61.2	11
28198344	ATP synthase subunit beta	atpD	C	51	43.8	13
28198365	50S ribosomal protein L5	rplE	C	20	58.1	10
28199791	Fimbrial protein	pilA	EC	15	78.4	9
28199622	Putative ABC transporter ATP-binding protein	PD1751	C	62	24.5	11
77747677	Ketol-acid reductoisomerase	ilvC	C	39	46.6	10
28199859	Temperature acclimation protein B	PD1993	C	8	87.7	6
28199798	Succinyl-CoA synthetase subunit alpha	sucD	C	30	62.8	11
28198651	Subunit C of alkyl hydroperoxide reductase	ahpC	C	21	53.2	8
28198689	Precursor of drug resistance protein	acrA	U	44	41.7	9
28199797	Succinyl-CoA ligase [ADP-forming] subunit beta	sucC	C	41	29.7	8
28198385	Trigger factor	tig	C	48	23.0	7
28198007	Cell division protein	hflB	CM	71	17.8	6
28199726	Protein translocase subunit secA	secA	C	103	15.3	9
28199849	Ribonuclease E	rne	U	126	15.1	8
28199810	50S ribosomal protein L9	rplI	C	16	57.7	4
28198614	Virulence regulator	PD0708	C	16	61.6	5
28199748	Lipase/esterase	estA	OM	64	29.0	10

28198477	Septum site-determining protein	minD	C	29	78.1	13
28198269	Succinate dehydrogenase flavoprotein subunit	sdhA	CM	65	14.3	6
28199826	Elongation factor Ts	tsf	C	31	39.4	8
28199039	Twitching motility protein	pilT	C	38	36.0	10
28199506	Integral membrane proteinase	hflC	U	32	32.8	7
28197955	Biopolymer transport ExbB protein	exbB	CM	27	28.3	6
28199627	Hypothetical protein	PD1756	OM	34	35.8	7
28199090	ABC transporter phosphate binding protein	pstS	U	39	26.4	6
28199405	Peptidyl-prolyl cis-trans isomerase	PD1525	OM	25	53.0	10
28199549	Bacterioferritin	bfr	C	18	54.5	6
28199381	3-oxoacyl-(acyl carrier protein) synthase II	fabB	CM	43	46.5	9
28198372	50S ribosomal protein L15	rplO	C	15	53.1	6
28199723	Putative uncharacterized protein	PD1854	U	23	29.9	5
28199057	UDP-glucose dehydrogenase	ugd	C	50	26.9	9
28198353	50S ribosomal protein L3	rplC	C	23	38.1	6
28198346	ATP synthase subunit alpha	atpA	C	56	22.3	7
28199146	Enolase	eno	U	46	30.5	7
77747646	Phosphoenolpyruvate synthase	ppsA	C	87	25.8	13
28198403	Glutathione S-transferase	gst	C	23	48.3	6
28198480	Putative uncharacterized protein	PD0570	OM	44	20.0	7
28198937	Organic hydroperoxide resistance protein	ohr	C	15	67.8	8

28198389	Histone-like protein	hup	C	10	76.6	5
28198923	Glutamine synthetase	glnA	C	52	25.4	7
77747643	GTP-binding elongation factor protein	typA	CM	68	21.4	9
28199916	Transcription termination factor Rho	rho	C	48	18.5	6
28198370	30S ribosomal protein S5	rpsE	C	19	45.8	6
28199872	Transcription antitermination protein nusG	nusG	C	21	58.9	7
28199293	Glutaredoxin-like protein	grx	C	33	28.6	6
28199554	Two-component system, regulatory protein	popP	C	25	27.8	5
28198378	50S ribosomal protein L17	rplQ	C	14	50.0	6
28199609	Putative uncharacterized protein	PD1736	U	18	44.0	5
28198663	Peptidoglycan-associated outer membrane lipoprotein	pcp	OM	16	34.0	4
28198177	NADH dehydrogenase subunit G	nuoG	C	80	16.4	7
28199869	50S ribosomal protein L10	rplJ	C	19	36.6	4
28198354	50S ribosomal protein L4	rplD	C	22	46.5	7
28199172	Periplasmic protease	mucD	P	54	25.1	7
28198021	50S ribosomal protein L19	rplS	C	15	50.7	6
28198032	Carbon storage regulator homolog	csrA	U	8	63.4	3
28199870	50S ribosomal protein L1	rplA	C	24	35.8	4
28198140	Phosphomannose isomerase-GDP-mannose pyrophosphorylase	xanB	C	51	18.0	5
28198657	30S ribosomal protein S9	rpsI	C	14	52.3	5

28199329	Inosine-5'-monophosphate dehydrogenase	guaB	C	52	16.3	4
28199917	Isocitrate dehydrogenase [NADP]	icd	C	81	16.7	6
28198121	Transcription elongation factor nusA	nusA	C	56	12.5	5
28198753	Chemotaxis-related protein kinase	cheA	C	195	4.4	5
28198661	cAMP-regulatory protein	clp	C	26	29.7	5
28198400	50S ribosomal protein L28	rpmB	C	9	48.7	5
28198149	6-phosphofructokinase	pfkA	C	47	26.9	7
28199331	UTP-glucose-1-phosphate uridylyltransferase	gtaB	C	33	19.3	4
28198467	Rod shape-determining protein	mreB	C	39	33.4	8
28199586	TonB-dependent receptor	PD1711	OM	98	14.1	9
28199680	Dihydrolipoamide acetyltranferase	pdhB	C	58	13.8	5
28198358	50S ribosomal protein L22	rplV	C	12	50.5	5
28198688	Multidrug-efflux transporter	acrF	CM	114	8.2	7
28199503	Glyceraldehyde-3-phosphate dehydrogenase	gapA	C	36	30.4	5
28198367	30S ribosomal protein S8	rpsH	C	14	38.6	5
28197993	Signal recognition particle protein	ffh	CM	50	20.4	6
28198752	Pilus biogenesis protein	pilJ	CM	74	16.0	7
28198338	Tryptophan repressor binding protein	wrbA	U	20	22.2	4
28198364	50S ribosomal protein L24	rplX	C	11	44.8	6
77747670	Thiamine biosynthesis protein	thiC	C	66	13.1	5
28199786	Two-component system, regulatory protein	colR	C	25	24.9	3

28198352	30S ribosomal protein S10	rpsJ	C	12	31.1	3
28199201	Chromosome-partitioning protein	parB	C	34	15.2	3
28199877	50S ribosomal protein L25	rplY	C	23	30.0	4
28198018	30S ribosomal protein S16	rpsP	C	10	58.1	5
28199194	5-methyltetrahydropteroyltriglutamate--homocysteine methyltransferase	metE	C	86	9.9	4
28198141	Phosphoglucomutase	xanA	C	49	23.6	6
28199678	Outer membrane protein	ompW	OM	23	32.6	4
161484696	Aconitate hydratase	rpfA	C	101	7.6	4
28199621	Serine hydroxymethyltransferase	glyA	C	45	18.9	6
28199385	Pyruvate dehydrogenase E1 component	aceE	C	100	14.8	9
28198233	Putative uncharacterized protein	PD0312	P	10	50.0	2
28198174	NADH dehydrogenase subunit D	nuoD	C	49	11.0	3
28198112	Preprotein translocase subunit SecD	secD	CM	68	6.6	3
28198125	30S ribosomal protein S15	rpsO	C	10	46.5	4
77747692	GumK protein	gumK	C	31	24.6	4
28198655	50S ribosomal protein L31 type B	rpmE2	U	9	63.8	4
28199865	30S ribosomal protein S12	rpsL	C	14	37.9	3
28197947	DNA polymerase III subunit beta	dnaN	C	42	15.6	4
28198567	Thiol:disulfide interchange protein	dsbA	P	28	24.6	5
28198030	Recombinase A	recA	C	38	18.2	4

28198270	Succinate dehydrogenase iron-sulfur protein	sdhB	CM	30	16.1	2
28198450	Putative uncharacterized protein	PD0540	U	15	43.8	4
28199283	Isopropylmalate isomerase large subunit	leuC	C	51	11.4	3
28199536	Lipoprotein precursor	vacJ	OM	39	13.1	4
28198316	Carbamoyl phosphate synthase large subunit	carB	U	117	7.7	4
28198298	Phage-related protein	PD0381	U	11	55.9	4
28198363	50S ribosomal protein L14	rplN	C	13	34.4	6
28199812	30S ribosomal protein S6	rpsF	C	16	33.6	4
28198387	ATP-dependent protease ATP-binding subunit	clpX	C	47	19.2	5
28198664	Dihydrolipoamide dehydrogenase	lpd	C	51	9.4	3
28199926	TonB-dependent receptor	cirA	OM	96	5.8	3
28198360	50S ribosomal protein L16	rplP	C	15	27.7	3
28199722	Zinc protease	PD1853	P	106	6.8	4
28199094	Phosphate regulon transcriptional regulator	phoU	C	27	10.8	2
28198033	Oligopeptidase A	prlC	C	76	7.3	3
28199633	Methionyl-tRNA formyltransferase	fmt	C	33	15.6	3
28198097	Phosphoribosylaminoimidazole-succinocarboxamide synthase	purC	C	34	17.2	3
28198774	Superoxide dismutase (Mn)	sodA	P	26	25.7	4
28198348	ATP synthase subunit b	atpF	CM	17	31.4	3
28198428	Putative uncharacterized protein	PD0518	U	179	2.4	3

28198416	Putative uncharacterized protein	PD0504	U	14	19.4	3
28198374	30S ribosomal protein S13	rpsM	C	14	34.7	4
28198334	TldD protein	tldD	C	51	9.1	3
28199839	Isocitrate dehydrogenase	icdA	C	36	27.5	6
28198362	30S ribosomal protein S17	rpsQ	C	10	39.3	3
28198195	Malic enzyme	maeB	C	83	5.9	2
28199783	Threonyl-tRNA synthetase	thrS	C	73	11.3	4
28198563	Glutamate-cysteine ligase precursor	gshI	C	51	9.7	4
28199282	Isopropylmalate isomerase small subunit	leuD	C	24	27.4	4
28198573	ATP-dependent Clp protease subunit	clpA	C	84	4.4	2
28199612	Bacterioferritin comigratory protein	bcp	U	18	30.2	4
28198746	Glycyl-tRNA synthetase beta subunit	glyS	C	80	9.3	3
28198052	Arginyl-tRNA synthetase	argS	C	63	10.3	4
28198187	Porin O precursor	oprO	OM	45	13.6	4
28199811	30S ribosomal protein S18	rpsR	C	9	40.8	2
28198173	NADH dehydrogenase subunit C	nuoC	C	28	11.6	2
28198336	PmbA protein	pmbA	C	48	10.3	2
28199089	Cation:proton antiporter	ybaL	CM	60	10.8	4
28199854	Superoxide dismutase	sodM	P	23	22.7	2
28198116	3-methyl-2-oxobutanoate hydroxymethyltransferase	panB	C	29	21.3	4
28198371	50S ribosomal protein L30	rpmD	U	7	30.2	2

28199290	Alcohol dehydrogenase	yahK	C	37	23.8	5
28198252	Ribosome-recycling factor	frr	C	21	33.5	4
28199681	Dihydrolipoamide dehydrogenase	lpdA	C	64	7.5	3
28199371	Elongation factor P	efp	C	21	21.8	2
28199871	50S ribosomal protein L11	rplK	C	15	12.0	1
28198658	50S ribosomal protein L13	rplM	C	16	29.6	3
28198503	RNA polymerase sigma factor	rpoD	C	70	6.6	3
28198369	50S ribosomal protein L18	rplR	C	13	29.4	3
28199794	Pilus biogenesis protein	pilB	C	63	8.7	3
28199040	Twitching motility protein	pilU	C	42	12.0	3
28198527	DNA-binding related protein	dps	C	19	30.9	3
28199504	Adenylosuccinate synthetase	purA	C	47	9.5	3
28199502	Nucleoside diphosphate kinase	ndk	EC	16	22.0	3
28198150	Adenylate kinase	adk	C	20	23.5	2
28198459	Electron transfer flavoprotein ubiquinone oxidoreductase	etfD	U	60	4.6	3
28198375	30S ribosomal protein S11	rpsK	C	14	26.2	2
28198185	3-oxoacyl-[ACP] reductase	fabG	C	26	23.2	3
28198388	ATP-dependent serine proteinase La	lon	C	92	3.9	3
28198936	ATPase	PD1039	C	45	8.5	2
28198848	Fumarate hydratase	fumB	C	55	8.1	2
77747623	Phospho-2-dehydro-3-deoxyheptonate aldolase	aroG	C	41	13.9	3

28198404	Malate dehydrogenase	mdh	U	35	35.4	6
28198517	Aspartate-semialdehyde dehydrogenase	asd	C	37	16.3	2
28197956	Biopolymer transport ExbD1	exbD1	CM	15	25.2	2
77747689	Polysaccharide export protein	mrp	CM	32	6.6	1
28198960	Preprotein translocase subunit SecB	secB	C	19	43.0	4
28197977	Transcription-repair coupling factor	mfd	U	132	4.4	3
28199058	Peptidyl-prolyl cis-trans isomerase	PD1168	OM	25	14.2	3
28198433	Small conductance mechanosensitive ion channel	yggB	CM	34	19.3	3
28198368	50S ribosomal protein L6	rplF	C	19	11.4	2
77747720	4-hydroxy-3-methylbut-2-en-1-yl diphosphate synthase	ispG	C	45	15.8	4
28199782	Translation initiation factor IF-3	infC	C	21	12.8	2
28199704	Peptidyl-prolyl cis-trans isomerase	surA	P	51	10.6	3
28198847	Aspartyl-tRNA synthetase	aspS	C	66	10.4	3
28198532	Cytochrome O ubiquinol oxidase subunit I	cyoB	CM	74	2.9	2
28199323	50S ribosomal protein L27	rpmA	C	9	25.9	2
28199511	DNA-binding protein	bbh3	U	14	33.1	3
28198444	Poly(Hydroxyalcanoate) granule associated protein	phaF	C	20	17.3	2
77747658	NAD-glutamate dehydrogenase	gdhA	U	186	1.6	2
28199878	Ribose-phosphate pyrophosphokinase	prs	C	35	5.9	1
77747631	Phosphomannomutase	algC	C	50	8.8	2
28198330	Outer membrane protein	omp28	P	26	11.6	2

28198345	ATP synthase gamma chain	atpG	C	32	11.5	2
28198558	Phosphoribosylformylglycinamidine synthase	purL	C	144	5.7	4
28198025	Succinyl-diaminopimelate desuccinylase	dapE	C	41	10.9	2
28198031	Alanyl-tRNA synthetase	alaS	C	96	2.4	1
28198600	ABC transporter ATP-binding protein	ynhD	C	31	9.7	2
28198952	Outer membrane protein Slp	slp	OM	18	20.0	2
28199569	Fimbrial assembly membrane protein	pilN	CM	25	14.1	2
28199623	Probable malate:quinone oxidoreductase	mqo	C	63	11.7	4
77747685	Catalase-peroxidase	katG	C	84	6.3	3
28198361	50S ribosomal protein L29	rpmC	U	8	26.2	2
28198638	General secretory pathway protein E	xpsE	C	65	5.3	2
28198068	Tyrosyl-tRNA synthetase	tyrS	C	47	6.5	1
28198733	Bifunctional purine biosynthesis protein purH	purH	C	57	8.0	2
28198325	Diaminopimelate decarboxylase	lysC	C	95	4.3	3
28199113	Inorganic pyrophosphatase	ppa	C	20	16.9	2
28199043	Putative uncharacterized protein	PD1151	OM	31	16.6	3
28199560	Chaperone protein ClpB	clpB	C	96	5.2	3
28198095	Acetyl-coenzyme A carboxylase carboxyl transferase subunit alpha	accA	C	36	19.1	4
28199809	Chromosome segregation protein	smc	C	131	4.3	2
28198800	2,3-bisphosphoglycerate-dependent phosphoglycerate mutase	gpmA	C	29	13.3	2

28198251	Undecaprenyl pyrophosphate synthase	uppS	C	29	9.8	2
28197982	Nitric oxide dioxygenase	hmp	C	44	8.1	2
28199255	Heat shock protein GrpE	grpE	C	19	26.7	2
28198261	6-phosphogluconolactonase	pgl	U	26	26.4	4
28199883	Peptide chain release factor 1	prfA	C	41	11.1	2
28198411	Colicin V secretion ABC transporter ATP-binding protein	cvaB	CM	79	7.5	2
28199563	Putative cytochrome P450 133B1	CYP133 B1	CM	45	21.6	4
28198026	Asparagine synthase B	asnB	C	63	8.3	3
28199369	3-demethylubiquinone-9 3-methyltransferase	ubiG	C	27	11.8	2
28199383	3-oxoacyl-[ACP] reductase	fabG	C	25	17.0	2
28198366	30S ribosomal protein S14	rpsN	C	12	18.8	2
28198213	Argininosuccinate synthase	argG	C	44	11.5	3
28199115	Thioredoxin domain-containing protein	trx	C	38	9.7	2
28198011	Dihydroxy-acid dehydratase	ilvD	C	65	7.2	3
28199318	Isoleucyl-tRNA synthetase	ileS	C	106	5.1	4
28199677	Membrane protein	PD1806	CM	29	13.4	2
28197999	Fimbrial subunit	PD0062	EC	19	34.8	2
28199334	Putative uncharacterized protein	PD1453	C	44	8.9	2
28199202	Chromosome partitioning protein	parA	CM	29	17.0	2
77747669	Quinolinate synthase A	nadA	C	37	16.5	3

77747710	(Dimethylallyl)adenosine tRNA methylthiotransferase miaB	miaB	C	55	8.7	2
28198405	Peptidyl-prolyl cis-trans isomerase	ppiB	C	18	30.5	3
28199780	50S ribosomal protein L20	rplT	C	14	16.8	2
28199573	Ribokinase	rbsK	C	33	9.1	2
28199399	Peptidyl-prolyl cis-trans isomerase	slyD	C	18	23.9	2
28199204	Seryl-tRNA synthetase	serS	C	47	9.6	3
28198633	Proline iminopeptidase	pip	C	36	9.9	3
28199173	GTP-binding protein LepA	lepA	CM	67	8.3	3
28198562	Acetylornithine aminotransferase	argD	C	44	7.3	2
28199705	LPS-assembly protein lptD	lptD	OM	91	2.9	2
28198958	Putative uncharacterized protein	PD1063	OM	21	32.1	3
28198323	Regulator of pathogenicity factors	rpfB	CM	63	7.0	3
28198668	Adenylosuccinate lyase	purB	C	51	7.0	2
28199552	S-adenosylmethionine synthase	metK	C	44	8.4	2
77747688	Putative uncharacterized protein	PD1329	U	15	16.0	2
28199860	Putative uncharacterized protein	PD1994	CM	78	6.1	3
28198652	Subunit F of alkyl hydroperoxide reductase	ahpF	CM	57	8.3	3
28199377	Type IV fimbriae assembly protein	pilZ	U	13	32.2	2
28199730	Cell division protein	ftsZ	C	42	12.9	2
28199351	Putative uncharacterized protein	PD1470	C	28	10.9	2
28198974	DNA mismatch repair protein mutS	mutS	C	97	4.4	2

77747682	Ferric enterobactin receptor	bfeA	OM	87	6.8	2
28199645	Stringent starvation protein A	sspA	C	24	10.9	2
28198552	UDP-N-acetylglucosamine 1-carboxyvinyltransferase	murA	C	45	11.3	2
28199572	Voltage-gated potassium channel beta subunit	tas	C	36	10.9	2
28198569	High frequency lysogenization protein hflD homolog	hflD	U	22	19.1	2
28198623	Sulfate adenylyltransferase subunit 2	cysD	C	35	7.6	2
28199157	Threonine synthase	thrC	C	46	4.9	2
28198591	Glucosamine--fructose-6-phosphate aminotransferase	glmS	C	36	8.4	2
28197957	Biopolymer transport ExbD2 protein	exbD2	CM	15	32.4	2
28199453	Recombination-associated protein rdgC	rdgC	C	34	9.9	2
28199717	Glutamyl-tRNA synthetase	gltX	C	53	5.4	2
28199174	Signal peptidase I	lepB	CM	30	8.6	2
28199773	Virulence regulator	xrvA	U	15	33.6	2
28198707	Putative uncharacterized protein	PD0802	U	20	15.7	2
28198260	6-phosphogluconate dehydratase	edd	C	67	4.8	2
28199814	Asparaginyl-tRNA synthetase	asnS	C	53	5.8	2
28199427	Cystathionine beta-synthase	cysM	C	50	11.0	2
28198357	30S ribosomal protein S19	rpsS	C	10	25.8	2
28199280	GumB protein	gumB	U	24	11.1	2
28198667	Putative uncharacterized protein	PD0761	C	48	7.8	2
28198559	Disulfide isomerase	dsbC	P	28	14.9	3

28198605	Putative uncharacterized protein	PD0697	CM	11	18.6	2
28198194	C4-dicarboxylate transport protein	dctA	CM	48	5.3	2
28199052	Putative uncharacterized protein	PD1162	C	47	3.0	2
28199241	P-protein	pheA	C	42	6.4	2
28198038	Valyl-tRNA synthetase	valS	C	111	3.2	2
28198855	Putative uncharacterized protein	PD0956	U	37	8.4	2
28199932	Type I restriction-modification system DNA methylase	hsdM	C	89	4.0	2
28198322	Response regulator	rpfG	CM	44	8.1	2

1: Protein accesion number at NCBI database (http://www.ncbi.nlm.nih.gov/);

2: Protein localization as prediceted by PSORTb v. 3.0.2 Subcellular Localization Prediction Tool (http://www.psort.org/psortb/;

C: Cytoplasmic; CM: Cytoplasmic Membrane; OM: Outer Membrane; P: Periplasmic; EC: Extracellular; U: Unknown);

3: Theoretical protein molecular weight shown in KDa.

Material and Methods

Xff strains and growth conditions.

The WT Temecula1 strain of *Xylella fastidiosa* subspecies *fastidiosa* (Xff; ATCC 700964) and a GFP-expressing variant, the KLN59.3 strain (41), were used in this study. The bacteria were grown in PD3 medium (42) with aeration (120 rpm) at 28°C, and solid cultures were prepared in the same medium with addition of 1.5% agar. PD3 media was supplemented with kanamycin (30 ug/mL) for selective growth of KLN59.3.

Isolation of secreted proteins and outer membrane vesicles from culture supernatants.

Xff cells were harvested by centrifugation at 8.000 x *g* for 15 min at 4°C. The culture supernatant was transferred to 38.5 mL tubes and centrifuged at 38,000 x *g* for 1 h at 4°C (Sw28 rotor, Beckman Coulter, USA). The supernatant was collected (the remaining pellet was discarded), transferred to 12 mL tubes and centrifuged at 150,000 x *g* for 3 h at 4°C (Sw41 Ti rotor, Beckman Coulter, USA). The supernatant containing secreted proteins was concentrated 75-100x using Amicon Ultra-15 3K filters units (Millipore). The remaining pellet containing OMVs was resuspended in 300 μL of PBS (pH 7.4) for subsequent SDS-PAGE analysis. For electron microscopy analysis, the vesicle pellet was resuspended in 50 mM HEPES buffer (pH 6.8).

Outer membrane and total protein extraction.

Outer membrane protein extraction was performed essentially as described before (29). For the preparation of total protein extracts, bacteria from 2 mL culture (4-6 days old) were harvested by centrifugation at 8.000 x *g* for 15 min at 4°C and washed three times with 1 mL of washing buffer containing 10 mM Tris (pH 8.8), 3 mM KCl, 50 mM NaCl, 5 mM EDTA and 1 mM PMSF, and centrifuged for 2 min at

3000 x *g*. The pelleted cells were then lysed with 200 μL of the following solution: 10 mM Tris (pH 8.8), 0.5% w/v SDS, 5 mM EDTA, 1 mM PMSF. After adding 100 mM DTT, the sample was boiled for 3 min and stored at -80°C.

Bacterial surface digestion.

Xff cells were harvested by centrifugation at 8.000 x *g* for 15 min at 4°C and washed three times with 1 mL of PBS. A total of 4 x 10^8 cells were resuspended in 100 μL of filtered sterilized 50 mM ammonium carbonate buffer (pH 7.5). Digestions were carried out with 20 μg of sequencing grade modified trypsin (Promega) in the presence of 5 mM DTT, for 15 min at 37°C. The digestion mixture was centrifuged at 3,500 x *g* for 10 min at 4°C, and the supernatant (containing the peptides) collected. Trypsin reaction was stopped with formic acid at 0.1% final concentration. The reaction was filtered using Amicon Ultra Microcon 3K filters units (Millipore), and the flowed through peptides were kept at -20°C until further analysis.

Grapevine leaf protein extraction.

Grapevine (*Vitis vinifera* L. c.v. 'Thompson Seedless') leaves from *Xff*-infected (n=5) and non-infected (n=5) plants were collected about one meter above the point of inoculation. Plant tissues were flash frozen in liquid nitrogen, lyophilized and kept at -80°C. Proteins were extracted using a phenol extraction procedure previously described (43). Each leaf was grinded in liquid nitrogen using a pestle and mortar containing 1% (w/w) PVPP. One hundred milligrams of plant material was resuspended in 600 μL of extraction buffer (0.7 M Sucrose, 0.1 M KCl, 0.5 M Tris-HCl pH7.5, 0.5 M EDTA, 1 mM PMSF and 2% β-mercaptoethanol). The suspension was homogenized 3 times (1 min each) using a MM300 TissueLyser (Qiagen). An equal volume of UltraPure™ Buffer-Saturated Phenol (Invitrogen) was added and the mixture was rehomogenized as described above. After centrifugation at 12,000 x *g* for 15 min at 4°C, the upper phenol phase was

removed and the remaining pellet used for re-extraction using extraction buffer. Proteins were precipitated from the phenol phase using 5 volumes of saturated ammonium acetate (100 mM) in methanol overnight at -20°C followed by centrifugation at 12,000 x *g* for 15 min at 4°C. Protein pellets were washed 4 times with 4 mL of saturated ammonium acetate (100 mM) in methanol and dried for 10 min in the hood. Proteins were solubilized with urea buffer (7 M Urea, 2 M Thiourea, 40 mM Tris, 2% Chaps and 18 mM DTT). The protein concentration was determined according to Bradford's method using BSA as standard.

Protein preparation and mass spectrometry analysis.

X. fastidiosa proteins extracted following the procedure described above were analyzed in the Proteomics Facility at University of California Davis. *Xff* soluble supernatant (SSPs) and OMV proteins were resolved by SDS-PAGE prior to in-gel digestion to reduce the amount of non-protein contaminants in the samples. Peptides from the cell shaving (surfaceome) procedure were de-salted using Aspire RP30 Desalting Tips (Thermo-Fisher Scientific) and directly subjected to LC/MSMS analysis. For the in-gel digestion used for SSPs and OMV proteome analysis, gel pieces were washed twice with 100-150 μL of 50 mM ammonium bicarbonate (AmBic; pH 8.0), followed by dehydration with acetonitrile (ACN; 3-4 times the total volume of gel pieces) for 10-15 min. Proteins were reduced for 30 min at 56°C in a solution of 10 mM DTT and 50 mM AmBic. Gel pieces were dehydrated again, followed by the replacement of ACN by 55 mM iodoacetamide in 50 mM AmBic. Gel pieces were incubated for 20 min in the dark at room temperature, followed by two washing steps with 150-200 μL of 50 mM AmBic for 15 min each. Gel pieces were dehydrated with ACN, dried by speed vacuum centrifugation and subjected to tryptic digestion overnight. Peptides were extracted by adding 60% ACN and 0.1% Trifluoroacetic acid (TFA) in the gel pieces, followed by sonication for 10 min. The solution containing the peptides was mixed with the supernatant resulted from the tryptic digestion, followed by speed vacuum centrifugation. Digested peptides were then de-salted using Aspire RP30 Desalting Tips (Thermo-Fisher Scientific) and resuspended in loading buffer.

The digested peptides were analyzed using a QExactive mass spectrometer (Thermo Fisher Scientific) coupled with an Easy-LC (Thermo Fisher Scientific) and a nanospray ionization source. The peptides were loaded onto a trap (100 micron, C18 100Å 5U) and desalted online before separation using a reverse phased column (75 micron, C18 200Å 3U). The gradient duration for separation of peptides was 60 minutes using 0.1% formic acid and 100% ACN for solvents A and B respectively. Data was acquired using a data dependent ms/ms method, which had a full scan range of 300-1600 Da and a resolution of 70,000. The ms/ms method's resolution was 17,500 and an isolation width of 2 m/z with normalized collision energy of 27. The nanospray source was operated using 2.2 KV spray voltage and a heated transfer capillary temperature of 250°C. Raw data was analyzed using X!Tandem and visualized using Scaffold Proteome Software (Version 3.01). Samples were searched against Uniprot databases appended with the cRAP database, which contains common laboratory contaminants. Reverse decoy databases were also applied to the database prior to the X!Tandem searches.

For the grapevine proteomic analysis, leaf proteins were precipitated using ProteoExtract^{TM} Protein Precipitation kit (Calbiochem) followed by dehydration overnight in a sterile fume hood. The protein pellet was then resuspended in 50 mM AmBic (pH 8.0) and subjected to an in-solution tryptic digestion. Digested peptides were then de-salted and subjected to LC/MSMS essentially as described above.

Electron microscopy analysis of outer membrane vesicles.

Outer membrane vesicles were resuspended in 50 mM HEPES buffer (pH 6.8) and fixed with 4% paraformaldehyde in 1 M Sorenson's phosphate buffer (pH 7.4). Copper grids (400 mesh) supported with formvar coating were used for electron microscopy. An amount of 10 μL of fixed OMVs were placed in the grids and allowed to settle for 10 min. The excess of sample was removed with filter paper, followed by quickly staining with 1% ammonium molybdate. Grids were air-

dried completely before visualization in a Philips CM120 (FEI/Philips Inc.) electron microscope at 80 KV.

Immunogold electron microscopy.

Immunogold Electron Microscopy (IEM) was performed using fresh cultures of *Xff*. The sample containing *Xff* cells as well as the filamentous network secreted in the culture supernatant were fixed with 4% paraformaldehyde in 1 M Sorenson's phosphate buffer (pH 7.4). The fixed sample was embedded in LR White resin essentially as described before (44). Ultra-thin sections were cut and placed onto coated grids (200 mesh; treated with glow-discharge), followed by blocking with 1% fish gelatin for 30 min. Grids were blotted with anti-LipA (1:500) antibody for 1 h at RT and washed with PBS. The primary antibody was detected using anti-rabbit (1:50) antibody coupled to 10 nm gold particles. Unbound conjugate was removed by a sequence of washing steps with PBS. The preparation was negatively stained with 1% ammonium molybdate, air-dried, and visualized in a Philips CM120 (FEI/Philips Inc.) electron microscope at 80 KV.

LipA detection in grapevine leaves by ELISA.

For the detection of LipA in grapevine (*Vitis vinifera* L. c.v. 'Thompson Seedless') by ELISA, leaves from *Xff*-infected (12 wpi) and non-infected plants were collected and divided in three sections (inside, middle and outside; ~2 cm of length each). An amount of 90 mg of leaf tissue was homogenized in 900 μL of coating buffer (0.1 M sodium carbonate buffer, pH 9.6) for 3 min using a MM300 TissueLyser (Qiagen, USA). The number of *Xff* cells present in each homogenized sample was determined using a double-antibody sandwich (DAS)-ELISA assay (Agdia Inc., USA), following manufacturer's instructions. For LipA detection, the homogenized solution was used to coat (100 μL/well) a ninety-six-well Maxisorp™ microtiter plate (NUNC, USA) for 2 h at RT. The wells were washed two times with PBS-T 0.1% (PBS plus 0.1% Tween 20) and blocked for 1 h at RT with PBS-M 5% (PBS plus 5% non-fat dried milk). The plate was washed three times with PBS-T

0.1%, followed by incubation with anti-LipA (1:1000) antibody in PBS-M 1% for 1 h at 37°C. The plate was washed three times with PBS-T 0.1% followed by incubation with HRP-conjugated anti-rabbit (1:1000) in PBS-M 1% for 1 h at 37°C. The plate was washed four times with PBS-T 0.1% and developed with TMB (3,3′,5,5′-tetramethylbenzidine).

Western-blot analysis.

For the detection of LipA in *Xff* and grapevine samples, a polyclonal antibody was generated in rabbit (GenScript, USA). In all cases, anti-LipA was used diluted in PBS-M 1% (PBS plus 1% non-fat dried milk) in a dilution of 1:1000, followed by detection using HRP-conjugated goat anti-rabbit antibody (1:2000 for grapevines and 1:4000 for *Xff* samples) (Life Technologies, USA). Blocking and washing steps were performed with PBS-M 5% and PBS-T 0.1% (PBS plus 0.1% Tween 20), respectively. Developments were carried out using ECL Plus Western Blotting Detection Reagents (GE Life Sciences, USA). For the detection o MopB and EF-Tu in *Xff* samples, polyclonal antibodies (dilutions of 1:20,000 for MopB and 1:10,000 for EF-Tu) were used, followed by detection using HRP-conjugated goat anti-rabbit antibody (1:20,000). Blocking and washing steps were carried out as described for LipA. Developments were carried out using SuperSignal West Dura Chemiluminescent Substrate (Thermo Scientific, USA).

RNA extraction and real-time RT-PCR.

Xff 3A2 (WT), rpfC$^-$ and rpfF$^-$ cells were grown in 50 mL PD3 liquid medium (3 flasks/condiction) until the cultures reach 10^7-10^8 cells/mL. RNA was extracted using miRNeasy Mini Kit (Qiagen, USA) following manufacture's instructions. The synthesis of cDNA was performed using SuperScript III First-Strand Synthesis SuperMix (Life Technologies, USA). RT-PCR reactions were performed using TaqMan Universal PCR Master Mix (Life Technologies, USA) on the StepOne Real-Time PCR System (PE Applied Biosystems, USA). The level of gene transcription was normalized to 16S rRNA and expressed as a relative difference.

The statistical analysis was performed using GraphPad Prism software, version 5 (Graph-Pad Software, San Diego, USA), using the Unpaired t test with Welch's correction. The data was considered significant when $p < 0.05$.

Lipase and esterase activity assays.

Tributyrin (C4), tricaprin (C10), and a mixture of tryglicerides (C2-C10) (Sigma-Aldrich, USA) were used as substrates for LipA activity in a plate assay (23, 45). The triglyceride substrates (0.5%; v/v) were prepared in a buffer containing 100 mM Tris-HCl (pH 8.0), 25 mM $CaCl_2$, sonicated at 30 W for 3 min to emulsify the substrates, mixed with an equal volume of 2% agarose solution and solidified in Petri plates. Fifty microliters of *Xff* soluble supernatant proteins (700 ng/μL) were added to the wells and assayed for a zone of clearance for 24-48 h at RT. The culture medium PD3 was used as negative control. For the LipA esterase activity, pNP butyrate (pNP-C4) was used as the substrate in a spectrophotometric assay, which was performed at OD_{405nm} after a incubation for 10 min of pNP-C4 (1-5 mM) with *Xff* soluble supernatant proteins (1 μg/well) in 50 mM Tris-HCl (pH 7.5) at 37°C.

Hypersensitive response assay in grapevine leaves.

The heterologous expression of the wild type LipA and its mutated version (LipAΔS165) - in which the amino acid Ser-165 of the active triad was replaced by Alanine - was accessed after cloning both genes in the pJexpress 401 (DNA2.0) vector for expression under the T5 promoter. The insertion of cloned genes was verified by PCR using primers flanking LipA genes, followed by transformation of ElectroMAX™ DH5α-E™ Competent Cells (Life Technologies, USA). For the heterologous expression, cells were grown in LB medium supplemented with Kanamycin (50 μg/mL) until OD_{600nm} of 0.8 at 37°C and 120 rpm. IPTG (1 mM) was added to the culture, followed by incubation for 3 h at 30°C and 120 rpm. Total protein was extracted from *E. coli* cells using CellLytic B Plus Kit (Sigma-Aldrich, USA). The protein concentration was determined according to Bradford's

method using BSA as standard. Total proteins from LipA, LipAΔS165, and empty vector-expressing *E. coli* were used for syringe infiltration in greenhouse-grown grapevine (*Vitis vinifera* L. c.v. 'Thompson Seedless') leaves. HR-like lesions in the infiltrated area were visualized 24 h after inoculation.

Discussion

PD symptoms development has long been thought to be the result of xylem vessels blockage by *Xff* biofilm, associated gels and tyloses that would ultimately result in water stress in the distal parts of the infected plant and lead to PD. The absence of a correlation between PD symptoms with *Xff* concentrations (16) along with the low level of xylem vessel occlusion (2-4%) (41) in infected plants, and lack of relationship between leaf scorch symptoms and bacterial population in well-watered plants, where high populations of bacteria also occurred, indicate that the idea of water stress as the main cause of PD symptoms should be reevaluated (2, 46, 47). We present here strong evidences of a putative pathogenic mechanism that is independent of the water stress hypothesis, supporting the concept that PD symptoms development is caused by a *Xff*-generated phytotoxin.

The first indication that *Xff* was secreting a virulence factor came from our bacterial secretome analysis, a proteomic approach generally used to identify crucial secreted and surface-associated proteins in several bacteria species (48-55), which led us to the finding of abundant lipase/esterase proteins. The high abundance of three specific putative lipases in our SSPs profile analysis raised the question whether this *Xff* lipase secretion was associated with the pathogenic process. A supporting evidence originated from an *in silico* analysis (Fig. S1) revealed that the most abundant SSP (PD1703) was an ortholog of the lipase/esterase and cell wall degrading protein LipA from *Xoo* and *Xcv*, which has been shown to play an important role in the virulence of both pathogens in rice (23, 33, 56) and tomato (24), respectively.

Interestingly, these lipase/esterase proteins were not characterized in the *Xf* extracellular proteome of the CVC-causing strain, although the genes are present in the genome (19, 57). The lipase/esterase proteins of the *Xf* CVC 9a5c strain (XF0357, XF0358 and XF2151), homologs of the three *Xff* Temecula 1 (LipA, PD1702 and PD1211, respectively), were not detected probably because of a mixture of proteins originated from the surface and from secretions, but the secreted fraction was underrepresented due to the cell washing, neglecting the

secretion in the media. However, we cannot discard the possibility of different secreted virulence factors among *Xf* subspecies.

The functional characterization of lipase/esterase properties of *Xff* SSPs confirmed the dual function of LipA (Fig. S2, A-B), presenting esterase activity on p-nitrophenol butyrate, but not on long chain triacylglycerides. This was also observed in *Xoo*, which is not a typical behavior of a true lipase (23). The LipA expression appears to be induced by Tween 80 (oleic acid monoester of polyoxyethylene sorbitan) (Fig. S2, C), as previously observed for both fungal and bacterial lipases (58, 59).

The second evidence of the *Xff* LipA role in the *Xff* pathogenesis were provided elsewhere (60), which described the complete absence of LipA in the *Xf* biocontrol strain EB92-1, isolated from elderberry in 1992 (61). EB92-1 is infectious to grapevines, but does not cause symptoms, and it survives for many years in the host, providing an effective biocontrol against PD. A genome draft of the EB92-1 strain revealed that 10 potential pathogenicity effectors were missing (60). Interestingly, among them, two are predicted type II secreted enzymes, including the lipase/esterase LipA and the serine protease PD0956, also identified in our SSPs profile.

Although our observations revealed that *Xff* LipA was being abundantly secreted *in vitro*, it was unknown whether the same level of expression was happening during infection and colonization, which led us to perform a proteomic analysis of a *Xff*-infected grapevine leaf (Table 3). This analysis revealed that LipA was one of the six *Xff* identified proteins, clearly indicating that LipA was also abundantly secreted by *Xff* during the plant infection/colonization, which is the third evidence that LipA is associated with PD symptoms. However, it remained to be demonstrated if the LipA was responsible for the leaf necrosis, and how this protein was distributed in the leaf.

One of the most typical symptoms of PD is the leaf scorch characterized by zones of chlorosis progressing into necrotic zones at the peripheral margins of the infected leaves. Our results also corroborate previous findings (16) demonstrating not only the absence of correlation between PD symptoms and bacterial

colonization patterns in leaves, but also a gradual decrease in bacterial concentration contrary to the symptoms development from edges (margins) to the center of the leaf blade (petiole) (Fig. 4). On the other hand, we have demonstrated that LipA accumulates abundantly in leaf regions where minimal *Xff* titer is found, and it was associated with PD symptoms (Fig. 4).

The co-localization of LipA and level of chlorosis/necrosis in leaves raised questions about LipA secretion and translocation mechanisms, and two major hypothesis were considered: i) immediate secretion as a soluble protein, or ii) entrapped in outer membrane vesicles (OMVs), which are small spherical structures that allow the interaction of gram-negative bacteria with their environment by releasing the vesicular contents to adjacent prokaryotic and eukaryotic cells, considered a major mechanism by which Gram-negative pathogens communicate with and intoxicate host cells (26). The first hypothesis is a fragile argument if we consider LipA as a phytotoxin, because necrotic lesions would occur everywhere, including in the proximity of bacterial aggregates, which was not observed. Our previous finding, showing that the bacteria do not translocate abundantly to the margins, supports the second hypothesis, which involve OMV formation and translocation to leaf margins releasing its cargo.

The outer membrane (OM) entraps the periplasmic constituents during the OMV formation, including soluble proteins, phospholipids, lipopolysaccharides (LPSs), and DNA as vesicle's cargo (25, 62, 63). The secretion mechanism mediated by OMVs have been shown to be used by many pathogenic bacteria for the releasing of virulence factors (64-68), quorum sensing signals (69), pathogen-associated molecular patterns (PAMPs) (70, 71) and other OM components, e.g., surface-exposed adhesins (72). Recently, it has been shown that *Xff* releases OMVs carrying the autotransporter XatA (27); however, the complete protein cargo was not elucidated, and apparently this protein impacts migration, colonization and biofilm formation, but a direct relationship between PD symptoms and the protein was not demonstrated. Therefore, we have further investigated whether OMVs were released during bacterial culture, which was demonstrated by ultracentrifugation and electron microscopic imaging. Additionally, a complete purification step followed by a comprehensive proteomic analysis was performed

to identify the major constituents of the cargo, and the major proteins found was the lipase/esterase, but not the XatA described elsewhere (27). This latter report does not present confirmation of the OMV purification through imaging and our data suggest that the membrane may be reorganized in order to release its cargo, because the proteomic analysis identified only few putative proteins.

The low protein content of *Xff* OMVs' cargo (Table 2) might be explained by the large LPS content that can exceed the total protein content of vesicles by ratios as high as 10:1 (73). The OMV proteomic analysis of the *Xff* closely related pathogen *Xcc* also resulted in the identification of a small number of proteins (28). Among the *Xff* OMV proteins found, four were identified as outer membrane proteins (MopB, OmpW, PspB and PD1283). MopB, OmpW and the TonB-dependent receptor PD1283 (Table S2) have been shown to be highly abundant in *Xff* outer membrane (29). The outer membrane proteins OmpA, closely related to MopB, OmpW3 and a TonB-dependent receptor were also identified in the OMV cargo of *Xcc* (28). The non-fimbrial adhesin XadA, which has been shown to contribute for the attachment and virulence of *Xff* (74) and *Xoo* (75), was abundantly found in our OMV's proteome, surfaceome and secretome analysis. Interestingly, the three secreted lipases (LipA, PD1702 and PD1211) were also found to be part of *Xff* OMV's cargo, supporting our hypothesis that OMVs are likely transporting these proteins to its site of action in the grapevine leaf margins.

Interestingly, the presence of LipA was highly concentrated in the leaf margins and was gradually decreased towards the petiole, where the bacteria had formed a biofilm network. SEM and TEM imaging (Fig. 3) identified major filamentous network formed with the presence of LipA, but in low concentration and well distributed, suggesting that it may only be active without being associated with the biofilm or could have limited digestive activity. Apparently, this is a protective mechanism that prevents tissue destruction close to the bacteria colonies allowing a controlled digestion and metabolism without causing major damage in the colonization site. It is also possible that the absence of biofilm formation due to the low bacteria concentration in the very thin leaf vessels may be responsible for the generation of higher levels of OMV cargos and release of LipA, which will occur only close to the margins. We propose that the release of LipA

through OMVs to distant sites without biofilm formation may be the major reason of tissue destruction, causing the relocation of nutrients from the leaf margins to the opposite direction towards the bacteria colonies (Fig. 7).

Another corroborating evidence linking biofilm formation and release of OMVs is provided by the analysis of quorum sensing mutants taking into account the Diffusible Signaling Factor (DSF) conditioned by two different mutant strains (*rpfC* and *rpfF*) involved in the production of the α,β unsaturated fatty acid, which modulates the *Xff* virulence by a cell–cell signaling. The *rpfF* gene encodes a protein similar to enoyl-CoA hydratases that synthesizes DSF and has been shown to be required for DSF production, while *rpfC* seems to be part of a putative two-component regulator involved in DSF signal sensing. *Xff rpfC* mutant exhibits a hyperattachment phenotype in culture (higher biofilm formation) that is associated with their inability to migrate in xylem vessels and cause disease (36). The *rpfF* mutant, deficient in DSF production, has the opposite phenotype (planktonic) for all of these traits (32). We postulate that the inability of the *Xff rpfC* mutants to cause PD symptoms in grapevine might be related to the decreased expression of LipA as well as other potential virulence factors regulated by *rpfC* (Fig. 5), as observed for *Xcc rpfC* mutants, which are deficient in the production of virulence factors such as extracellular polysaccharide (EPS) and also in the secretion of extracellular enzymes (76). Interestingly, the lack of significant differences of LipA expression in the *rpfF* mutant relative to the wild type also suggests that the lower production of biofilm may generate higher OMV cargos released to distant sites, or uncontrolled distribution of LipA may cause immediate damage to tissues.

Another corroborating evidence of the LipA role in pathogenesis was shown elsewhere (77) through the two-component system of GacS/GacA, which is involved in the environmental signaling and control of secondary metabolites and extracellular enzymes production. It regulates the virulence of many pathogenic and environmental bacteria, including *Xf*. GacA is a response regulator that controls various physiological processes and pathogenicity factors thought the transcriptional activation of genes involved in the regulation of pathogenesis, e.g., genes involved in quorum sensing, toxin production, motility, biofilm formation, and

extracellular polysaccharide production (78-82). Several putative pathogenicity-related genes are regulated by *gacA* in *Xff*, including the two secreted lipases LipA (PD1703) and PD1702. Interestingly, *Xff gacA* mutants present lower expression levels of LipA and developed significantly less severe disease symptoms when inoculated in grapevines (77). In addition, the global activator *gacA* has been shown to act positively on the synthesis of the quorum-sensing autoinducer BHL (N-butyryl-homoserine lactone) in *P. aeruginosa* strain PAO and thereby on BHL-controlled virulence factors expression, including a lipase (83). In a human isolate of *P. aeruginosa*, a *gacA* mutant showed significant reduced pathogenicity on both mice and infiltrated *Arabidopsis* plants (84). Similarly to *Xff rpfC* mutants, *gacA* mutants are likely deficient in pathogenesis due to the low expression level of virulence factors such as LipA.

To further demonstrate the toxicity of LipA in leaf tissue, we have produced a recombinant LipA and a mutant at the Ser165 in the catalytic triad (ΔS165LipA), and we were able to confirm the predicted catalytic site due to the significant reduction of leaf damage followed by grapevine leaf infiltration. This evidence strongly supports the concept of LipA as a causal factor of necrosis during *Xff* pathogenesis, similar to what has been observed in *Xoo* (23, 33, 56).

In conclusion, we propose a model of *Xyllela fastidiosa* pathogenesis in Pierce's Disease (PD) based on the secretion, movement and accumulation of a lipase/esterase (LipA) in grapevine's infected leaves that lead to chlorosis and leaf scorching. *Xff* secretes LipA through two mechanisms: i) secretion into a biofilm filamentous network close to the bacterial colonization site, which is mainly localized close to the petiole with restricted movement, and ii) secretion through outer membrane vesicles (OMVs), which are increasingly accumulated as migration occurs towards leaf margins, and movement of virulence factors is possibly related to OMV translocation and release of LipA, which accumulates in leaf margins causing PD symptoms.

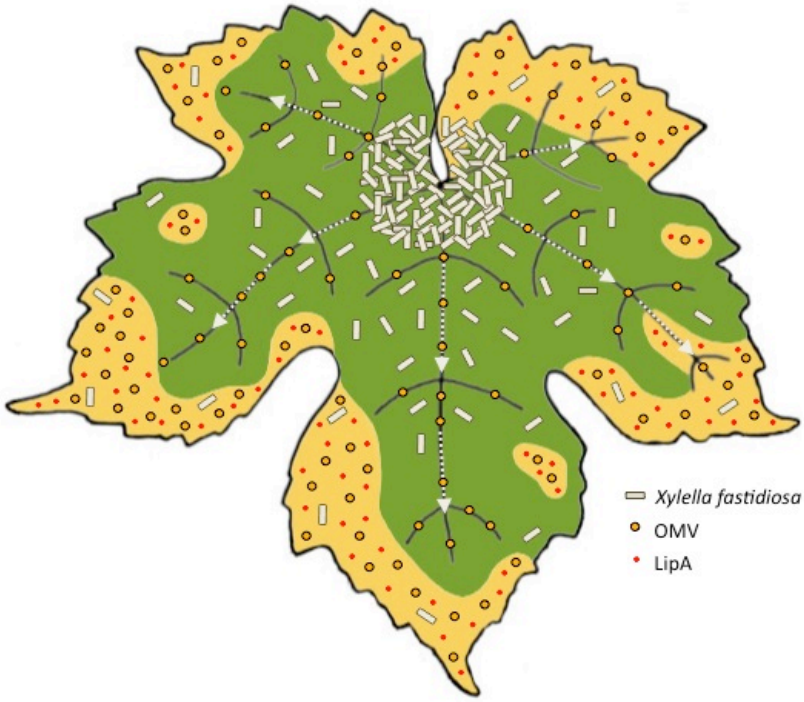

Fig. 7: Model of *Xyllela fastidiosa* pathogenesis in Pierce's Disease (PD). We propose that *Xff* virulence is caused by LipA, which is secreted by bacteria by two mechanisms: i) secretion into a biofilm filamentous network close to the bacterial colonization site (petiole), and ii) secretion through outer membrane vesicles (OMVs), responsible for the LipA transport and release. LipA accumulation in grapevine leaf margins is associated with PD symptoms (chlorosis and necrosis, yellow areas). OMVs (orange spheres) are increasingly accumulated as migration occurs towards leaf margins. Bacterial cells (white rods), mainly localized in the center of the leaf (petiole), present a restricted movement, and transport of virulence factors is possibly related to OMV translocation and release of LipA (red dots), which accumulates in leaf margins causing PD symptoms.

Acknowledgements

The authors acknowledge research support obtained from the Citrus Research Board of California and RN is grateful to Brazilian agency CAPES for scholarship's support. We thank David Dolan for his contributions to experimental procedures in the greenhouse. We also express our gratitude to Grete Adamson and Patricia Kysar (Electron Microscopy Laboratory, School of Medicine, University of California at Davis) for technical support.

References

1. Davis MJ, Purcell AH, Thomson SV (1978) Pierce's disease of grapevines: isolation of the causal bacterium. *Science* **199**(4324):75-77.

2. Chatterjee S, Almeida RP, Lindow S (2008) Living in two worlds: the plant and insect lifestyles of Xylella fastidiosa. *Ann Rev Phytopath* **46**:243-271.

3. Purcell AH, Hopkins DL (1996) Fastidious xylem-limited bacterial plant pathogens. *Ann Rev Phytopath* **34**:131-151.

4. Redak RA*, et al.* (2004) The biology of xylem fluid-feeding insect vectors of Xylella fastidiosa and their relation to disease epidemiology. *Ann Rev Entomol* **49**:243-270.

5. Hopkins DL (1989) Xylella fastidiosa: xylem-limited bacterial pathogen of plants. *Ann Rev Phytopath* **27**(1):271-290.

6. Chatterjee S, Almeida RPP, Lindow S (2008) Living in two worlds: The plant and insect lifestyles of Xylella fastidiosa. *Ann Rev Phytopath* **46**:243-271.

7. Esau K (1948) Anatomic effects of the viruses of Pierce's disease and phony peach. *Hilgarida* **18**:423-482.

8. Alves E, Marucci CR, Lopes JRS, Leite B (2004) Leaf symptoms on plum, coffee and citrus and the relationship with the extent of xylem vessels colonized by Xylella fastidiosa. *J Phytopath* **152**(5):291-297.

9. Baccari C, Lindow SE (2011) Assessment of the process of movement of Xylella fastidiosa within susceptible and resistant grape cultivars. *Phytopathology* **101**(1):77-84.

10. Chatelet DS, Wistrom CM, Purcell AH, Rost TL, Matthews MA (2011) Xylem structure of four grape varieties and 12 alternative hosts to the xylem-limited bacterium Xylella fastidious. *Ann Botany* **108**(1):73-85.

11. Fogaca AC*, et al.* (2010) Effects of the antimicrobial peptide gomesin on the global gene expression profile, virulence and biofilm formation of Xylella fastidiosa. *Fems Microbiol Lett* **306**(2):152-159.

12. Fritschi FB, Lin H, Walker MA (2008) Scanning electron Microscopy reveals different response pattern of four Vitis genotypes to Xylella fastidiosa infection. *Plant Dis* **92**(2):276-286.

13. Goodwin PH, Devay JE, Meredith CP (1988) Roles of water-stress and phytotoxins in the development of Pierces disease of the grapevine. *Physiol Mol Plant Pathol* **32**(1):1-15.

14. Daugherty MP, Lopes JRS, Almeida RPP (2010) Strain-specific alfalfa water stress induced by Xylella fastidiosa. *Europ J Plant Pathol* **127**(3):333-340.

15. McElrone AJ, Sherald JL, Forseth IN (2003) Interactive effects of water stress and xylem-limited bacterial infection on the water relations of a host vine. *J Experim Botany* **54**(381):419-430.

16. Gambetta GA, Fei J, Rost TL, Matthews MA (2007) Leaf scorch symptoms are not correlated with bacterial populations during Pierce's disease. *J Experim Botany* **58**(15-16):4037-4046.

17. Van Sluys MA*, et al.* (2002) Comparative genomic analysis of plant-associated bacteria. *Ann Rev Phytopath* **40**:169-189.

18. Ray SK, Rajeshwari R, Sonti RV (2000) Mutants of Xanthomonas oryzae pv. oryzae deficient in general secretory pathway are virulence deficient and unable to secrete xylanase. *Mol Plant-Microbe Interact: MPMI* **13**(4):394-401.

19. Simpson AJ*, et al.* (2000) The genome sequence of the plant pathogen Xylella fastidiosa. The Xylella fastidiosa Consortium of the Organization for Nucleotide Sequencing and Analysis. *Nature* **406**(6792):151-159.

20. Darvill AG, Albersheim P (1984) Phytoalexins and their elicitors - a defense against microbial infection in plants. *Ann Rev Plant Physiol* **35**(1):243-275.

21. Ryan CA, Farmer EE (1991) Oligosaccharide signals in plants: a current assessment. *Ann Rev Plant Physiol Plant Mol Biol* **42**(1):651-674.

22. Braun EJ, Rodrigues CA (1993) Purification and properties of an endoxylanase from a corn stalk rot strain of Erwinia chrysanthemi. *Phytopathology* **83**(3):332-338.

23. Aparna G, Chatterjee A, Sonti RV, Sankaranarayanan R (2009) A cell wall-degrading esterase of Xanthomonas oryzae requires a unique substrate recognition module for pathogenesis on rice. *The Plant Cell* **21**(6):1860-1873.

24. Tamir-Ariel D, Rosenberg T, Navon N, Burdman S (2012) A secreted lipolytic enzyme from Xanthomonas campestris pv. vesicatoria is expressed in planta and contributes to its virulence. *Mol Plant Pathol* **13**(6):556-567.

25. Kulp A, Kuehn MJ (2010) Biological functions and biogenesis of secreted bacterial outer membrane vesicles. *Ann Rev Microbiol* **64**:163-184.

26. Kuehn MJ, Kesty NC (2005) Bacterial outer membrane vesicles and the host-pathogen interaction. *Genes Developm* **19**(22):2645-2655.

27. Matsumoto A, Huston SL, Killiny N, Igo MM (2012) XatA, an AT-1 autotransporter important for the virulence of Xylella fastidiosa Temecula1. *MicrobiologyOpen* **1**(1):33-45.

28. Sidhu VK, Vorholter FJ, Niehaus K, Watt SA (2008) Analysis of outer membrane vesicle associated proteins isolated from the plant pathogenic bacterium Xanthomonas campestris pv. campestris. *BMC Microbiology* **8**:87.

29. Dandekar AM, *et al.* (2012) An engineered innate immune defense protects grapevines from Pierce disease. *Proc Natl Acad Sci USA* **109**(10):3721-3725.

30. Kunze G, *et al.* (2004) The N terminus of bacterial elongation factor Tu elicits innate immunity in Arabidopsis plants. *The Plant Cell* **16**(12):3496-3507.

31. Zipfel C, *et al.* (2006) Perception of the bacterial PAMP EF-Tu by the receptor EFR restricts Agrobacterium-mediated transformation. *Cell* **125**(4):749-760.

32. Newman KL, Almeida RP, Purcell AH, Lindow SE (2004) Cell-cell signaling controls Xylella fastidiosa interactions with both insects and plants. *Proc Natl Acad Sci USA* **101**(6):1737-1742.

33. Jha G, Rajeshwari R, Sonti RV (2007) Functional interplay between two Xanthomonas oryzae pv,. oryzae secretion systems in modulating virulence on rice. *Mol Plant-Microbe Interact: MPMI* **20**(1):31-40.

34. Chatterjee S, Sonti RV (2002) rpfF mutants of Xanthomonas oryzae pv. oryzae are deficient for virulence and growth under low iron conditions. *Mol Plant-Microbe Interact: MPMI* **15**(5):463-471.

35. Barber CE, *et al.* (1997) A novel regulatory system required for pathogenicity of Xanthomonas campestris is mediated by a small diffusible signal molecule. *Mol Microbiol* **24**(3):555-566.

36. Chatterjee S, Wistrom C, Lindow SE (2008) A cell-cell signaling sensor is required for virulence and insect transmission of Xylella fastidiosa. *Proc Natl Acad Sci USA* **105**(7):2670-2675.

37. Combet C, Jambon M, Deleage G, Geourjon C (2002) Geno3D: automatic comparative molecular modelling of protein. *Bioinformatics* **18**(1):213-214.

38. Konagurthu AS, Whisstock JC, Stuckey PJ, Lesk AM (2006) MUSTANG: a multiple structural alignment algorithm. *Proteins* **64**(3):559-574.

39. Larkin MA, *et al.* (2007) Clustal W and Clustal X version 2.0. *Bioinformatics* **23**(21):2947-2948.

40. Gouy M, Guindon S, Gascuel O (2010) SeaView version 4: A multiplatform graphical user interface for sequence alignment and phylogenetic tree building. *Mol Biol Evolution* **27**(2):221-224.

41. Newman KL, Almeida RP, Purcell AH, Lindow SE (2003) Use of a green fluorescent strain for analysis of Xylella fastidiosa colonization of Vitis vinifera. *Appl Environm Microbiol* **69**(12):7319-7327.

42. Almeida RP, Mann R, Purcell AH (2004) Xylella fastidiosa cultivation on a minimal solid defined medium. *Curr Microbiol* **48**(5):368-372.

43. Schuster AM, Davies E (1983) Ribonucleic acid and protein metabolism in pea epicotyls: I. The aging process. *Plant Physiol* **73**(3):809-816.

44. Erickson PA, Anderson DH, Fisher SK (1987) Use of uranyl acetate en bloc to improve tissue preservation and labeling for post-embedding immunoelectron microscopy. *J Elect Microsc Technique* **5**(4):303-314.

45. Smeltzer MS, Hart ME, Iandolo JJ (1992) Quantitative spectrophotometric assay for staphylococcal lipase. *Appl Environm Microbiol* **58**(9):2815-2819.

46. Choat B, Gambetta GA, Wada H, Shackel KA, Matthews MA (2009) The effects of Pierce's disease on leaf and petiole hydraulic conductance in Vitis vinifera cv. Chardonnay. *Physiol Plantarum* **136**(4):384-394.

47. Thorne ET, Stevenson JF, Rost TL, Labavitch JM, Matthews MA (2006) Pierce's Disease symptoms: comparison with symptoms of water deficit and the impact of water deficits. *Amer J Enol Viticult* **57**(1):1-11.

48. Rodriguez-Ortega MJ*, et al.* (2006) Characterization and identification of vaccine candidate proteins through analysis of the group A Streptococcus surface proteome. *Nat Biotech* **24**(2):191-197.

49. Berlec A, Zadravec P, Jevnikar Z, Strukelj B (2011) Identification of candidate carrier proteins for surface display on Lactococcus lactis by theoretical and experimental analyses of the surface proteome. *Appl Environm Microbiol* **77**(4):1292-1300.

50. Solis N, Larsen MR, Cordwell SJ (2010) Improved accuracy of cell surface shaving proteomics in Staphylococcus aureus using a false-positive control. *Proteomics* **10**(10):2037-2049.

51. Tjalsma H, Lambooy L, Hermans PW, Swinkels DW (2008) Shedding & shaving: Disclosure of proteomic expressions on a bacterial face. *Proteomics* **8**(7):1415-1428.

52. Cordwell SJ (2006) Technologies for bacterial surface proteomics. *Curr Opin Microbiol* **9**(3):320-329.

53. Buist G, Ridder AN, Kok J, Kuipers OP (2006) Different subcellular locations of secretome components of Gram-positive bacteria. *Microbiology* **152**(Pt 10):2867-2874.

54. Tjalsma H*, et al.* (2004) Proteomics of protein secretion by Bacillus subtilis: separating the "secrets" of the secretome. *Microbiol Mol Biol Rev: MMBR* **68**(2):207-233.

55. Poetsch A, Wolters D (2008) Bacterial membrane proteomics. *Proteomics* **8**(19):4100-4122.

56. Rajeshwari R, Jha G, Sonti RV (2005) Role of an in planta-expressed xylanase of Xanthomonas oryzae pv. oryzae in promoting virulence on rice. *Mol Plant-Microbe Interact: MPMI* **18**(8):830-837.

57. Smolka MB, *et al.* (2003) Proteome analysis of the plant pathogen Xylella fastidiosa reveals major cellular and extracellular proteins and a peculiar codon bias distribution. *Proteomics* **3**(2):224-237.

58. Boekema BK, *et al.* (2007) Hexadecane and Tween 80 stimulate lipase production in Burkholderia glumae by different mechanisms. *Appl Environm Microbiol* **73**(12):3838-3844.

59. Chang RC, Chou SJ, Shaw JF (1994) *Multiple forms and functions of Candida rugosa lipase*. *Biotechnol Appl Biochem* **19**(1):93-97.

60. Zhang S, *et al.* (2011) The Xylella fastidiosa biocontrol strain EB92-1 genome is very similar and syntenic to Pierce's disease strains. *J Bacteriology* **193**(19):5576-5577.

61. Hopkins DL (2005) *Biological control of Pierce's disease in the vineyard with strains of Xylella fastidiosa benign to grapevine*. *Plant Dis* **89**(12)1348-1352.

62. Deatherage BL, *et al.* (2009) Biogenesis of bacterial membrane vesicles. *Mol Microbiol* **72**(6):1395-1407.

63. Renelli M, Matias V, Lo RY, Beveridge TJ (2004) DNA-containing membrane vesicles of Pseudomonas aeruginosa PAO1 and their genetic transformation potential. *Microbiology* **150**(Pt 7):2161-2169.

64. Wai SN, *et al.* (2003) Vesicle-mediated export and assembly of pore-forming oligomers of the enterobacterial ClyA cytotoxin. *Cell* **115**(1):25-35.

65. Kato S, Kowashi Y, Demuth DR (2002) Outer membrane-like vesicles secreted by Actinobacillus actinomycetemcomitans are enriched in leukotoxin. *Microb Pathogene* 32(1):1-13.

66. Kadurugamuwa JL, Beveridge TJ (1996) Bacteriolytic effect of membrane vesicles from Pseudomonas aeruginosa on other bacteria including pathogens: conceptually new antibiotics. *J Bacteriology* **178**(10):2767-2774.

67. Kadurugamuwa JL, Beveridge TJ (1995) Virulence factors are released from Pseudomonas aeruginosa in association with membrane vesicles during normal growth and exposure to gentamicin: a novel mechanism of enzyme secretion. *J Bacteriology* **177**(14):3998-4008.

68. Kolling GL, Matthews KR (1999) Export of virulence genes and Shiga toxin by membrane vesicles of Escherichia coli O157:H7. *Appl Environme Microbio* **65**(5):1843-1848.

69. Mashburn LM, Whiteley M (2005) Membrane vesicles traffic signals and facilitate group activities in a prokaryote. *Nature* **437**(7057):422-425.

70. Bauman SJ, Kuehn MJ (2006) Purification of outer membrane vesicles from Pseudomonas aeruginosa and their activation of an IL-8 response. *Microbes Infection / Institut Pasteur* **8**(9-10):2400-2408.

71. Fritz JH, Ferrero RL, Philpott DJ, Girardin SE (2006) Nod-like proteins in immunity, inflammation and disease. *Nature Immuno* **7**(12):1250-1257.

72. Tavano R*, et al.* (2009) The membrane expression of Neisseria meningitidis adhesin A (NadA) increases the proimmune effects of MenB OMVs on human macrophages, compared with NadA-OMVs, without further stimulating their proinflammatory activity on circulating monocytes. *J Leukocyte Biology* **86**(1):143-153.

73. Ellis TN, Kuehn MJ (2010) Virulence and immunomodulatory roles of bacterial outer membrane vesicles. *Microbio Mol Biol Rev: MMBR* **74**(1):81-94.

74. Feil H, Feil WS, Lindow SE (2007) Contribution of fimbrial and afimbrial adhesins of Xylella fastidiosa to attachment to surfaces and virulence to grape. *Phytopathology* **97**(3):318-324.

75. Ray SK, Rajeshwari R, Sharma Y, Sonti RV (2002) A high-molecular-weight outer membrane protein of Xanthomonas oryzae pv. oryzae exhibits similarity to non-fimbrial adhesins of animal pathogenic bacteria and is required for optimum virulence. *Mol Microbio* **46**(3):637-647.

76. Slater H, Alvarez-Morales A, Barber CE, Daniels MJ, Dow JM (2000) A two-component system involving an HD-GYP domain protein links cell-cell signalling to pathogenicity gene expression in Xanthomonas campestris. *Mo Microbio* **38**(5):986-1003.

77. Shi XY, Dumenyo CK, Hernandez-Martinez R, Azad H, Cooksey DA (2009) Characterization of regulatory pathways in Xylella fastidiosa: genes and phenotypes controlled by gacA. *Appl Environm Microbio* **75**(8):2275-2283.

78. Heeb S & Haas D (2001) Regulatory roles of the GacS/GacA two-component system in plant-associated and other gram-negative bacteria. *Mol Plant-Microbe Interact: MPMI* **14**(12):1351-1363.

79. De la Torre-Zavala S*, et al.* (2011) Gene expression of Pht cluster genes and a putative non-ribosomal peptide synthetase required for phaseolotoxin production is regulated by GacS/GacA in Pseudomonas syringae pv. phaseolicola. *Resear Microbio* **162**(5):488-498.

80. Brencic A*, et al.* (2009) The GacS/GacA signal transduction system of Pseudomonas aeruginosa acts exclusively through its control over the transcription of the RsmY and RsmZ regulatory small RNAs. *Mol Microbio* **73**(3):434-445.

81. Yan Q, Wu XG, Wei HL, Wang HM, Zhang LQ (2009) Differential control of the PcoI/PcoR quorum-sensing system in Pseudomonas fluorescens 2P24 by sigma factor RpoS and the GacS/GacA two-component regulatory system. *Microbiolog Resear* **164**(1):18-26.

82. Reimmann C, Valverde C, Kay E, Haas D (2005) Posttranscriptional repression of GacS/GacA-controlled genes by the RNA-binding protein RsmE acting

together with RsmA in the biocontrol strain Pseudomonas fluorescens CHA0. *J Bacteriology* **187**(1):276-285.

83. Reimmann C, *et al.* (1997) The global activator GacA of Pseudomonas aeruginosa PAO positively controls the production of the autoinducer N-butyryl-homoserine lactone and the formation of the virulence factors pyocyanin, cyanide, and lipase. *Mol Microbio* **24**(2):309-319.

84. Rahme LG, *et al.* (1995) Common virulence factors for bacterial pathogenicity in plants and animals. *Science* **268**(5219):1899-1902.

ANEXO

An engineered innate immune defense protects grapevines from Pierce disease

Abhaya M. Dandekar[a], Hossein Gouran[a], Ana María Ibáñez[a], Sandra L. Uratsu[a], Cecilia B. Agüero[b], Sarah McFarland[a], Yasmin Borhani[a], Paul A. Feldstein[c], George Bruening[c], Rafael Nascimento[a], Luiz R. Goulart[d], Paige E. Pardington[e], Anu Chaudhary[e], Meghan Norvell[e], Edwin Civerolo[f], and Goutam Gupta[e,1]

[a]Plant Sciences Department, [b]Viticulture and Enology Department, [c]Plant Pathology Department, and [d]Medical Microbiology and Immunology Department, University of California, Davis, CA 95616; [e]Biosciences Division, Los Alamos National Laboratory, Los Alamos, NM 87545; and [f]US Department of Agriculture, Agricultural Research Service, San Joaquin Valley Agricultural Science Center, Parlier, CA 93648

Edited by Eugene W. Nester, University of Washington, Seattle, WA, and approved January 20, 2012 (received for review September 29, 2011)

We postulated that a synergistic combination of two innate immune functions, pathogen surface recognition and lysis, in a protein chimera would lead to a robust class of engineered antimicrobial therapeutics for protection against pathogens. In support of our hypothesis, we have engineered such a chimera to protect against the Gram-negative *Xylella fastidiosa* (Xf), which causes diseases in multiple plants of economic importance. Here we report the design and delivery of this chimera to target the Xf subspecies *fastidiosa* (Xff), which causes Pierce disease in grapevines and poses a great threat to the wine-growing regions of California. One domain of this chimera is an elastase that recognizes and cleaves MopB, a conserved outer membrane protein of Xff. The second domain is a lytic peptide, cecropin B, which targets conserved lipid moieties and creates pores in the Xff outer membrane. A flexible linker joins the recognition and lysis domains, thereby ensuring correct folding of the individual domains and synergistic combination of their functions. The chimera transgene is fused with an amino-terminal signal sequence to facilitate delivery of the chimera to the plant xylem, the site of Xff colonization. We demonstrate that the protein chimera expressed in the xylem is able to directly target Xff, suppress its growth, and significantly decrease the leaf scorching and xylem clogging commonly associated with Pierce disease in grapevines. We believe that similar strategies involving protein chimeras can be developed to protect against many diseases caused by human and plant pathogens.

disease protection | pathogen clearance | symptom suppression

Innate immune response is the first line of host defense against invading pathogens. This response occurs readily after pathogen recognition by the host cell through intracellular signaling and subsequent expression of effector molecules, such as lytic antimicrobial peptides, cytokines, and reactive oxygen species, that are involved directly or indirectly in pathogen clearance (1). However, many pathogens successfully circumvent the innate immune defense and manage to grow inside the host, establish infection, and cause disease (2, 3). It is our hypothesis that although a pathogen might be able to block the individual functions (i.e., pathogen recognition by host cells, intracellular host signaling, and function of the effector molecules), it would have difficulty overcoming a combination of two innate immune functions in the same molecule (4). Specifically, we believe that the synergistic combination of pathogen recognition protein and lytic peptide in a chimera would be very effective in blocking infection and thus represent a unique class of protein therapeutics. The efficacy of these chimeras would depend on the degree of synergism achieved between the chimera components and how effectively these chimeras were delivered to sites of pathogen colonization.

For a demonstration of chimera efficacy, we targeted *Xylella fastidiosa* (Xf), a Gram-negative bacterial pathogen with a wide range of plant hosts of economic importance (5–8). Xf is vectored primarily by sharpshooter insects and colonizes in the plant xylem (6, 7). The Xf subspecies *fastidiosa* (Xff), as exemplified by the California strain Temecula1, causes Pierce disease (PD) in grape. In this paper, we report that a transgene expressing a protein chimera containing recognition and lysis domains, expressed in multiple grape lines, significantly reduced the Xff level in the xylem and ameliorated the symptoms of PD. Transgenic model and crop plants expressing antimicrobial peptides (e.g., insect cecropins) have been shown to display resistance against various bacterial and fungal pathogens (9). Given that the level of protection by a single antimicrobial peptide is only moderate at best, efforts have been made to fuse two antimicrobial peptides (e.g., cecropin and melittin) to improve their efficacy in disease protection (10). Moreover, because antimicrobial peptides are inherently unstable due to their susceptibility to plant proteases, amino acids have been altered to improve their stability in plant tissues (11). However, to the best of our knowledge, an effective protein chimera combining recognition and lysis domains and targeting two different but conserved moieties on the pathogen surface has not yet been reported. We describe the anti-Xff properties of our chimera and propose an explanation for its much greater effectiveness compared with an antimicrobial peptide alone.

Results

Outer-Membrane Protein MopB Is a Logical Xf Recognition Target for Our Strategy. Our first step in designing a chimera was selecting an appropriate recognition target on the Xf surface. We selected MopB as our recognition target based on four main observations. First, MopB is the most abundant protein in Xff membrane preparations detected on mass spectrometry analysis (Fig. S1). Second, the sequence of MopB was identical in all Xf subspecies sequenced thus far (12–14). Third, MopB is accessible on the Xff cell surface, as evidenced by strong staining of the Xf cell surface by Alexa Fluor 488-labeled rabbit anti-MopB polyclonal antibody (Fig. 1*A*). Fourth, sequence and structure analysis revealed that MopB contains recognition and cleavage sites for human neutrophil elastase (HNE), a host defense protein. Our cleavage studies confirmed that MopB is indeed a target for HNE (Fig. 1*B*), although the membrane-bound MopB appears to be partially protected relative to the soluble MopB. In addition, as a member of the multifunctional porin family, MopB is an attractive Xff target because it is likely critical for bacterial growth and viability (15, 16) and, like other porins, is an expected target for host defense (17, 18). The observation that porin deletion

Author contributions: A.M.D., G.B., E.C., and G.G. designed research; H.G., A.M.I., S.L.U., C.B.A., S.M., Y.B., P.A.F., G.B., R.N., P.E.P., A.C., and M.N. performed research; C.B.A. performed plant transformations; L.R.G. supervised the mass spectrometric work of R.N.; L.R.G. analyzed data; and A.M.D., G.B., and G.G. wrote the paper.

The authors declare no conflict of interest.

This article is a PNAS Direct Submission.

Freely available online through the PNAS open access option.

[1]To whom correspondence should be addressed. E-mail: gxg@lanl.gov.

This article contains supporting information online at www.pnas.org/lookup/suppl/doi:10.1073/pnas.1116027109/-/DCSupplemental.

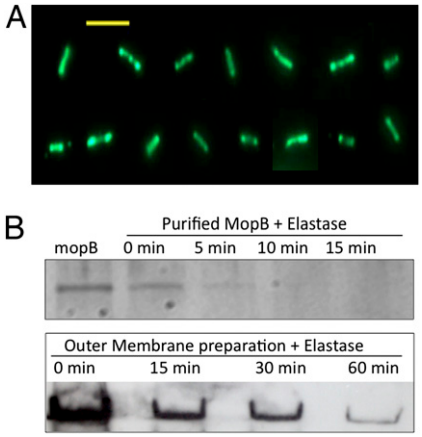

Fig. 1. HNE–MopB interactions. (*A*) Staining of *X. fastidiosa* sbsp. *fastidiosa* Temecula1 strain (Xff, causal agent of PD disease of grapevines) by fluorescently labeled IgG from rabbit polyclonal antibody raised against Xf-MopB purified from bacterial culture. The images were assembled from seven fields to be representative of cells with their long axis parallel to the substrate. (Scale bar: 5 μm.) (*B*) Visualization of the digestion of Xff MopB by HNE on denaturing gels using purified MopB (detection by Coomassie stain) (*Upper*) and an Xf outer membrane preparation (detection by immunoblotting with anti-MopB polyclonal antibody) (*Lower*). Approximately 5 ng of purified MopB was incubated with 0.5 μg of HNE for the indicated times before analysis by electrophoresis. Aliquots of Xff cell suspension were incubated with 0, 0.1, 0.3, and 1 μg of elastase (Calbiochem) at 37 °C for 1 h before immunoblotting.

mutants of bacteria are more susceptible to bactericidal effects (19) is particularly noteworthy for our strategy.

HNE Enhances the Bactericidal Effect of Cecropin B. As the lysis component of our chimera, we selected the peptide cecropin B, which shows a preference in its lytic action for Gram-negative bacteria (20). Because HNE, through cleavage, can make Xff more vulnerable to bactericidal agents, as was observed for porin deletion (19), it was of interest to test whether HNE does indeed enhance the bactericidal effect of cecropin B on Xff. Fig. 2*A* shows the effect of HNE, cecropin B, and HNE plus cecropin B on survival of Xff over a 1-h period as assessed by subsequent plating on solid periwinkle wilt (PW) medium (Fig. S2). We found that 50 nM HNE had a negligible effect on Xff viability relative to the untreated control, but that 5 μM cecropin B reduced the number of viable Xff cells. More interestingly, treatment with HNE plus cecropin B produced a synergistic effect, as evidenced by the dramatic reduction in the number of viable Xff cells (from 10^7 to 10^3 CFU/mL, compared with reductions to 10^6 for HNE alone and 10^5 for cecropin B alone). The synergy may be due to MopB cleavage by HNE facilitating Xff lysis and/or Xff lysis exposing MopB cleavage sites in the Xf outer membrane and periplasm.

Design of (HNE-Cecropin B) Chimeras to Facilitate Pathogen Recognition and Lysis and Delivery into the Plant Xylem. The results of our Xff cell viability studies prompted us to design a chimera of covalently linked HNE and cecropin B with the intent of enhancing the synergistic effect of the two modules. The design of such a chimera was subject to two criteria: (*i*) Each domain should retain its native folding and function, and (*ii*) the two domains should be joined in such way that both are able to act simultaneously on their target sites on Xff. Clearly, an appropriate choice of a linker is critical to meeting these criteria. We performed molecular dynamics and energy minimization (21) to obtain stable structures of the chimera, in which a flexible linker with the amino acid sequence GSTA joins the HNE and cecropin B domains. Fig. 2*B* shows a ribbon diagram of such a chimera. The flexibility of GSTA and neighboring amino acids were used to model a stable structure of the chimera in which HNE and cecropin B assumed their correct folding. A chimeric gene was constructed by fusing DNA sequences encoding the amino-end secretory signal peptide of HNE to the HNE-GSTA-cecropin B chimera. This construct is designated HNEsp-HNE-GSTA-cecropin B (Fig. S3). The secretory pathway is expected to facilitate the native folding of the secreted HNE and cecropin B domains in the chimera (22, 23). We tested the HNE activity by spectrophotometric enzyme assay (24), and tested the folding of cecropin B by binding to polyclonal antibody (Fig. S4). As expected, the secreted HNEsp-HNE-GSTA-cecropin B construct was more effective than HNE plus cecropin B in killing Xff (Fig. S5). In addition to the observed synergy, HNEsp-HNE-GSTA-cecropin B was delivered in the grape xylem, suggesting that the HNE secretion signal, HNEsp, is sufficient for the xylem delivery in a heterologous host (see below).

We created a second construct, designated PGIPsp-HNE-GSTA-cecropin B, using a plant-specific signal sequence for delivery of the chimera into the plant xylem. In this construct, we replaced the HNEsp with the signal peptide sequence from the pear polygalacturonase-inhibiting protein (PGIP) gene. PGIP, an innate defense protein, is secreted to the apoplast of plants and blocks cleavage of the pectin component of the middle lamella between plant cells by bacterial and fungal polygalactouranases (25). In a previous study (26), we demonstrated that the expression of PGIP in grapevines resulted in the secretion of PGIP first to the apoplast and then to the xylem. The chimeric genes (optimized for plant codon use) were cloned into a plant vector to create the two binary plasmids pDA05.0525 with PGIP signal peptide PGIPsp and pDU04.6105 with HNEsp (Fig. S6).

Our Chimera Protects Against Development of PD-Like Symptoms in Tobacco Plants. Disarmed *Agrobacterium tumefaciens* strain EHA 105 was electroporated with binary plasmid pDA05.0525, containing the PGIP signal peptide PGIPsp, and then used to transform *Nicotiana tabacum* cv. SR1, which has been established as a model host for the bioassay of Xf strains (27, 28). A total volume of 250 μL containing 2.5×10^7 Xff cells was injected at three sites, one on either side of the base of the midrib and the third in the middle of the midrib. As shown in Fig. 2*C*, at 2 mo after inoculation, extreme leaf scorching was observed on the untransformed plants, but only minimal scorching was seen on the transformed plants. Thus, expression of PGIPsp-HNE-GSTA-cecropin B in the xylem provided significant protection against the development of Xff-induced symptoms in tobacco.

Expression and Activity of the Chimera in Transgenic Grape Lines. Our results from the model tobacco system encouraged us to generate transgenic grapevines expressing the chimera with HNE signal peptide sequences (Fig. S6). As described previously, pre-embryogenic callus of *Vitis vinifera* variety Thompson seedless (TS) was used for plant transformation (29). Thirty-eight independent transgenic grape lines were generated from pDU04.6105 and grown in a greenhouse. Fig. 3*A* shows the expression of the HNEsp-HNE-GSTA-cecropin B gene as determined by real-time PCR in two transformed TS lines (89 and 146) in leaf and stem samples. A higher level of chimera expression is observed in leaf tissue compared with stem tissue. Plant transgenes under control of the CaMV 35S promoter reportedly are expressed at higher levels in the leaves than in other tissues (30). However, as shown in Fig. 3*B*, even the relatively low expression level in the stem was sufficient to provide in vitro anti-Xff activity in xylem sap. The presence and activity of the chimera in the xylem sap of the transgenic grape lines were examined by monitoring the growth of Xff for 5 h in the corresponding xylem saps. Fig. 3*B* shows the mortality of Xff in the

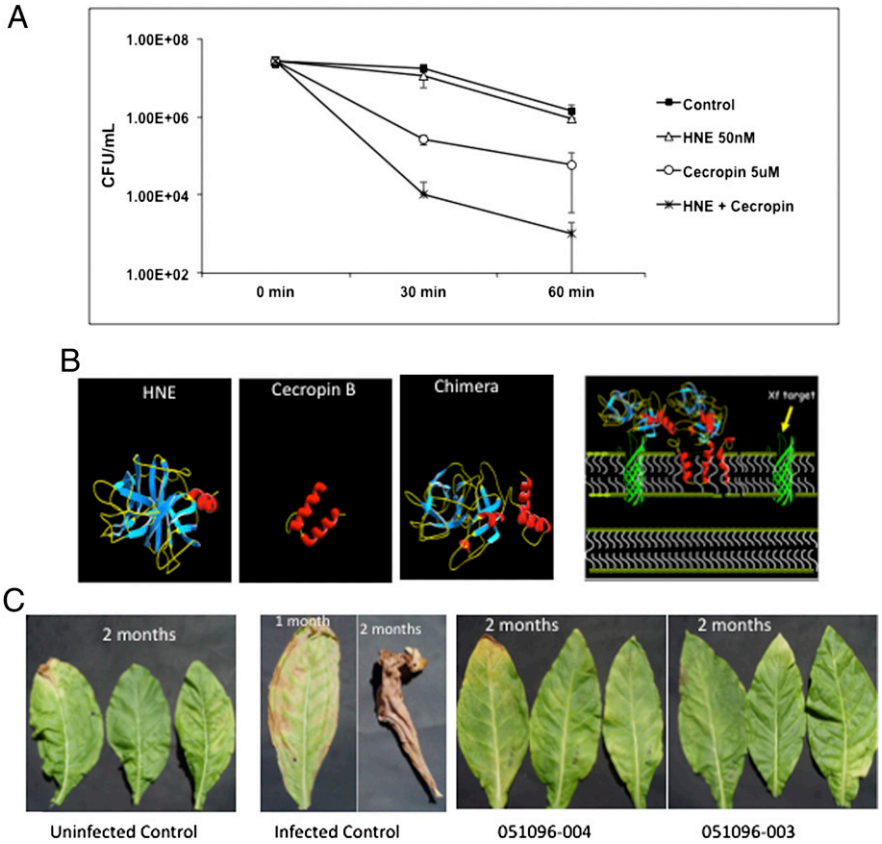

Fig. 2. Structures and biological activities of HNE, cecropin B, and HNE-GSTA-cecropin B. (*A*) The Xff-killing activity of HNE and cecropin B against 10^7 CFU/mL of Xff at indicated times after addition of buffer (control), 50 nM HNE, 5 μM cecropin B, and 50 nM HNE plus 5 μM cecropin B. Viable Xf was estimated by diluting aliquots and plating them on PW solid plates. (*B*) (*Left*) Ribbon diagrams of HNE (PDB ID: 1HNE) and cecropin B (PDB ID: 2IGR) generated from their coordinates and the energy-minimized model of the HNE-GSTA-cecropin B chimera. The flexibility of GSTA and a few residues of HNE and cecropin B were used to obtain a stable model using the AMBER force field (21) with the objective of having both HNE and cecropin B retain their native fold (and function). (*Right*) A schematic model of how oligomerization of the hydrophobic part of cecropin B leads to creation of pores in the outer membrane and also can allow cleavage of MopB. (*C*) Protection against development of PD symptoms demonstrated by two transgenic tobacco lines (051096-004 and 051096-003) expressing the HNE-GSTA-cecropin B chimera in the xylem and generated by *Agrobacterium*-mediated transformation using the PGIPst-HNE-GSTA-cecropin B–containing pDA05.0525 binary vector. Photographs were taken 1 or 2 mo postinoculation with Xff Temecula1 strain, as indicated.

xylem of the transgenic TS (89 and 146) lines relative to that in the xylem of the untransformed TS or in buffer. It appears that the endogenous signal sequence of HNE is sufficient to secrete the HNE-GSTA-cecropin B chimera to the xylem, where it confers the expected anti-Xff effect.

Transgenic Grape Lines Expressing the Chimera Are Protected Against Xff-Induced PD. The protection of the transgenic TS grapevine against PD was demonstrated by visual monitoring of leaf scorching (Fig. 4*A*) and NMR imaging of xylem blocking (Fig. 4*B*) after stem inoculation with Xff. Fifteen individuals each from 14 transgenic TS plant lines and one untransformed (control) plant were examined for 7–14 wk after Xff inoculation in a greenhouse. Representative leaves were selected from the eighth node above the point of inoculation at 10–14 wk postinoculation. Fig. 4*A* shows representative leaves from the untransformed TS and transgenic TS lines (89 and 146). We used a scaling system that assigned a score of 0 to a leaf with no scorching and 5 to a leaf with 100% scorching, a leaf that usually had dropped. The average "leaf scorching" scores for the transformed lines were ≤2 at the 10th week postinoculation and ∼2.5 at the 14th week postinoculation, compared with ≥4.2 for the untransformed plants at 10 wk or later postinoculation. Differences between the scores for transformed and untransformed plants were statistically significant with P values < 0.001.

Blocking of the xylem vessels was monitored by proton density NMR imaging of stem cross-sections (31) obtained from each plant at 15–20 cm above the point of inoculation. The bright patches in the proton image correspond to the presence of water, whereas the dark patches imply the absence of water. Fig. 4*B* shows the proton density maps of the stem cross-sections from the untransformed TS and transgenic TS lines at 10 wk after Xf inoculation. The stem cross-sections from the infected untransformed TS show central dark patches, suggesting lack of water flow due to xylem clogging, whereas the corresponding stem cross-sections in the transgenic lines show higher water density, implying relatively open xylem.

A selected set of "PD-protected" grape lines bearing the HNEsp-HNE-GSTA-cecropin B construct is currently being tested in the field. Grape lines bearing the PGIPsp-HNE-GSTA-cecropin B construct have been generated and are ready to be tested in the greenhouse and in the field.

Discussion

Here we describe a therapeutic approach for clearing a pathogen from the site of colonization in the host. This approach is based on two key steps: (*i*) designing a protein chimera containing recognition and lysis domains targeting conserved moieties on the pathogen surface, and (*ii*) specifically expressing this chimera at the site of pathogen colonization in the host. Such a protein chimera has been successfully designed to protect against PD caused

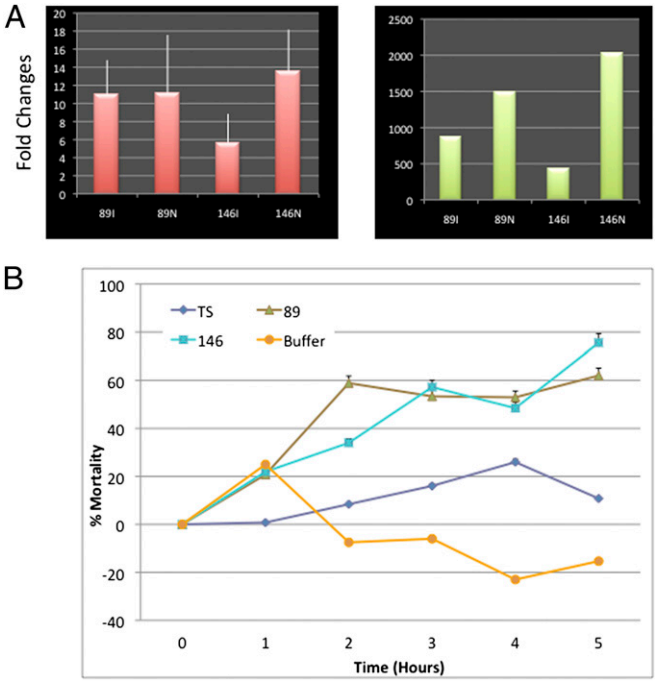

Fig. 3. Expression of HNEsp-HNE-GSTA-cecropin B and the biological effect of its gene product. (*A*) Level of expression of the chimera HNEsp-HNE-GSTA-cecropin B gene in the stem (red bars) and leaf tissues (green bars) of the transgenic TS-89 and TS-146 lines in inoculated (89I and 146I) and non-inoculated (89N and 146N) states, as determined by quantitative real-time PCR. The fold changes are relative to the expression levels in the untransformed TS. (*B*) The effect of the xylem sap collected from the transgenic TS lines 89 and 146 on the in vitro accumulation of the Xff strain KLN59.3 cells (28), which express GFP. For each sample extruded under pressure from stem sections, 450 μL of xylem sap was mixed with 50 μL of PBS (pH 7.4) containing 10^6 KLN59.3 cells. Three different dilutions of Xf/xylem sap mixture were plated on PW nutrient agar plates at 1-h intervals for 5 h. Xylem sap from the untransformed TS and buffer was used as controls.

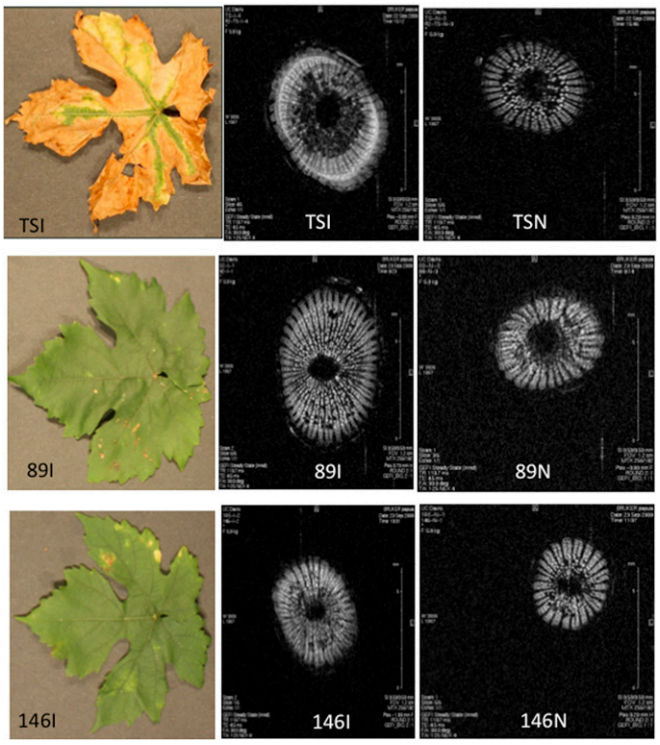

Fig. 4. Protective effects of HNE-GSTA-cecropin B in transgenic grapes. (*Left*) Monitoring of leaf scorching in the untransformed TS line and in the transgenic TS-89 and TS-146 lines expressing the HNE-GSTA-cecropin B chimera. Each leaf scorch monitoring experiment was performed using 30 plants from each transgenic line, 15 for Xff KLN59.3 inoculation and 15 for untreated controls. Transgenic TS and control TS plants were stem-inoculated with a total of 20 μL of the GFP-expressing Xff KLN59.3. The symptoms of leaf scorching were monitored after 10–14 wk of Xff KLN59.3 inoculation. A 10-μL drop of inoculum containing 10^7 Xf CFU/mL was placed near the base of the main stem 10 cm above the soil, and the stem was pricked through the liquid 5–10 times with a number 0 entomological pin. Fifteen plants were examined for the untransformed TS and for each of the transgenic TS lines. Representative leaves were selected from the eighth node above the point of inoculation at 10–14 wk postinoculation. (*Right*) ^{1}H-MRI images of the stems from the untransformed TS and the transgenic lines (89 and 146) inoculated with Xff strain KLN59.3 and of the stems from the same lines without inoculation. The images were obtained using an Avance 400 spectrometer equipped with Bruker DRX console microimaging accessories. The magnet is an Oxford vertical wide-bore (89 mm) magnet at 9.4 T (proton frequency, 400.1 MHz). At 10 wk postinoculation, the stems were cut under water from sections 10–20 cm above the point of inoculation and then completely wrapped with paraffin sheets to prevent further cavitation. Wrapped sections (10-12 cm) were placed inside the volume coil, and six transverse image slices were acquired simultaneously using a gradient-echo pulse sequence with a tip angle of 30 degrees, a repetition time of 110.7 ms, and an echo time of 4.5 ms. The images with the highest resolution were selected for further analysis. The images were acquired using 256 × 192 pixels with a field of view of 1.2 cm and slice thickness of 1.2 mm.

by Xff. We have demonstrated anti-Xff activity of the chimera in the grape xylem (Fig. 3*B*) and protection against PD in grapevine (Fig. 4 *A* and *B*). Our approach provides a viable alternative to conventional breeding of PD-resistant grapes. Note that in general, multiple genes clusters control PD resistance in natural grape cultivars, and these genes assort independently, resulting in very few resistant progeny in breeding populations. However, the recent discovery of PD resistance in the *Vitis arizonica* grape occurring in a single locus (designated *Pdr1*) suggests much promise for conventional breeding because of single-gene inheritance (32). In contrast to a conventional gene for resistance, the chimeric transgene described here has a defined mode of action, does not result in the introduction of adverse traits through linkage drag, and can be manipulated to alter its strength of action and other characteristics. Finally, because MopB is identical in all Xf strains, the same chimera also should effectively protect against Xf-induced diseases of economically important tree fruits and nuts, such as citrus, almond, coffee, peach, and plum.

Traditionally, the lytic antimicrobial peptides have been characterized as the next-generation antibiotics for their ability to target and kill bacteria. However, these peptides have limitations, being active only at high (μM) concentration (33) and often rendered inactive by bacterial resistance (34, 35). The appropriate linking of the recognition protein with a lytic peptide increases the overall antimicrobial activity of the chimera by several-fold over a lytic peptide alone (such as cecropin) or a combination of two lytic peptides (such as cecropin and melittin) with similar modes of action. The use of a protein chimera of recognition and lysis domains targeting two different but conserved moieties on a pathogen's surface should significantly overcome the problem of pathogenic resistance, because simultaneous mutations of the two sites are likely to occur at a very low frequency. Although proteins with multiple functional domains are quite common, antimicrobial protein chimeras synthetically designed by linking of pathogen recognition and lysis domains are not. This strategy of creating antipathogen chimeric proteins is applicable to a broad spectrum of pathogen-induced diseases, as we advocated several few years ago (4). We have recently completed preliminary studies showing that a protein chimera with recognition and clearance domains can completely inhibit the in vitro growth of *Staphylococcus aureus* at nM concentrations.

Materials and Methods

MopB was extracted and purified from the Xff grown on PD3 agar. IgG polyclonal antibody was purified from New Zealand White rabbit anti-sera collected after 100 d of MopB injection. The distribution of MopB on the Xff accessible on the surface was assessed by fluorescent imaging of Xff cells stained with Alexa Fluor-labeled anti-MopB IgG. The digestion of MopB was studied for the purified protein fraction, intact Xff, and membrane fraction by monitoring the product on a denaturing gel detected by either Coomassie blue staining or anti-MopB polyclonal IgG.

The HNE-GSTA-cecropin B chimera gene was cloned into pBacPAK8 baculovirus vector and expressed in High Five insect cells. The chimera was purified from the supernatant using elastin affinity beads that bound to HNE in the chimera. The antimicrobial activity of HNE, cecropin B, and the chimera was determined by measuring the CFU/mL of Xff plated on PW medium.

Two binary plasmids carrying HNEsp-HNE-GSTA-cecropin B and PGIPsp-HNE-GSTA-cecropin B genes were constructed. Each binary plasmid was introduced into a disarmed *Agrobacterium* strain to create a functional plant transformation system. Tobacco (*N. tabacum* cv. SR1) was transformed using the binary plasmid carrying PGIPsp-HNE-GSTA-cecropin B. TS grapevine embryogenic callus cultures were transformed using both binary plasmids.

mRNA levels of the chimera in the leaf, petiole, and stem tissues of the transformed and untransformed grape lines were measured by quantitative real-time PCR. Xylem sap was collected from the transformed and untransformed grapevines, and the activity of the chimera in xylem sap was tested by measuring the bactericidal effect on the Xff KLN59.3 strain grown in PW medium. The *in planta* efficacy of the HNEsp-HNE-GSTA-cecropin B chimera was determined by comparing (*i*) leaf scorching in transformed and untransformed grape lines and (*ii*) blockage of water by NMR in the xylem of transformed and untransformed grape lines.

More details are provided in *SI Materials and Methods*.

ACKNOWLEDGMENTS. This project was supported by funding from the Pierce's Disease Control Board of the California Department of Food and Agriculture (various awards to A.M.D., G.B., and P.A.F.), the US Department of Energy, and the US Department of Agriculture (USDA-ARS Agreement 58-5302-4-544).

1. Janeway CA, Jr., Medzhitov R (2002) Innate immune recognition. *Annu Rev Immunol* 20:197–216.
2. de Wit PJ (2007) How plants recognize pathogens and defend themselves. *Cell Mol Life Sci* 64:2726–2732.
3. Kraus D, Peschel A (2008) *Staphylococcus aureus* evasion of innate antimicrobial defense. *Future Microbiol* 3:437–451.
4. Kunkel M, et al. (2007) Rapid clearance of bacteria and their toxins: Development of therapeutic proteins. *Crit Rev Immunol* 27:233–245.
5. Strange RN, Scott PR (2005) Plant disease: A threat to global food security. *Annu Rev Phytopathol* 43:83–116.
6. Dow JM, Daniels MJ (2000) *Xylella* genomics and bacterial pathogenicity to plants. *Yeast* 17:263–271.
7. Redak RA, et al. (2004) The biology of xylem fluid-feeding insect vectors of *Xylella fastidiosa* and their relation to disease epidemiology. *Annu Rev Entomol* 49:243–270.
8. Chatterjee S, Almeida RPP, Lindow SE (2008) Living in two worlds: The plant and insect lifestyles of *Xylella fastidiosa*. *Annu Rev Phytopathol* 46:243–271.
9. Montesinos E (2007) Antimicrobial peptides and plant disease control. *FEMS Microbiol Lett* 270:1–11.
10. Yevtushenko DP, et al. (2005) Pathogen-induced expression of a cecropin A-melittin antimicrobial peptide gene confers antifungal resistance in transgenic tobacco. *J Exp Bot* 56:1685–1695.
11. Owens LD, Heutte TM (1997) A single amino acid substitution in the antimicrobial defense protein cecropin B is associated with diminished degradation by leaf intercellular fluid. *Mol Plant Microbe Interact* 10:525–528.
12. Simpson AJ, et al.; *Xylella fastidiosa* Consortium of the Organization for Nucleotide Sequencing and Analysis (2000) The genome sequence of the plant pathogen *Xylella fastidiosa*. *Nature* 406:151–159.
13. Bhattacharyya A, et al. (2002) Whole-genome comparative analysis of three phytopathogenic *Xylella fastidiosa* strains. *Proc Natl Acad Sci USA* 99:12403–12408.
14. Chen J, et al. (2010) Whole genome sequences of two *Xylella fastidiosa* strains (M12 and M23) causing almond leaf scorch disease in California. *J Bacteriol* 192:4534.
15. Achouak W, Heulin T, Pagès JM (2001) Multiple facets of bacterial porins. *FEMS Microbiol Lett* 199:1–7.
16. Benz R (1988) Structure and function of porins from Gram-negative bacteria *Ann. Rev Microbiol* 42:359–393.
17. Wang Y (2002) The function of OmpA in *Escherichia coli*. *Biochem Biophys Res Commun* 292:396–401.
18. Belaaouaj A, Kim KS, Shapiro SD (2000) Degradation of outer membrane protein A in *Escherichia coli* killing by neutrophil elastase. *Science* 289:1185–1188.
19. Fu H, Belaaouaj AA, Dahlgren C, Bylund J (2003) Outer membrane protein A-deficient *Escherichia coli* activates neutrophils to produce superoxide and shows increased susceptibility to antibacterial peptides. *Microbes Infect* 5:781–788.
20. Moore AJ, Beazley WD, Bibby MC, Devine DA (1996) Antimicrobial activity of cecropins. *J Antimicrob Chemother* 37:1077–1089.
21. Hong-Geller E, Möllhoff M, Shiflett PR, Gupta G (2004) Design of chimeric receptor mimics with different TcRVβ isoforms: Type-specific inhibition of superantigen pathogenesis. *J Biol Chem* 279:5676–5684.
22. Ellgaard L, Molinari M, Helenius A (1999) Setting the standards: Quality control in the secretory pathway. *Science* 286:1882–1888.
23. Chevet E, Cameron PH, Pelletier MF, Thomas DY, Bergeron JJ (2001) The endoplasmic reticulum: Integration of protein folding, quality control, signaling and degradation. *Curr Opin Struct Biol* 11:120–124.
24. Bieth J, Spiess B, Wermuth CG (1974) The synthesis and analytical use of a highly sensitive and convenient substrate of elastase. *Biochem Med* 11:350–357.
25. Roper MC, Greve LC, Warren JG, Labavitch JM, Kirkpatrick BC (2007) *Xylella fastidiosa* requires polygalacturonase for colonization and pathogenicity in *Vitis vinifera* grapevines. *Mol Plant Microbe Interact* 20:411–419.
26. Agüero CB, et al. (2005) Evaluation of tolerance to Pierce's disease and *Botrytis* in transgenic plants of *Vitis vinifera* L. expressing the pear PGIP gene. *Mol Plant Pathol* 6: 43–51.
27. Lopes SA, et al. (2000) *Nicotiana tabacum* as an experimental host for the study of plant–*Xylella fastidiosa* interactions. *Plant Dis* 84:827–830.
28. Francis M, Civerolo EL, Bruening GE (2008) Improved bioassay of *Xylella fastidiosa* using *Nicotiana tabacum* cultivar SR1. *Plant Dis* 92:14–20.
29. Aguero CB, Meredith CP, Dandekar AM (2006) Genetic transformation of *Vitis vinefera* L. Cvs Thompson Seedless and Chardonnay with pear PGIP and GFP encoding genes. *Vitis* 45:1–8.
30. Wally O, et al. (2008) Comparative expression of β-glucuronidase with five different promoters in transgenic carrot (*Daucus carota* L.) root and leaf tissues. *Plant Cell Rep* 27:279–287.
31. Pérez-Donoso AG, Greve LC, Walton JH, Shackel KA, Labavitch JM (2007) *Xylella fastidiosa* infection and ethylene exposure result in xylem and water movement disruption in grapevine shoots. *Plant Physiol* 143:1024–1036.
32. Krivanek AF, Famula TR, Tenscher A, Walker MA (2005) Inheritance of resistance to *Xylella fastidiosa* within a *Vitis rupestris* × *Vitis arizonica* hybrid population. *Theor Appl Genet* 111:110–119.
33. Guaní-Guerra E, Santos-Mendoza T, Lugo-Reyes SO, Terán LM (2010) Antimicrobial peptides: General overview and clinical implications in human health and disease. *Clin Immunol* 135:1–11.
34. Weidenmaier C, Kristian SA, Peschel A (2003) Bacterial resistance to antimicrobial host defenses—an emerging target for novel antiinfective strategies? *Curr Drug Targets* 4: 643–649.
35. Gutsmann T, et al. (2005) Lipid-mediated resistance of Gram-negative bacteria against various pore-forming antimicrobial peptides. *J Endotoxin Res* 11:167–173.

Supporting Information

Dandekar et al. 10.1073/pnas.1116027109

SI Materials and Methods

Xf Strains and Growth Conditions. The WT Temecula1 strain of *Xylella fastidiosa* subspecies *fastidiosa* (Xff; ATCC 700964) and a GFP-expressing variant, the KLN59.3 strain (1), were used in these studies. The bacteria were grown in periwinkle wilt (PW) medium with 1.5% agar at 28 °C, and liquid cultures were prepared in the same medium and grown with aeration (150 rpm) at 28 °C. PW media (2) was supplemented with kanamycin (30 mg/mL) for selective growth of KLN59.3.

Immunostaining of Xf Cells. Xff Temecula1 cells were harvested from PD3 agar medium (3) by suspending plate scrapings in SCP (3.7 mM sodium succinate, 3.4 mM trisodium citrate, 8.6 mM KH_2PO_4, and 7.4 mM K_2HPO_4), and then washed once with SCP and once with water. Then 4 mL of A_{600} = 20–25 cell suspension was diluted and mixed gently in a final volume of 50 mL in 40 mM Tris-HCl, 10 mM sodium EDTA, 8 mg/mL SDS, and 0.2 mg/mL mercaptoethanol (pH 8.5). The suspension was incubated at 30 °C for 30 min. The precipitate was collected by centrifugation at 210,000 × *g* for 30 min at 15 °C and then suspended in 1.2 mL of water. The suspension was heated in SDS/PAGE disruption solution, and the equivalent of 2 A_{600} units of the original Xf cell suspension was applied to each lane of a 12.5% polyacrylamide SDS-permeated gel. An unstained gel was aligned with neighboring lanes of stained gel to locate a band with migration corresponding to molecular mass of 45 kDa. The unstained band was excised and crushed, and protein was eluted. Gel fragments were removed by centrifugal flow through a 45-μm filter. Eluted protein from four lanes was injected into a New Zealand White rabbit at 0, 40, and 60 d, and serum was collected at 100 d. IgG was purified (4) and treated with Alexa Fluor 488 (fluorescein active ester; Molecular Probes A-10235) in accordance with the manufacturer's protocol. Approximately 0.25 A_{600} units of Xff Temecula1 cells were collected and washed once with 500 μL of PBS containing 1 μL/mL of Tween 20 nonionic detergent (PBS-T). The cells were incubated overnight with fluorescent antibody against Xf Temecula1 MopB, washed three times with PBS-T, suspended in 20 μL of PBS-T, and examined with a fluorescence microscope under 488-nm illumination.

Digestion of Cells and Outer Membrane Fraction of Xff with HNE. For HNE digestion of an outer membrane preparation, 3 μg of membrane preparation derived from 50 mL of Xff cell culture was mixed with 1.2 μM of HNE and incubated for the indicated times in a volume of 50 μL. Membrane preparations were obtained according to the method of Fujiki et al. (5) with modifications. Xff Temecula1 strain cells were grown in 50 mL of PD3 media for 10 d at 28 °C and 120 rpm. Cells were washed three times with washing buffer [10 mM Tris (pH 8.8), 3 mM KCl, 50 mM NaCl, 5 mM EDTA, and 1 mM PMSF] and collected by centrifugation at 5,000 × *g* for 5 min. The cell pellet was diluted in 5 mL of 50 mM Tris-HCl (pH 7.3) containing 0.6 mg of DNase I (Qiagen). The cells were ruptured by sonication on ice, and the unbroken cells were removed by centrifugation at 8,500 × *g* for 10 min. The supernatant was diluted with ice-cold 0.1 M sodium carbonate (pH 11.0) to a final volume of 50 mL and stirred slowly on ice for 1 h. The carbonate-treated membranes were collected by ultracentrifugation at 115,000 × *g* for 1 h at 4 °C. The supernatant was discarded, and the membrane pellet was resuspended and washed in 50 mL of 50 mM Tris-HCl (pH 7.3). The pellet was collected by centrifugation at 115,000 × *g* for 1 h at 4 °C, resuspended in PBS (pH 7.4), and stored at −80 °C. For HNE digestion of an outer membrane preparation, 3 μg of membrane preparation derived from 50 mL of Xff cell culture was mixed with 1.2 μM HNE and incubated for the indicated times in a volume of 50 μL. Cells were incubated with HNE under similar conditions and collected by centrifugation, and were heated in SDS disruption solution before being applied to the gel.

Mass Spectrometry Analysis of the Xff Membrane Fraction. Xff membrane fractions, extracted following the procedure described above, were analyzed in the Proteomics Facility at University of California Davis. After digestion with trypsin, the samples were resuspended in 2% acrylonitrile and 0.1% trifluoracetic acid and loaded directly onto the mass spectrometer. A paradigm MG4 HPLC system (Michrom Bioresources), coupled to a Finnigan LTQ Ion-Trap Mass Spectrometer (Thermo Scientific) was used for peptide separation and analysis. Each digested sample (10 μg) was loaded onto a trap column (Zorbax 300SB-C18, 5 μm, 5 × 0.3 mm; Agilent Technologies) and desalted online. Peptides were then eluted from the trap and separated on a reverse-phase Michrom Bioresources Magic C18AQ (200 μm × 150 mm) capillary column at a flow rate of 2 μL/min. Peptides were eluted using a 120-min gradient of 2% B–35% B over 80 min and 35% B–80% B for 25 min, held at 80% B for 1 min and 80% B–2% B in 1 min, and re-equilibrated for 13 min at 2% B (A, 0.1% formic acid; B, 100% ACN) and then sprayed directly into the mass spectrometer by/through a Michrom Bioresources advance captive spray ionization source with a spray voltage of 1.5 kV, a heated capillary temperature of 180 °C, and a full scan range of 350–1400 mass-to-charge ratio. Data-dependent MS/MS spectra (6) were collected with the following parameters: 10 MS/MS spectra for the most intense ions from the full scan (minimum signal required, 500.0; isolation width, 2.0) with 35% collision energy for collision-induced dissociation. Dynamic exclusion of the same abundant peptides was enabled with a repeat count of 2 and an exclusion duration of 1 min. The protein database of Xff Temecula 1 strain was downloaded from Uniprot.org, which contains the most common contaminants of such samples as human keratin and BSA, to allow identification of and correction for such contaminants in our samples. The MS/MS-generated data were analyzed using Scaffold software (Proteome Software). Fig. S1 shows the relative abundance of MopB among Xf outer membrane proteins.

Measurement of Bactericidal Activity Using Xff Culture. The Xff Temecula1 strain or KLN59.3 variant was grown to midlog suspension in PW medium, and A_{550} nm was measured. Cells were centrifuged and resuspended in 0.15 M NaCl to obtain an A_{550} nm of 0.5. The culture was diluted and treated with different protein concentrations (50 nM HNE, 50 μM cecropin, or both together), with water used as a control. After the treatment, the samples were removed to measure A_{550} nm, and the cells were centrifuged, resuspended, diluted, and plated on PW medium to enumerate viable cell counts. Fig. S2 shows Xf colonies without any treatment and with treatment with HNE, cecropin B, and HNE plus cecropin B.

Mortality Assay with Xylem Sap from Transgenic and Untransformed Thompson Seedless Plants. Xylem sap was extracted from mature plants grown in the greenhouse using a pressure chamber. Stems were severed 15–20 cm above the soil, and the remaining lower part of the plant, including roots, was placed inside a chamber

with only the top of the stem exposed. The root system was kept intact to prevent dilution of the sap. The chamber was pressurized with industrial nitrogen gas to ~5 bars. Collected sap was filter-sterilized with a 0.2-μm low protein binding filter (Millipore) and kept at 4 °C. Xff KLN59.3 variant was inoculated in 5 mL of liquid PW media containing kanamycin (30 μg/mL) with 50 μL of Xff stock cells at a concentration of 10^9 CFU/mL and incubated at 28 °C under shaking at 100 rpm for 4–6 d. For each sample extracted from transgenic vines, 450 μL of xylem sap was mixed with 50 μL of PBS (pH 7.4) containing 10^6 Xf cells. Three different dilutions of the Xff–xylem sap mixture was plated on PW solid plates at one-hour time points for five hours.

Real-Time Quantitative PCR of mRNAs from Grape Tissue Samples. Leaf, petiole, and stem samples were collected from greenhouse, immediately frozen in liquid nitrogen, and kept at −80 °C before extraction. For each sample, 100 mg of tissue was ground in liquid nitrogen using a mortar and pestle, and the powdered tissue was processed using Concert Plant RNA Reagent (Invitrogen) following the manufacturer's instructions. RNA concentration and purity were analyzed using a Nanodrop spectrophotometer and an Experion bioanalyzer. Primers for the relative quantitation of the chimera gene in the transgenic (89 and 146) and untransformed Thompson Seedless (TS) lines were designed using OligoPerfect software (Invitrogen). Amplification reactions were done with an Applied Biosystems 7900HT Real-Time PCR System (7) using Express SYBR Green ER reagents (Invitrogen), performed in duplicate across all six transformed lines and the TS control line from both inoculated and noninoculated plants. The reaction volume was 20 μL, with 70 ng of total RNA per reaction. Samples were amplified under the following temperature cycling conditions: 5 min incubation at 50 °C, 2 min incubation at 95 °C, and 40 cycles of 95 °C for 15 s and 60 °C for 1 min, followed by a final temperature dissociation of 65 °C to 95 °C. Dissociation profiles were analyzed for a lack of primer dimer formation, and the expression levels were computed from the Ct values of the chimeric gene in the transgenic 89 and 146 lines relative to the untransformed TS.

Expression of the NE-GSTA-Cecropin B Chimera in Insect High Five Cells and Measurement of in Vitro Activity. The *HNEsp-HNE-GSTA-cecropin B* chimera gene was synthesized and cloned into pBacPAK8 baculovirus vector (8). Fig. S3 shows the protein sequence. The chimeric gene inserted into pBacPAK8 was cotransfected with BacPAK6 viral DNA into Sf21 cells. Recombinant viruses formed by homologous recombination were amplified, and protein expression was optimized in High Five cells (Invitrogen), derived from *Trichoplusia ni* egg cell homogenates. Compared with Sf9 and Sf21 cells, High Five insect cells produced significantly higher levels of secreted recombinant proteins. Optimal conditions for expression were determined in High Five cells by monitoring the infection of suspension cells in logarithmic growth with recombinant baculovirus, with a multiplicity of infection (MOI) of 10, and grown for 72 h (Fig. S4*A*). Approximately 25–50% of the expressed chimeric protein was secreted into the supernatant and was detected as a single band on Western blot analysis (Fig. S4*B*). The supernatant was collected, concentrated, and dialyzed, and concentrated supernatant was then run on an elastin affinity column. The chimeric protein-containing fractions were pooled and dialyzed, and the dialyzed fractions were run on a weak cation exchange column. All chromatography steps were carried out by gravity flow (Fig. S4*C*). The chimeric protein-containing fractions were pooled and dialyzed and tested for elastase activity and anti-cecropin antibody binding. For elastase activity, a spectrophotometric assay (9) was used to monitor the increase in the UV absorbance at 410 nM on cleavage of the model substrate, succinyl-(L-alanine)$_3$-p-nitroanilide. Cecropin B binding was assessed using the antibody ab27571 (Abcam). By these methods, we were able to purify 250 μg of active protein from 50 mL of supernatant. By scaling up the culture, we were able to obtain milligram quantities of purified protein for our in vitro efficacy studies. Fig. S5 shows the in vitro anti-Xff activity of the HNE-GSTA-cecropin B chimera relative to HNE plus cecropin B.

Construction of Plant Expression Vectors. The coding sequences HNEsp-HNE-GSTA-cecropin B and PGIPsp-HNE-GSTA-cecropin B were directionally cloned using XbaI and BamHI into our CaMV35 S cassette-containing vector, designated pDE00.0113, such that the coding regions were downstream from the *Cauliflower mosaic virus* (CaMV) 35S promoter and upstream from an octopine synthase gene (*ocs*) 3′-UTR regulatory region required for proper polyadenylation. The resultant cassettes carrying HNEsp-HNE-GSTA-cecropin B and PGIPsp-HNE-GSTA-cecropin B genes were then ligated into our binary pDU99.2215 vector using AscI. This led to the new binary vectors pDU04.6105 and pDU04.6105 (Fig. S6). The amino acid sequences of these chimeric proteins are shown in Fig. S3. These binary vectors were introduced into a disarmed *Agrobacterium* strain as described above to create functional plant transformation systems.

Transformation of Tobacco and Grapevine and Testing for Disease Resistance. *Agrobacterium* vectors carrying the two binary plasmids (Fig. S6) were provided to the Ralph M. Parsons Plant Transformation facility at University of California Davis. Fifteen independent transgenic lines for pDU04.6105 and 24 lines for pDA05.0525 were obtained and confirmed by PCR analysis of their DNA. TS grapevine embryogenic callus cultures were transformed as described previously (10). Transgenic grapevines were confirmed by GUS (β-glucuronidase) activity and by sequencing to check for the presence of the incorporated gene. The transgenic tobacco lines were challenged with Xff Temecula1 strain. Three leaves of three plants of each line were inoculated with 1–2 million Xff at the base of each leaf on either side of the midvein ("eye"). Log phase cultures of Xff grown in PW medium were centrifuged and resuspended in 0.15 M NaCl to 10^7 cells/mL, and 100 μL was inoculated using a tuberculin syringe (11). Controls were not inoculated or inoculated with 100 μL of 0.15 M NaCl. At the end of 1 mo and again at 2 mo, the tobacco leaves were scored. In vitro grape plants transformed with the constructs pDU04.6105 (HNE-GSTA-cecropin B) and pDA05.0525 (*N*-Term PGIP-HNE-cecropin B) were received from the Parsons Plant Transformation Facility. A total of 69 HNEsp-HNE-GSTA-cecropin B plants and 18 pgipSP-HNE-CECB plants were screened by PCR on DNA isolated from leaves using the Qiagen DNeasy Plant Mini Kit to verify the individual transformation events. The following primers were used for detection of elastase: CaMV355-2: 5′-GACGTAAGGGATGACGCACAAT; 3HNEb: 5′-TTACTAGAGTGCTTTTGCTTCTCCCAG. The 36 resulting HNE-CECB plants were micropropagated in the laboratory and transferred to the greenhouse for acclimation and for RNA and protein analysis. Five of 10 PGIPsp-HNE-GSTA-cecropin B in vitro lines were transferred to the greenhouse.

Each acclimated transgenic line was propagated to obtain between four and six plants for use as mother plants for further propagation to provide cuttings for *Xylella* infection and grafting experiments. From each line, 25–35 plants were propagated (from cuttings) at the same time. *Xylella* infection experiments were done in multiple rounds. Each round consisted of five or six transgenic lines and two controls, WT TS as a negative control and TS50 as a positive control. Each round of experiments included 30 plants from each transgenic line, including 15 inoculated plants and 15 noninoculated controls. The positive control, T50, was a transgenic PGIP-expressing grapevine described previously.

Transgenic TS and controls (untransformed TS and TS50) plants were inoculated with 20 μL of the GFP-expressing *X. fastidiosa* KLN59.3 containing ~2×10^7 cells. The plants were inoculated with

10 μL on the first day and reinoculated with 10 μL on the second day, with an independently grown *Xylella* culture used for each inoculation. The *Xylella* was introduced to each plant at ~3–4 inches above the soil level using a number 0 insect pin as described previously (11). Plants were pruned regularly and maintained at a height of ~90–100 cm until PD symptoms appeared. Each round of Xf challenge took 33–37 wk from the time of the transfer of in vitro plants to the greenhouse until the appearance of the first PD symptoms.

1. Newman KL, Almeida RPP, Purcell AH, Lindow SE (2003) Use of a green fluorescent strain for analysis of *Xylella fastidiosa* colonization of *Vitis vinifera*. *Appl Environ Microbiol* 69:7319–7327.
2. Davis MJ, French WJ, Schaad NW (1981) Axenic culture of the bacteria associated with phony disease of peach and plum leaf scald. *Curr Microbiol* 5:311–316.
3. Davis MJ, Purcell AH, Thompson SV (1980) Isolation media for the Pierce's disease bacterium. *Phytopathology* 70:425–429.
4. Rowhani A (1992) Use of F(Ab')$_2$ antibody fragment in ELISA for detection of grapevine viruses. *Am J Enol Vitic* 43:38–40.
5. Fujiki Y, Hubbard AL, Fowler S, Lazarow PB (1982) Isolation of intracellular membranes by means of sodium carbonate treatment: Application to endoplasmic reticulum. *J Cell Biol* 93:97–102.
6. Brown RN, Romine MF, Schepmoes AA, Smith RD, Lipton MS (2010) Mapping the subcellular proteome of *Shewanella oneidensis* MR-1 using sarkosyl-based fractionation and LC-MS/MS protein identification. *J Proteome Res* 9:4454–4463.
7. Schefe JH, Lehmann KE, Buschmann IR, Unger T, Funke-Kaiser H (2006) Quantitative real-time RT-PCR data analysis: Current concepts and the novel "gene expression's CT difference" formula. *J Mol Med (Berl)* 84:901–910.
8. Trowitzsch S, Bieniossek C, Nie Y, Garzoni F, Berger I (2010) New baculovirus expression tools for recombinant protein complex production. *J Struct Biol* 172:45–54.
9. Moore AJ, Beazley WD, Bibby MC, Devine DA (1996) Antimicrobial activity of cecropins. *J Antimicrob Chemother* 37:1077–1089.
10. Aguero CB, Meredith CP, Dandekar AM (2006) Genetic transformation of *Vitis vinefera* L. Cvs Thompson seedless and Chardonnay with pear PGIP- and GFP- encoding genes. *Vitis* 45:1–8.
11. Almeida RPP, Purcell AH (2003) Biological traits of *Xylella fastidiosa* strains from grapes and almonds. *Appl Environ Microbiol* 69:7447–7452.

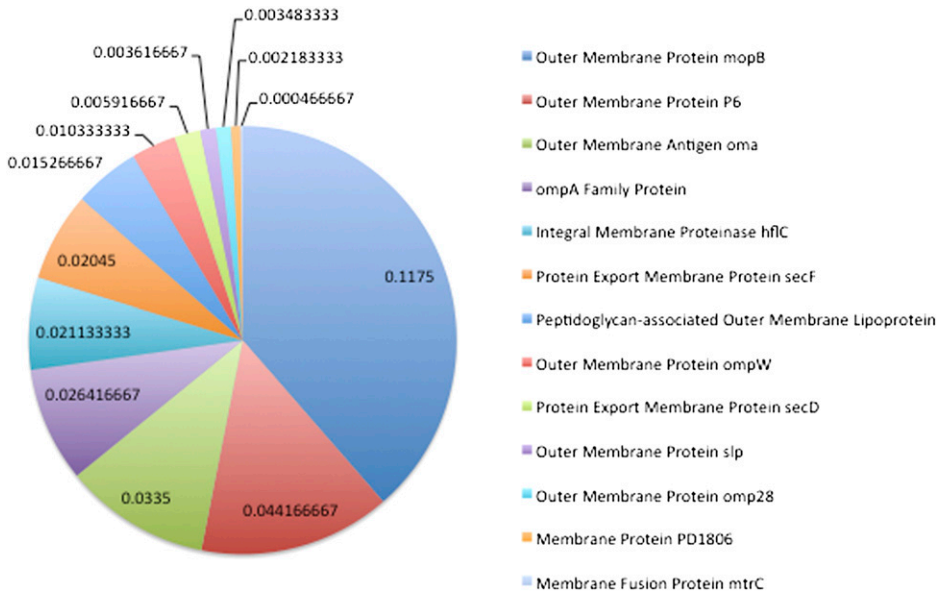

Fig. S1. Relative abundance of the Xf outer membrane proteins. The numbers correspond to the fraction of number of spectra obtained for a listed protein relative to the total number of spectra attributed to all identified proteins.

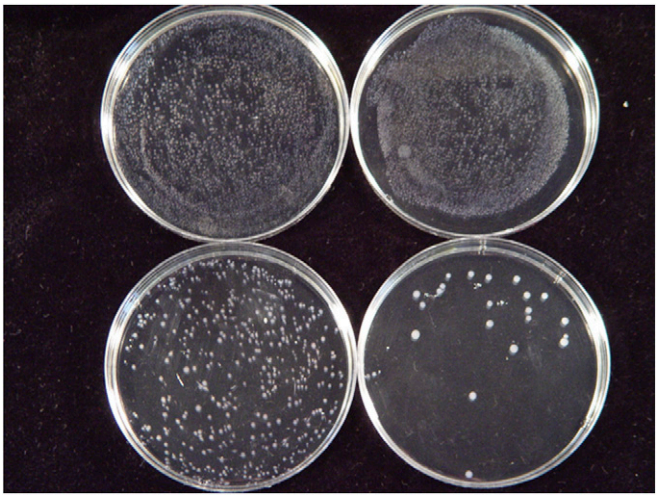

Fig. S2. Antimicrobial activity against Xff Temecula1 strain. Visualization of CFU without treatment (control; *A*) and with treatment with HNE (*B*), cecropin B (*C*), and HNE plus cecropin B (*D*). These experiments were performed in replicate to obtain the data shown in Fig. 2*A*.

MTLGRRLACLFLACVLPALLLGGTALASE

MELKFSTFLSLTLLFSSVLNPALSIVGGRRARPHAWPFMVSLQLRGGHFCGA

TLIAPNFVMSAAHCVANVNVRAVRVVLGAHNLSRREPTRQVFAVQRIFED

GYDPVNLLNDIVILQLNGSATINANVQVAQLPAQGRRLGNGVQCLAMGW

GLLGRNRGIASVLQELNVTVVTSLCRRSNVCTLVRGRQAGVCFGDSGSPLV

CNGLIHGIASFVRGGCASGLYPDAFAPVAQFVNWIDSIIQGSTA

KWKVFKKIEKMGRNIRNGIVKAGPAIAVLGEAKAL

Fig. S3. Amino acid sequences of the two chimeras, one with the intrinsic HNE N-terminal signal (designated HNEsp; upper sequence in orange) and the other with the pear N-terminal PGIP signal (designated PGIPsp, lower sequence in orange).

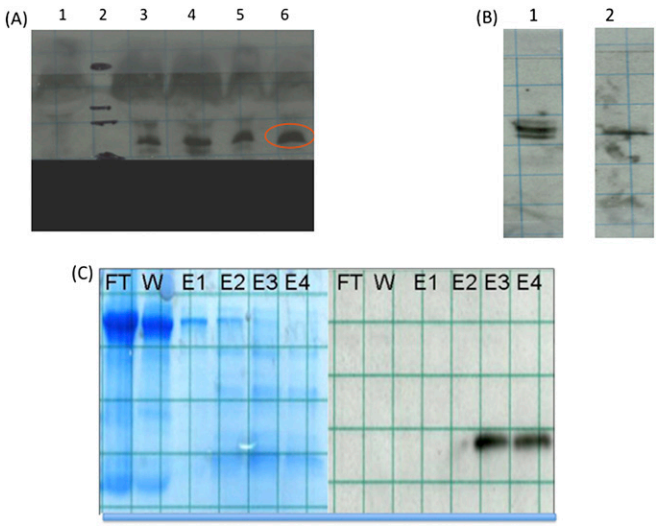

Fig. S4. (*A*) Expression of the HNE-GSTA-cecropin B chimera in the insect High Five cell supernatant at 72 h postinoculation as assessed by the intensity of the band that migrated at 25 kDa during SDS/PAGE. The MOI was 1 for lane 3, 2 for lane 4, 5 for lane 5, and 10 for lane 6. Lanes 1 and 2 correspond to no transfection and the markers. An MOI of 10 was used in subsequent experiments. (*B*) Relative intracellular (lane 1) and extracellular (lane 2) expression of the chimera in the insect High Five cells. The extracellular fraction shows a single band of chimera on the gel. (*C*) SDS/PAGE and Western blot analysis of the chimera eluted from the elastin column. (*Left*) Fractions from batch chromatography on an elastin-agarose column were run on a denaturing gel, with samples designated flow-through (FT), wash (W), and elution (E). (*Right*) Recombinant chimera was detected in E3 and E4 by Western blot analysis.

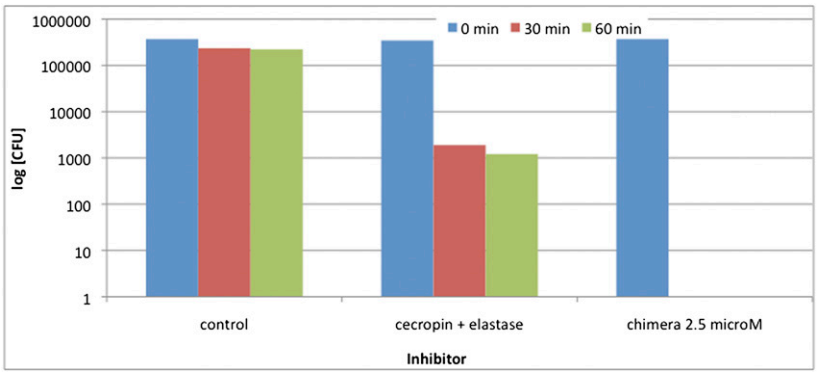

Fig. S5. Measurement (CFU/mL) of Xf Temecula1 in the presence of HNE plus cecropin B and the chimera, at the indicated concentrations, expressed in the insect HiFive cells for incubation times of 0, 30, and 60 min. The cecropin B (5 μM) and HNE (50 nM) concentrations are same as in Fig. 2*A* and Fig. S2.

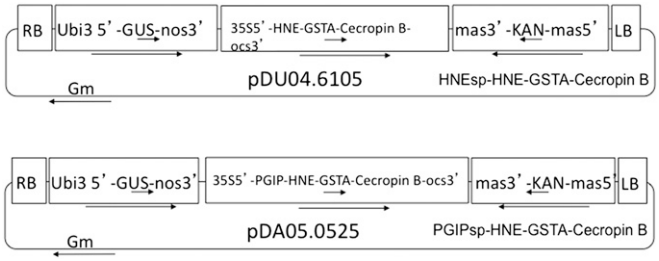

Fig. S6. Schematic representations of the pDU04.6105 and pDA05.0525 vectors carrying HNEsp-HNE-GSTA-cecropin B (*Upper*) and PGIPsp-HNE-GSTA-cecropin B genes (*Lower*).